Oct-4 GENE EXPRESSION IN THE PREATTACHMENT PORCINE CONCEPTUS AND MURINE EMBRYO WITH REGULATION OF PLURIPOTENCY THROUGH PROTEIN TRANSDUCTION

By

DIANA SPENCER

Bachelor of Arts in Science Education
University of Houston at Clear Lake City
Clear Lake City, Texas
1978

Master of Science in Math/Science Education
The University of Tulsa
Tulsa, Oklahoma
1994

Submitted to the Faculty of the
Graduate College of the
Oklahoma State University Center for Health Sciences
in partial fulfillment of
the requirements for
the Degree of
DOCTOR OF PHILOSOPHY
July, 2005

Oct-4 GENE EXPRESSION IN THE

PREATTACHMENT PORCINE CONCEPTUS AND

MURINE EMBRYO WITH REGULATION OF

PLURIPOTENCY THROUGH PROTEIN

TRANSDUCTION

Dissertation Approved:

Lee Rickords, Ph.D.

Dissertation Adviser

Earl Blewett, Ph.D.

Kirby Jarolim, Ph.D.

Rodney Geisert, Ph.D.

A. Gordon Emslie, Ph.D.

Dean of the Graduate College

ACKNOWLEDGEMENTS

I wish to express my sincere appreciation to Dr. Lee Rickords for inviting me into his molecular biology lab and generating many research ideas. I especially appreciate my committee members, Dr. Kirby Jarolim, Dr. Rodney Geisert and Dr. Earl Blewett for much support and guidance. A special thanks is extended to Dr. Earl Blewett for incredible hours of support most recently, but also for years of technical guidance.

I have received much help from a number of scientists. I appreciate Heather Schafstall and Crystal Shults for help in my early molecular education with a special appreciation for Crystal finding our "KKL" ligation protocol. I thank Dr. Geisert and Jason Ross for much technical assistance with the porcine specimen at OSU, Stillwater. Dr. Greg Sawyer and Tami Ross provided much help with numerous lab protocols. I appreciate Dr. Julie Marino and Rhonda Massengale in the lab of Dr. Teague at OU-HSC for early help with Real Time PCR. I extend a very special thanks to Kim Urick for her tireless hours of protein purification in Logan, Utah. My favorite times in the lab involved optimizing protocols with my fellow new scientist colleagues; Sarah Myer and Kim Urick and I were able to discuss new techniques in a new language to advance our projects in Real Time and protein purification, respectively.

I appreciate many professionals of the scientific community. I thank Drs. Austin Cooney, Guang Zhao, Hans Scholer and Steven Dowdy who sent specific plasmids and cDNA. I also thank the Oklahoma State University Recombinant DNA/Protein Resource Facility for sequencing our constructs.

I especially thank the people who provided emotional support and guidance through these years. Drs. Conrad, John and Jarolim were especially supportive to the completion of this project. I've been continuously supported by lifelong friends Paulette Ramsey, Janie Johnson and Dot Woods. My colleagues at Jenks High School and Tulsa Community College have been constantly supportive.

Of course, my greatest appreciation is given to my family. My mom and dad, Carol and Richard Blake gave me an incredible amount of curiosity and modeled a persistent work ethic. My daughters, Jessica and Julia have supported my goal for many years of their young lives; they never slowed in their support, even when it meant our household would run less smoothly. Through their elementary, middle, high and now college years they openly advocated for their employed and night school working mom. And Mark, my wonderful husband, who chose to live through his accident, see this project to fruition, and make me forever grateful.

TABLE OF CONTENTS

LIST OF TABLES

Table Page

Chapter III

Chapter IV

LIST OF FIGURES

Figure Page

Chapter III

Chapter IV

Chapter V

LIST OF ABBREVIATIONS

APP	Amyloid Precursor Protein
BLASTN	Basic Local Alignment Search Tool for Nucleotides
BMP8b	Bone Morphogenetic Protein 8b
cDNA	Complementary Deoxyribonucleic Acid
COUP-TF	Chicken Ovalbumin Upstream Promoter Transcription Factor
DE	Distal Enhancer
DFC	Dense Fibrillar Components
EC	Embryonic Carcinoma
EGFP	Enhanced Green Fluorescent Protein
EMBL	European Molecular Biology Laboratory
ES	Embryonic Stem
FACS	Fluorescence Activated Cell Sorting
FC	Fibrillar Centers
FGF	Fibroblastic Growth Factor
FITC	Fluorescein Isothiocyanate Conjugate
GC	Granular Components
GCNF	Germ Cell Nuclear Factor
GDNF	Glial Line Derived Neurotrophic Factor
GFP	Green Florescent Protein
GNT	Granulosa Cell Nuclear Transfer
GOF	Genomic Oct-4 Fragment
HCG	Human Chorionic Gonadotropin
HIV	Human Immunodeficiency Virus
HMG	High Mobility Group
HPRT	Hypoxanthine-Guanine Phosphoribosyltransferase
HRE	Hormone Response Element
HSC	Hematopoietic Stem Cell
HSC	Heat Shock Cognate
ICM	Inner Cell Mass
IFN	Interferon
IGF	Insulin Growth Factor
IGFBP	Insulin Growth Factor Binding Protein
IVF	In vitro Fertilization
LIFR	Leukemia Inhibitory Factor Receptor
LTR	Long Terminal Repeat
MFF	Murine Fetal Fibroblasts
MHC	Major Histocompatibility Complex
mRNA	Messenger Ribonucleic Acid

MZT	Maternal to Zygotic Transition
NCBI	National Center for Biotechnology Information
NSC	Neural Stem Cell
NT	Nuclear Transfer
OPN	Osteopontin Protein
P4CC	Post-4-Cell Cleavage
PDGF	Platelet Derived Growth Factor
PE	Proximal Enhancer
PGC	Primordial Germ Cell
PMSG	Pregnant Mare Serum Gonadotropin
PORE	Palindromic Octamer Recognition Element
POU	Pit, Oct, *Unc* Related Domain
PTD	Protein Transduction Domain
RA	Retinoic Acid
RARE	Retinoic Acid Response Element
RBP	Retinol Binding Protein
RT-PCR	Reverse Transcription Polymerase Chain Reaction
RXR	Retinoid X Receptor
SOD	Superoxide Dismutase
TAR	Tat-responsive Element
TAT	Transcription-Activating Factor
TAT-HA	TAT with Hemagglutinin Tag
TE	Trophectoderm
TIGR	The Institute for Genomic Research

CHAPTER 1

INTRODUCTION

Pluripotent stem cells, derived from embryonic tissues, have the unique capacity to theoretically produce every cell type in the body. By studying this cellular plasticity and elucidating the properties and mechanisms of pluripotency, an understanding of how to induce the pluripotent state in a variety of cell types may be developed. This would be significant in that cells induced to become pluripotent in nature may be used in the treatment of diseases such the muscular dystrophies, leukemias, diabetes, Parkinson's, and Alzheimer's. An understanding of the properties of cellular pluripotency has the potential to enhance stem cell development and ultimately be used to take stem cell-based treatments into the clinic.

A classical marker of embryonic stem (ES) cells (cultured cells derived from the pluripotent inner cell mass (ICM) cells of pre-implantation embryos) and *in vivo* embryonic blastocyst cells is the transcription factor, Oct-4. Oct-4, exclusively expressed by embryonic and germ cells, plays a critical role in the establishment and/or maintenance of pluripotency [1-3]; this transcription factor binds specifically to an octamer sequence of DNA, ATGCAAAT [4]. The structure of this DNA binding domain allows for such flexibility that it can profoundly influence the activity of transcriptional regulators. Two fused heterodimers are brought together to form a single DNA-binding

unit. The linker has little apparent structure and increases the versatility in its interaction with DNA [5]. The *Oct-4* gene transcript is found in the totipotent and pluripotent stem cells of the early mouse embryo and is down regulated when the cells differentiate [4, 6]. *Oct-4* is active in the ICM cells and down regulated in the pre-trophectoderm cells, or cells of the outer layer of the blastocyst. The ICM cells are pluripotent and give rise to cell types of the three embryonic germ layers, i.e., ectoderm, mesoderm, and endoderm [7]. The Oct-4 transcript levels are maintained in the epiblast, but expression soon becomes gradually restricted to cells of the germline as gastrulation proceeds [3, 8]. Oct-4 is the first described protein which appears to be specific for the mammalian totipotent cycle [8, 9]. The Oct-4 protein can either repress or activate transcription in particular target genes during embryonic development. These varied, initiating molecular events remain uncertain and complex, and deciphering these cell differentiation pathways is pivotal to the growth of stem cell technology [10].

The *Oct-4* gene has been found only in mammals, and the human sequence is 87% identical to that of the mouse [10, 11]. The 5' upstream regulatory region of the human, bovine and murine *Oct-4* genes reveal four conserved regions of homology between these species, and the murine *Oct-4* gene is highly conserved in humans and cows as evidenced by 87% and 81.7% overall protein sequence identity, chromosomal mapping to the major histocompatibility complex (MHC) and the genomic organization into five exons of the three species [2, 12]. The *Oct-4* gene, also designated *Oct-3* or *POU5F1* [12] has a transcript encoded of about 1.5 Kb [13, 14]. Understanding the molecular basis of the pluripotent phenotype is critical to isolating and propagating human stem cells. Elucidation of the mechanisms that govern cell signaling will provide a

paradigm for understanding tissue differentiation and growth control in later stages of development [15].

Pluripotency reflects a cellular diversity which is driven by an adaptive response to a functional pressure [16]. With the expression of *Oct-4*, a connection has been investigated on fetal germ cells, between the retention of pluripotency, and the ability to transform into variable tumors [17]. A high abundance of Oct-4 in carcinoma *in situ* (CIS) cells is consistent with pluripotent characteristics. Gidekel and co-workers demonstrated that Oct-4 is a critical player in the genesis of testicular germ cell tumors [18]. Deregulation of homeobox genes is functionally relevant for carcinogenesis [18]. Oct-4, which is essential for the development of pluripotent murine cells, is often used as a marker of pluripotency in primates, and ES cells provide a model to study human embryology and investigate novel growth factors and medicines [19]. The transcription factor, Oct-4 is regarded as a candidate master regulator for the initiation, maintenance, and differentiation of pluripotent cells [15, 20-22]. An understanding of this gene's expression will provide experimental evidence for clarification of target genes controlled by *Oct-4* [22]. Because the quantitative expression of Oct-4 defines differentiation and self-renewal of ES cells [20], the ability to regulate *Oct-4* expression is a vehicle to understanding tumorigenesis, increasing pluripotency of somatic cells, and modeling of the multiple layers of transcription and growth factors involved in embryology.

Protein transduction, the internalization of proteins into the cell from the external environment, is an emerging technology which relies on the property of some proteins to penetrate the cell membrane [23]. Although protein transduction is still in its infancy, it holds potential for the basis of an entirely new form of therapy. Expressed and purified

fusion proteins permit the study of stem cells and their regulation. Oligopeptides and oligonucleotides transduced with the Transcription-activating factor (TAT) vehicle could change transcription expression and provide an integration of the two broad fields of mammalian gene regulation and stem cell biology through protein fusion. This interdisciplinary study could have vast implications for the development of therapeutic applications described above.

Proteins participate in signal transduction, gene transcription, intracellular movement and cell to cell communication [24]. New, non-invasive methods of delivery of functional peptides to cells have been developed. These proteins translocate across the plasma membrane in an energy independent pathway [25]. A peptide derived from the homeodomain of the transcription factor encoded by the *Antennapedia* gene can translocate across the plasma membrane of living cells and permits the transport of conjugated oligopeptides and oligonucleotides [25]. A similarly functioning protein is the herpes simplex virus type 1 protein, VP22, which is secreted from, and then re-internalized by live cells [25]. TAT, our protein of interest, is encoded by a portion of the Human Immunodeficiency Virus (HIV). The TAT domain is 86-102 amino acids in length, depending on the viral strain of the HIV [25]. It is divided into three functional domains: 1) an acidic N-terminal region; 2) a cysteine-rich DNA binding region and 3) a basic region responsible for nuclear entry (amino acids 48-59 which include six arginine and two lysine amino acids). TAT is also secreted and then re-internalized by the living cells that encode the TAT protein in a time- and concentration-dependent manner [25]. The commonality between each protein transduction domain (PTD) is the presence of the basic amino acids (lysine and arginine), which might be important for penetration of the

membrane, or lipid interactions, or both [26, 27]. TAT is the region responsible for the protein's ability to transduce membranes. The TAT fusion protein has several advantages over the VP22 delivery system. TAT fusion proteins are rapidly internalized so that timing can be controlled precisely; also, virtually all eukaryotic cell types tested to date are susceptible to transduction, excluding yeast [28, 29]. TAT fusion proteins have readily transduced into nucleated and enucleated whole blood cells, peripheral blood lymphocytes, diploid human fibroblasts, keratinocytes, bone marrow stem cells, osteoclasts, glioma cells, renal carcinoma and hepatocellular carcinoma cells [30]. Internalization has been demonstrated with more than ten TAT-derived short peptides; this transduction occurs within minutes and is not altered by lowering the temperature to 4°C [25]. PTD proteins have been introduced into mice and exhibit delivery of active enzymes across the blood-brain barrier [28]. PTDs have potential to deliver drug compounds and proteins to combat viral infections, kill cancer cells and regulate gene transcription [28]. Schwarze and co-workers introduced a 120 kDa enzyme that is 200 times larger than compounds that are normally able to cross cell membranes into all cells of a mammal. This was the first intraperitoneal delivery of TAT-fusion proteins *in vivo* with TAT-β-galactosidase into mice [27, 29].

Of prime importance is sifting through the milieu of environmental signals to determine which specific factors can selectively coax cells down a specific pathway. Elucidating the molecules that orchestrate specific developmental programs are important steps in determining the key components of stem cell regulation [31]. Currently, one of the best candidates for an embryonic regulatory factor is the transcription factor Oct-4 [10]. Future experiments focusing on Oct-4 protein expression and repression are

necessary to establish the unique biological functions of Oct-4 in both murine and human cells [15, 32]. While the pharmacology of protein transduction is poorly understood, it requires extensive study to realize its therapeutic potential [23]. Melding the technology of protein transduction with the early embryonic pluripotency factor, Oct-4, implicated in patterning of the vertebrate embryo, will clarify pluripotent regulation in embryonic cells.

Our first hypothesis is that porcine trophoblastic elongation and placental differentiation is associated with the *Oct-4* gene expression. Studying the gene expression of the porcine embryos exhibiting epithelialchorial placentation requires a collection and pooling of conceptuses for day 10, 12, 13, 15 and 17 of development. We will perform quantitative real-time analysis on the conceptus mRNA using a one-step RT-PCR amplification.

Our second hypothesis is that we'll find a murine up-regulation of Oct-4 in the 4-cell, 8-cell, and blastocyst whole embryos, and the individual pluripotent cells will show an increase in single cell gene expression. Testing this hypothesis will involve mastering the techniques to perform whole murine embryo messenger ribonucleic acid (mRNA) extraction and quantification. In order to elucidate the quantification of the Oct-4 transcript present in our model murine organism, it is necessary to investigate the steps needed to collect whole embryos, extract and reverse transcribe the RNA in individual embryos and then perform Real Time PCR on the individual 4-cell, 8-cell and blastocyst embryos. While Oct-4 transcripts have been studied in murine organisms through immunocytochemistry, whole embryo expression of the *Oct-4* gene has not been quantified. An analysis of the production of Oct-4 in these mammalian species (murine and porcine) will be the first reported documentation of the specific quantities of Oct-4

during various stages of development of the preimplantation embryos using Real Time polymerase chain reaction.

Our goal in this study is to construct plasmids within a prokaryotic expression system capable of expressing our particular genes, *GCNF*, *Bmp8b*, and *Oct-4*, fused to the TAT transduction domain and test the recombinant proteins, with transduction trials, on somatic and pluripotent cells. We hypothesize that through proper cloning with 5' restriction site mutagenesis, cloning of the PCR products, and protein expression in bacteria and purification through FPLC, we can quantitate the protein, and prove protein acquisition through SDS-PAGE and Western Blotting. We can also indicate transduction of the proteins through immunocytochemistry of Vero cells. This study is a necessary step toward the transduction of the repressor and promoter of the distal enhancer for the *Oct-4* gene in somatic cells and ES cells. The purification of TAT fusion proteins will allow for the subsequent mimicry of various internal cellular environments with suitable regulation of pluripotent characteristics. TAT fused to an *Oct-4* enhancer, bone morphogenetic protein 8b (BMP8b) and an *Oct-4* repressor, germ cell nuclear factor (GCNF) will allow for future data analysis of Oct-4 regulation and pluripotency.

This proposed research leads to our ultimate goal of investigating regulation of nuclear transfer (NT) derived preimplantation embryos. This proposed research investigates the regulatory components of nuclear transcription in embryonic cells. Protein transduction is a biotechnology tool that can be used to improve our understanding of stem cell regulation.

If pluripotent stem cells derived from human embryos behave like their murine counterparts, they could be used to treat a wide variety of human diseases [1]. These

murine and porcine models will contribute to understanding our own species' developmental biology [1]. Certainly, the homology seen between these models and the human will allow for the opportunity to study stem cell characteristics without human embryonic cells.

Human ES cell research is in its initial stages and to date, there is no universally accepted standard to determine what characteristics will predict the ability of such cells to be useful for the development of therapies. Some scientists require evidence of the expression of certain genes such as *Oct-4* before cell types will be used in ES cell studies [33]. While our hypotheses use animal models, it is understood that these results will differ specifically to human stem cells.

CHAPTER II

REVIEW OF LITERATURE

Introduction

A powerful approach for studying cellular function is found in the internalization of exogenous macromolecules by living cells. New therapeutic approaches will be developed from the understanding of the mechanism of transfer from the extracellular milieu to the cytoplasm and nucleus [34]. All eukaryotic cell types (except yeast) appear transducible with proteins linked to PTDs. Since *Oct-4* is expressed almost exclusively in stem cells of the early embryo, both maternally and zygotically [14], an understanding of its effect on embryonic cells, and somatic cells coupled with protein transduction requires a review of *Oct-4* expression, structure and regulation. Protein transduction vehicles will be studied with specific attention to the HIV TAT protein history of development through studies conducted by Frankel, Green, and Fawell [35-37]. A review of recent work completed with TAT fusion proteins will reveal the specific capabilities of the technology. Successful embryonic development requires specific gene expression for placental and embryonic differentiation; a study of the early embryonic murine and porcine environment is essential to understanding normal embryo development. This review of *Oct-4* and protein transduction domains is necessary

background to meld these topics into a complete biotechnology study in stem cell research.

Oct-4 Expression and Characteristics

Oct-4, an octamer binding protein stimulates transcription and is found in primary germ cells (PGCs), unfertilized oocytes and pluripotent ES cells; when the stem cells are induced to differentiate, the amount of the octamer binding factor decreases [13, 38]. It was suggested by Scholer and co-workers that the Oct-4 protein was not only present in oocytes but could be synthesized *de novo* by zygotic expression in the embryo [13]. Oct-4 was shown to be the first transcription factor described for the early stages of mouse development and maps to murine chromosome 17 near the MHC [39].

This mammalian transcription factor is exclusively expressed by embryonic and germ cells. Transcription factors are DNA binding proteins that can control the rate of transcription of certain genes. Understanding how transcription factors are expressed and function is a requirement for comprehending developmental processes. Oct-4 plays an important role during the early stage of mouse embryogenesis and in the germline as an essential component of regulation for germline maintenance [11]. Developmental lineage begins at the end of the cleavage stage of an embryo with compaction and leads to the development of the blastocyst. The trophectoderm, or outer layer of the blastocyst, generates the trophoblastic components of the placenta, while the ICM cells develop into the pluripotent progenitors of all of the fetal cell types, including the germ cells and the nontrophoblastic extraembryonic tissues [15]. Understanding the molecular basis of these pluripotent cells is critical to efforts to propagate stem cells. The explanation of

molecular interaction that governs the trophoblast and ICM development will provide an outline of complex tissue interaction in further development [15]. Oct-4 can either repress or activate transcription in particular target genes and is one of the best candidates for an embryonic regulatory factor. These varied, embryonic initiating molecular events remain uncertain and complex, while Oct-4 has emerged as a critical transcription factor that establishes pluripotency [10]. Deciphering the cell differentiation pathways is pivotal to growth of stem cell technology.

Murine *Oct-4* Expression

Oct-4 expression is crucial to the success of murine preimplantation development [38-42]. Maternal Oct-4 mRNA and protein are present in unfertilized murine oocytes [4] and in the nuclei of subsequent cleavage stages [4, 14, 43]. During the first two cleavage stages, the levels of Oct-4 mRNA decrease to background and then steadily increase thereafter. After cavitation, in murine hatched blastocysts, Oct-4 mRNA is found in the ICM which differentiates into epiblast and hypoblast (second extraembryonic lineage) [2]; as the murine blastocyst forms, *Oct-4* expression is downregulated, and with expansion, Oct-4 protein and mRNA are primarily found in the ICM [3, 4]. As the ICM differentiates into the epiblast (embryonic ectoderm) and the hypoblast (embryonic endoderm), and the hypoblast cells migrate along the inner surface of the trophectoderm, high levels of Oct-4 protein are found within these tissues [3, 39, 43]. The *Oct-4* gene transcript is found in totipotent and pluripotent stem cells of the early mouse embryos and is only down regulated when the cells begin to differentiate [4, 6]. Palmieri and co-workers (1994) found Oct-4 at high levels in the hypoblast that

differentiate and migrate along the inner surface of the trophectoderm. The Oct-4 protein levels increase in cells of the hypoblast, but decrease drastically as the hypoblast differentiates [4, 42]. Detection of the Oct-4 transcripts were identified in the postimplantation mouse embryonic ectoderm at day 7, but not in the endoderm, allantois or other extraembryonic tissues forming at day 7.5 [39]. Within the murine epiblast, *Oct-4* expression is high until the germ layers form. Thereafter, expression is downregulated from anterior to posterior as the somatic lineages form and gastrulation proceeds. As gastrulation ends, neurulation and somitogenesis progress and restrict the potency of ectodermal and mesodermal cells [2]. After 8.5 dpc, the expression of *Oct-4* is restricted to PGCs, or primordial germ cells [2, 6, 11, 12, 44-46]. The pluripotent cells of the murine embryo and germ line, and ES cells in culture are characterized by expression of the homeobox gene, *Oct-4* [47].

It also appears that expression of *Oct-4* differs between species. High levels of human Oct-4 were detected in the oocyte, not in the two-cell or four-cell embryos and then embryonic Oct-4 was detected in human blastocysts with a lower expression than found in the 10 week fetus [48]. Similar to murine embryos, human blastocyst mean *Oct-4* expression was 31 times higher in totipotent ICM cells than in differentiated trophectodermal (TE) cells [49]. Microarrays containing more than 16,000 oligonucleotides examined the gene expression in six of the 11 available human ES cell lines. A common subset of 92 genes was identified that included *Oct-4* and then verified through a variety of techniques including comparison with databases, RT-PCR and immunocytochemistry. The human ES cell lines appear similar to each other and express a unique molecular signature of 92 genes which includes *Oct-4* [50].

The three best characterized types of stem cells in vertebrates are embryonic (ESC), neural (NSC) and hematopoietic (HSC) stem cells. Transcriptional profiles of these cell types were compared by Ramalho-Santos and co-workers [51] to define a genetic program unique to stem cells. Using the stem cell samples and amplification probes hybridized to DNA microarrays, the scanned arrays were analyzed with software to identify transcripts specific to certain cell lines and those which intersected all three cell lines. Stem cells were determined to be distinct and clearly identified by specific genes identified. Interestingly, the human chromosome 17 contains 3.7 times the number of SC-enriched genes that would be present if the genes were randomly distributed, and *Oct-4* was identified as a nucleic acid binding ES cell-enriched gene [51].

Using a gene construct of portions of the upstream region, five exons of the *Oct-4* gene, and enhanced green fluorescent protein (EGFP) as a reporter, expression of the gene was monitored in porcine, murine and bovine with *in vitro* and *in vivo* models. Different from the murine pattern of expression, the bovine and porcine expression of *Oct-4* was detected in both the ICM and the TE [43]. The unique *Oct-4* expression pattern found in murine embryos was extended to pluripotent cells of the rhesus monkey [52]. Embryonic genome activation in the monkey initiates at 4-8-cell stage and *Oct-4* gene expression was first obvious at the 16-cell stage. At the hatched blastocyst stage of the rhesus monkey, only ICM cells were positive for Oct-4 protein, similar to the human expression [49, 52].

POU Transcription Factor Characteristics

The Oct-4 POU (Pit-1, Oct-1, *unc*-86) domain (pronounced 'pow') was first reported by Herr and co-workers, in 1988, with a sequence homology seen between the *pit-1*, *oct-1*, *oct-2* and *unc-86* mammalian gene products. [42, 48, 53-55]. The octamer motif ATGCAAAT is recognized by the Oct-4 family of transcription factors, while similar domains are present in the pituitary-specific transcription factor Pit-1 and the *Caenohoabditis elegans unc*-86 cell line product. Within this shared POU domain lie two subdomains: a POU-related homeo box and a POU-specific box[53] . The DNA-binding domain confers specificity of transcriptional activation and targets the *trans*-activator to the promoter carrying the corresponding octamer DNA-binding site. Oct-4 was first found with gel-shift analysis in embryonal carcinoma (EC) cells and cDNA was cloned independently as Oct-3 and Oct-4 [6, 41, 42, 45]. The earliest expressed gene known to encode the transcription factor is also referred to as *Pou5f1* (murine) *POU5f1* (human) and *bPOU5F1* (bovine) [42].

Transcription factors are proteins that bind DNA and can modulate the rate of transcription of various genes. The POU transcription factors have been isolated from a variety of different invertebrates and vertebrates and have been grouped into six or seven classes according to their amino acid sequence similarity [55, 56]. Conservation through functional constraints on the protein products is supported by the high degree of sequence conservation in proteins present in organisms as diverse as nematodes and humans [54]. Either of the two structurally independent helix-turn-helix domains, specific or homeodomain, can bind alone to the DNA. However, specificity and stability of binding are increased when the POU transcription factors bind simultaneously to opposite sides of

the DNA helix and cooperate functionally as a fused heterodimeric DNA-binding unit [5, 55, 57]. The length of the linker region, which ranges in size from 15 to 56 amino acids within the POU family of proteins, probably plays an important role in enabling the POU-specific domain to assume various orientations relative to the homeodomain, thus enabling the recognition of various DNA elements [55]. POU domain proteins regulate key developmental processes and Class V POU domain proteins are expressed almost exclusively during the early stages of embryonic development. The ability of the DNA octamer to allosterically modulate the specificity of the POU domain coactivator interaction coupled with the understanding that POU domain proteins utilize specific coactivators, provide the molecular foundation by which specific POU domain proteins can regulate transcription both temporally and spatially [55]. The embryonic Oct-4 has the following characteristics: a more conserved N-terminal domain of about 75 residues (POU_S), a more divergent C-terminal homeodomain of approximately 60 amino acids (POU_{HD}), and a linker to connect the two domains that is variable in sequence and length [5, 6, 11, 55, 58]. The fused heterodimer protein binds specifically to the octamer motif of ATGCAAAT, while the bipartite flexible structure of the two domains allows the protein to bind in different conformations. The two domains bind to the major groove on opposite sides of the DNA molecule. The POU_S domain consists of four α-helices surrounding a hydrophobic core while the $\alpha 3$ helix makes specific contact to the first half of the octamer motif (ATGC). The POU_{HD} domain has three α-helices and the helix $\alpha 3$ makes specific base contacts with the second half of the octamer motif (AAAT). The second and third helices of the homeodomain form a helix-turn-helix motif [46]. The

Oct-4 mRNA encodes a 352 amino acids long protein (with 324 amino acids in the open reading frame) [5, 6, 11, 46, 55, 59].

Regulation of *Oct-4* Expression

Promoters and Enhancers

Oct-4 is the earliest known gene of the mammalian embryo that is differentially regulated [60]. The 5' upstream regulatory region of the human, bovine and murine *Oct-4* genes reveal four conserved regions of homology (CR 1 to 4) between these species with a 66-94% conservation [12]. The *Oct-4* gene has five exons with a transcript encoded of about 1.5 Kb [14, 39]. The gene lacks a TATA box promoter, but contains a GC-box to which Sp1-family (specificity protein) members bind *in vitro* [58, 60]. Members of the Sp family of transcription members bind with varying affinities to GC-boxes, CACCC-boxes, and basic transcriptional elements. Murine *Oct-4* maps to chromosome 17 near the MHC while the human homologue of the *Oct-4* gene is mapped to chromosome 6 [11, 39].

Oct-4 gene expression is dependent on at least three regulatory *cis*-regions [10], the promoter region, the proximal enhancer and the distal enhancer. The first of the three, is the promoter region, located within 250 bp of the transcriptional initiation site. The TATA-less promoter of *Oct-4* contains a set of well-characterized sequences that are highly conserved in mice and humans [14, 61]. Within the basal promoter, a cluster of binding sites overlap. A hormone response element (HRE), partially overlaps with the GC-box and is recognized by a number of steroid-thyroid hormone receptor family

members such as retinoic acid (RA) [11, 62]. The HRE of the mouse *Oct-4* basal promoter has three repeats (R1, R2, R3) of an AGGTCA-like sequence which might interfere with specific members of the nuclear receptor family. This HRE can function as a positive regulator of transcription or as a director of an adjacent binding factor such as Sp1. The Sp1 transcription factor is thought to bind to the GC-box and as such regulates initiation of transcription from promoters that lack a TATA box. A point mutation that abolishes Sp1 binding in band shift assays decreased *Oct-4* gene activity more than 25-fold in different ES and EC cells lines [63]. The HRE might also function as a repressor of *Oct-4* production [11, 12]. This region resembles the RARE (retinoic acid response element), and is recognized by receptors including retinoic acid and retinoid X receptors (RAR, RXR, respectively) [10, 60]. Through upstream region deletion mutagenesis, the *cis* element (RAR1) was recognized as an enhancer, yet RA-repressible [61]. Recently, it has been determined that the direct repeats are bound by two factors; the initial repression of *Oct-4* by RA coincides with the disappearance of one factor and then the appearance of a transiently induced factor as evidenced in electrophorectic mobility shift assays [44]. Also, several members of the orphan nuclear hormone receptors superfamily preferentially bind to the direct repeat DR1 between R1 and R2 and are thought to be involved in *Oct-4* down-regulation [44].

Transgenic analysis revealed two upstream regulatory regions of the *Oct-4* gene [8]. The proximal enhancer (PE) is located approximately 1.2 Kb upstream of the initiation site; this particular site is mediated by RA down-regulation of *Oct-4* [61]. Another regulatory region, the distal enhancer (DE) is about 2 Kb upstream, and its

activity is restricted to totipotent cell types [11]. The switch from DE to PE occurs around implantation [8, 10].

Expression patterns of the *Oct-4* gene were studied through a *lacZ* gene inserted into an 18kb genomic fragment encompassing the *Oct-4* gene with the endogenous embryonic expression pattern of *Oct-4* in transgenic mice [8]. Similarly, transgenic mice expressing green fluorescent protein (GFP) in the germ cell line were generated using the same genomic fragments. Expression patterns were analyzed in detail through all stages of germ cell development [9]. In each study, the transgene expression in pre-implantation embryos and PGCs is driven by the DE, while the PE is necessary for the expression in the epiblast. ES, EC, and embryonic germ (EG) cells respectively resemble cells found in the ICM of blastocysts, epiblast cells and PGCs [11]. A DE is active in ICM cells of the preimplantation embryo, ES and EG cell lines and PGCs, while a PE, is active in the epiblast and EC cells [8, 9, 59, 64].

Additional Mechanisms of Down-Regulation

Complete physiological processes of down-regulation of *Oct-4* in some blastomeres are still unknown, however location of cells within the embryo might be one mechanism [32]. Another possible mechanism of down-regulation involves cell to cell proximity with a signal cascade from E-cadherin to β-catenin to lymphoid enhancer factor; E-cadherin deficient mouse embryos fail to form TE [2, 3, 10].

Extinction of the *Oct-4* gene expression is accompanied by a change in activity of trans-acting factors (either induction of repressors or loss of activators) acting on the upstream region of the gene. Suppression of *Oct-4* expression in EC fibroblast somatic

cell hybrids and RA treated EC cells is achieved through changes in methylation, chromatin structure and trans-acting factors on the upstream regulatory region [58]. *Oct-4* is expressed in EC cells and is repressed in (RA)-differentiated EC cells. The promoter for the gene has no RARE, however, it harbors a RARE motif, RAREoct, which acts as a binding site for positive regulators of transcription; in RA differentiated EC cells, it acts as a binding site for negative regulators [62, 65].

While *Oct-4* is expressed in EC cells and repressed in RA-differentiated EC cells, the complexity of modulation of gene expression is described in P19 and RA-treated P19 cells. Orphan receptors from the chicken ovalbumin upstream promoter transcription factors [60] ARP-1/COUP-TFII and EAR-3/COUP-TFI repress *Oct-4* activity through the RAREoct site [62]. Three different RA receptor: retinoid X receptor (RAR:RXR) heterodimers activate *Oct-4* transcription through the RAREoct site. *Oct-4* expression is modulated through the antagonism between the orphan receptors and the RAR:RXR heterodimers. Transcription of the gene is controlled by a complex interaction of positive and negative regulatory elements. ARP-1/COUP-TFII and EAR-3/COUP-TFI interfere with the binding and transactivation ability of the RAR:RXR heterodimers. Thus, in RA-treated EC cells, the kinetics of *Oct-4* repression inversely correlates with the kinetics of the orphan receptor activation. Inhibition of *Oct-4* expression occurred through the binding of the orphan receptors to the RAREoct site [62, 65, 66]. RARs by themselves are inefficient DNA binders and require auxiliary nuclear proteins such as RXRs for effective responses [66]. The upstream regulatory region contains an RA-negative element in the enhancer and at least one in the promoter region. Pikarsky and co-workers [66] suggested that these repressors are differentially used at specific stages of

development and since suppression of *Oct-4* expression is crucial during embryogenesis, several RA-negative regulators may be employed for accurate development.

Regulation Through *Oct-4* Expression

Specific Genes Regulated by Oct-4

Oct-4 belongs to a group of octamer-binding proteins that bind by the POU domain to promoter and enhancer regions of various genes with octamer sites [32]. At this time, about nine genes have been found to contain Oct-4 binding sites; some of these sites are negatively and others positively regulated by the *Oct-4* gene [10, 15]. The α and β subunits of human chorionic gonadotrophin (hCG) are repressed while the platelet-derived growth factor (PDGF) α receptor is activated by Oct-4 [32]. The Oct-4 repression of both human chorionic α and β (hCG α, β) shows that Oct-4 not only activates genes expressed in stem cells, but also prevents the expression of genes which are activated during differentiation pathways [67]. While the concensus view is that Oct-4 prevents differentiation by maintaining the expression of key embryonic genes, Oct-4 may also silence transcription of genes that are associated with differentiation into the TE [68]. Oct-4 appears to be a potent silencer of bovine IFN-τ promoters when the transactivator, Ets-2 is overexpressed. Ezashi and co-workers [68] described the silencing as a quenching when the protein interferes with the ability of the DNA-bound transactivator to interact with the basic transcriptional machinery. Fibroblast growth factor-4, *Fgf4*, and osteopontin, *Opn* were described as top candidates for genes that Oct-

4 regulate [11]. Possibly, Oct-4 controls the expression of *Opn* [10, 52, 56, 69] and *Esg 1* [52].

Through suppression-subtractive hybridization, identification of putative downstream genes were identified by Du and colleagues [67]. *Oct-4*, Rex-1, Sox-2, Creatine kinase B (a pivotal enzyme in cellular energy metabolism), Makorin 1, Importin β (a cytosolic receptor for nuclear transport), Histone H2A.Z, Ribosome protein S7 and four new genes were identified as putative downstream genes of the Oct-4 protein in ES cells [67].

Transcriptional Activation by Oct-4 Through Cooperation With Partners: E1A, Sox2, Rox-1

Oct-4 action appears to go beyond a simple repression of trophoblastic lineage and activation of ES cells; it activates transcription of genes through cooperation of protein "partners." Thus, Oct-4 regulates expression of multiple genes via interactions with other transcription factors such as: Sry-related (Sex determining region on the Y) Sox-2 [15, 20, 67] , a stem-cell-restricted E1A-like protein [10, 15, 20, 67, 70], and the transcription factor Rox-1 [20].

Transactivation by Oct-4 is stimulated in the presence of E1A in differentiated cells. The distance-independent transcriptional activation suggests that E1A functions as a bridging factor allowing the Oct-4 protein to interact with downstream enhancers. It is suggested that an E1A-like factor recognizes through coactivation one surface of Oct-4 and with another surface recognizes the basal initiation complex, thus activating transcription from a distance [70]. It has been suggested that the product of the

adenoviral gene, E1A, will synergize with Oct-4 and mimic stem cell-specific bridging factors. Interaction of the Oct-4 POU domain with the E1A may induce conformational changes in the Oct-4 molecule which enables transactivation to occur [59]. Scholer led a research group at the European Molecular Biology Lab (EMBL) on gene expression during 1996 and proposed that not only E1A, but other viral oncoproteins of several tumor viruses share the ability to mimic embryonal E1A-like activity in order to convey a permissivity for proliferation that is typical of embryonic tissues [71]. It appears that transactivation of various genes is dependent on connecting a remotely bound Oct-4 molecule with the transcription sites mediated by E1A, while binding of Oct-4 with Sox2, a cofactor, to adjacent sequences enables transactivation of *Fgf4* and *Utf1* genes [72].

Sox-2 acts as a positive or negative regulator of Oct-4 activity. The *Fgf4* gene has an octamer-containing enhancer in its 3' noncoding regions and responds to Oct-4 in a Sox2-dependent fashion [15, 59, 73]. Sox2 forms a ternary complex with the Oct-4 protein on FGF-4 enhancer DNA sequences. Yuan and co-workers (1995) identified FGF-4 as the first known embryonic target for Oct-4 or any of the Sox factors [73]. Fibroblastic growth factor 4 (FGF4) maintains normal trophoblast precursors and the Oct-4 directed secretion of FGF4 by the ICM and epiblast may sustain the diploid trophoblast [15]. The FGF-4 produced by undifferentiated ICM cells acts in the peri-implantation period of embryogenesis to influence the endoderm cells derived from the ICM cells [74]. FGF-4 mRNA is found at all stages of preimplantation mouse embryos from 1-cell through blastocyst; the *FGF-4* gene promoter contains a response element for the octamer binding factor. In the preimplantation mouse, *Oct-4* and *FGF-4* have temporally and spatially overlapping expression patterns [74]. Oct-4/Sox2

heterocomplexes also activate transcription of *Utf1* (undifferentiated embryonic cell transcription factor 1) whose protein displays further characteristics of transcriptional coactivator in early embryogenesis [75]. That the *UTF1* gene is a target gene of Oct-4 and also regulated by the synergistic action of Oct-4 and Sox-2, indicates the Oct-4/Sox2 transcription requirement of *FGF-4* enhancer is a general mechanism of activation of Oct-4 [76].

Oct-4 was also found by Ben-Shushan and co-workers to activate or repress the Rex-1 promoter depending on the cellular environment[65] . The Rex-1 promoter contains an octamer motif that is a binding site for Oct-4; Rex-1 is a developmentally regulated zinc finger gene regulated in a dose dependent manner. A novel regulatory element found within 11-bp of the Rex-1 sequence binds a protein, Rox-1 and plays a key role in expression of Rex-1 in stem cells [65]. Rex-1 repression was also enhanced by E1A. Activation and repression of the *Rex-1* gene by Oct-4 depends on cellular environment, amount of Oct-4 protein present and the *Rox-1* binding site; these factors provide the specificity of the expression of the *Rex-1* gene in early embryogenesis [65].

Transcriptional Control Through Conditional Expression

Niwa and co-workers used conditional expression and repression in ES cells to deliver a precise level of Oct-4 [20]. Three distinct fates were found in the ES cells. A less than twofold increase in expression caused differentiation into hypoblast and mesoderm. To maintain the undifferentiated stem cell, the expression had to remain within 50% plus or minus of normal diploid expression, and when the *Oct-4* expression is decreased, stem cells are directed into the TE lineage [20]. Also, the transcriptional

responses of five target genes to changed Oct-4 level were studied. *Otx1* and *Ebaf* were upregulated on induction of the *Oct-4* transgene, while *Upp* and *Zfp42* were downregulated and *Fgf4* expression wasn't appreciably changed [20]. Thus, increased expression of Oct-4 had divergent effects on different target genes. The expression, or quantity of mRNA of various marker genes was also examined. *Gata4* mRNA found in the endoderm of embryos and the mesodermal marker, brachyury *T* were activated during elevation of *Oct-4* expression. Two transcription factors implicated in trophoblast differentiation, Hand1 and Cdx2 were induced upon suppression of Oct-4 [20]. Thus, up-regulation of Oct-4 caused commitment to extraembryonic lineages, and down regulation enhanced trophoblastic development. Niwa and co-workers, show that maintaining *Oct-4* expression within a certain range appears to be crucial for stem-cell renewal, while any increase or decrease triggers differentiation to endoderm/mesoderm or TE, respectively [20]. Oct-4 is a master regulator of pluripotency that determines lineage commitment and illustrates the complexity of critical transcriptional regulators with the need for quantitative analyses [20, 56].

In mouse ES cells, down-regulation of Oct-4 through transfection of *Oct-4* specific short interfering RNA was accompanied by an increased expression of the endoderm-associated gene *Gata6*. The human Oct-4 knockdown induced the overtly differentiated cells coincident with up-regulation of *Gata6* [77].

Oct-4 and Osteopontin

Oct-4 and *Opn* are coexpressed in murine premigratory endodermal cells; this is consistent with the proposal that Oct-4 is involved in the regulation of the *Opn* gene, and

that osteopontin is involved in cell migration [10]. Homodimer formation with elevated Oct-4 may enhance expression of the target osteopontin gene [20, 69]. The osteopontin (OPN) protein, secreted by cells of the preimplantation embryo binds to specific integrin subtypes and can modulate cell adhesion and migration. Immunoprecipitation studies of the first intron of osteopontin (i-opn) in the murine preimplantation embryo show that Oct-4 and OPN are coexpressed and that Oct-4 binds to this fragment*in vivo* . POU proteins can homo- or heterodimerize on a novel palindromic Oct factor recognition element (PORE) found on the osteopontin fragment. The dimerization of Oct-4 depends on the palindromic motif ATTTG-CAAAT, which has to be spaced by more than five nucleotides [69]. Botquin and co-workers isolated an Oct-4 recognition sequence within the osteopontin gene [69]. Sox-2, a transcriptional factor, also coexpressed with Oct-4, represses Oct-4 mediated activation of i-opn by way of a Sox element that is located close to the PORE found on osteopontin. *Sox*-2 belongs to the *Sox* (*Sry*-related High Mobility Group (HMG) box-containing) gene family. The HMG box of Sry is DNA-binding and induces a strong architectural bend on binding to the DNA [69]. Botquin and colleagues (1998) suggested that the *Opn* gene is tightly regulated by Oct-4 and Sox-2 in ICM and also in hypoblast cells, which will migrate along the TE and become parietal endoderm[69]. OPN is an extracellular protein that mediates adhesion to and migration along the surface of cell types. A GenBank-EMBL sequence database search of the Sox element within 40 bp of the octamer motif identified 17 sequences and OPN was the only candidate with respect to adhesion and migration [69]. Through *in situ* hybridization experiments, OPN was expressed selectively in the ICM of early murine blastocysts (3.5 dpc) and in cells destined to form the hypoblast (4.0 dpc). OPN becomes undetectable in

the embryo by 5.5 dpc. The coexpression of Oct-4 and OPN with overlapping expression domains found in the preimplantation embryos along with the previously mentioned immunoprecipitation of the two expressed proteins clearly suggest a physiological link between the cell adhesion molecule OPN and the transcription factor, Oct-4 [10, 59, 69]. Sox-2, expressed in EC and undifferentiated cells of the early embryo [11], is a candidate for modulator of Oct-4 transcription; Sox-2 Oct-4 mediated repression of the osteopontin enhancer is directly opposed to the Sox-2 Oct-4 mediated activation of the *fgf*–4 gene enhancer [69].

Opn expresses mRNA at the morula stage and is involved in cell migration [10]. OPN binds to cells displaying particular integrins on their surface; the murine *Opn* gene encodes a secreted phosphoprotein which binds through integrins to cells as well as to components of the extracellular matrix [69]. The particular murine integrins include: $\alpha_v\beta_1$, $\alpha_v\beta_3$, $\alpha_v\beta_5$. The formation of the hypoblast derivities, parietal and visceral endoderm, depend on the proper interaction between the ICM and integrins [69]. Murine Oct-4 expression precedes the onset of OPN expression in preimplantation mouse embryos and *Opn* is likely a direct target gene of Oct-4 in murine preimplantation embryos [69]. Of interest is the observation that Palmieri and colleagues concluded that Oct-4 protein expression in the early endodermal migrating cells is higher than in the ICM [4].

Implications of Abnormal *Oct-4* Expression

Less than half of all somatic cell clones develop to the blastocyst stage, and of those, less than one-third develop beyond implantation. A favored hypothesis for the

developmental incompetence of clones is inadequate reprogramming of the transplanted nucleus. Abnormal *Oct-4* expression in clones alone account for the majority of failures currently observed for somatic cell cloning [21]. While the blastocyst is the most meaningful preimplantation stage at which to analyze participation of the transplanted nucleus in development, the improper spatial Oct-4 distribution or observed lack of expression in cloned blastocysts may be caused by failure of onset of gene expression or down-regulation in development [21].

Pluripotent cells can be isolated from pre-implantation mouse embryos as ES cells and maintained indefinitely as a pluripotent population *in vitro* in the presence of cytokines of the IL-6 family [47]. The cells can be reintroduced into a host blastocyst and contribute to all adult tissues of the mouse including germ cells [47]. Nichols and colleagues [15] studied mouse embryos with a homozygous deletion for the *Oct-4* gene; the mice produced structures that resembled blastocysts but they did not form a pluripotent ICM. They died shortly after implantation with an inability to form embryonic tissues. An absence of Oct-4 results in peri-implantation lethality before the murine egg cylinder forms [15]. Inactivation of the endogenous *Oct-4* gene through short interfering RNAs and knock-out technology has defined the role of Oct-4 during embryogenesis [15, 52, 78] The mouse embryos deficient in Oct-4 developed to blastocysts that lacked an ICM.

Oct-4 and *Oct-4 GFP* transgene were used as markers for gene reprogramming and were directly related to developmental potential of somatic cell clones [21]. While the *Oct-4* temporal activation in somatic cell clones appeared to be normal, the maintenance of expression and cell type-specific *Oct-4* regulation in the TE and ICM

were not. The abnormalities of *Oct-4* expression in clones suggested that pluripotency was compromised. Activation of *Oct-4* is not due to a general opening of chromatin after NT. Thus, gene regulation in later stage clones may involve transcription factors available in the oocyte cytoplasm or the chromatin remodeling might become dysfunctional [21].

Theoretically, totipotency can be restored to the nuclei of somatic cells by reprogramming the nucleus with the technique of NT. A change in gene expression of the somatic cells must accompany this nuclear reprogramming. The expression of the regulatory control gene, *Oct-4*, was chosen as an ideal marker to check for proper gene re-activation following NT since *Oct-4* expression is specifically expressed in mouse oocytes, preimplantation embryos and becomes restricted to the epiblast at murine implantation [79].

Experiments using systems to up- and downregulate Oct-4 protein *in vivo* are necessary to determine whether modifications of its level determine a "reprogramming" of cell fate during murine development. A perturbation of the Oct-4 equilibrium through artificial modification of *Oct-4* expression levels might result in specific phenotypic changes of stem cells [72].

Complementation of non-cell-autonomous defects of genetically identical, but epigenetically different embryos result in improved expression of *Oct-4* [80]. Boiani and co-workers [80] observed that in somatic mouse cell clone blastocysts, a higher number of cells correlated with the correct expression of *Oct-4*. When somatic cell clones at the 4-cell stage were combined with each other to generate aggregate blastocysts, *Oct-4* expression was normal in most embryos and rates of post-implantation and full-term

development increased. Aggregation of the cells at the 4-cell stage would precede onset of *Oct-4* expression and blastomere polarization at the morula stage; gap junctional intercellular communication at the 4-cell stage and subsequent development could compensate for defects. Perhaps more developmental potential with complementation via intercellular signaling between clone components can occur subsequent to aggregation [80].

Abnormal expression of members of different families of homeobox genes is attributed to the development of leukemias, lymphomas and solid tumors. Jin and co-workers [81] found that the expression of the embryonic transcription factor, Oct-4 was only detected in breast cancerous cells as compared to normal human breast tissue samples. Homeobox genes exert their functions mainly by programmatically controlling the expression of downstream target genes involved in morphogenesis, cell growth and/or cell cycle. The studies by Jin and colleagues indicate that breast cancer cells re-gain their ability to express Oct-4 [81]. This expression implies that cancer cells may regain their ability to express this gene that is normally only active in germ and embryonic cells. In an effort to find a possible cancer antigen associated with the initiation of deprogramming (demethylation) and a return to the proliferative stem cell state associated with the immortality and/or invasiveness of cancer cells, candidates to target in cancer treatment or development of a cancer vaccine, human embryo-specific expressed genes were tested for their expression in a panel of human cancers [82]. The *Oct-4* gene was expressed in blastocysts and various cancer cell line cDNA's, but not expressed in fibroblasts. Processes occurring during tumorigenesis may be similar to

early developmental processes; both processes exhibit genome-wide demethylation, promoter hypermethylation and silencing of other genes [82].

The transcription factor, Oct-4 occupies a preeminent position of transcriptional regulator of stem cell fate. Understanding the molecular basis of the pluripotent phenotype is critical to studies to isolate and propagate stem cells from humans [15]. Elucidation of the mechanisms that govern the cellular signaling will provide a paradigm for understanding tissue differentiation and growth control in later stages of development [15]. Maintaining *Oct-4* expression within a certain level appears to be critical for stem-cell renewal. Future experiments focusing on the Oct-4 protein expression and repression are necessary to establish the biological functions of the gene in mammalian embryos.

Protein Transduction

Cells are designed to exclude invaders, while the AIDS virus HIV transactivating factor of transcription (TAT) protein passes through the cellular membrane and has recently been synthetically mimicked in the laboratory for drug delivery. Just one part of the HIV molecule is responsible for the ability to cross the membrane. Paul Wender of Stanford University, California has studied these cell-smuggling feats and has synthesized 'peptoid' molecules that mimic this portion of the TAT molecule [83]. The basic domain $TAT_{49—57}$ (RKKRRQRRR) was the template for a series of analogues. The cellular uptake of the fusion protein into Jurkat cells was determined by flow cytometry. Work on protease resistent transporters are being studied for drug delivery, while at

present, a nona-peptide of high arginine content is primarily responsible for the cellular uptake of $TAT_{49—57}$ [83, 84].

The ability to introduce full-length proteins in a concentration-dependent fashion would alleviate the technological problems found in transfection or viral introduction of cDNA expression vectors (overexpression, broad intracellular concentration ranges, low percentage of cells targeted) [29, 30]. Antisense approaches also have both specific gene and cell-type restrictions. Protein transduction is a highly efficient method of infusing proteins into cells. Often called protein therapy, it is an alternative to gene therapy. Rather than giving deficient cells the gene to make a missing protein, protein transduction is the science of the delivery of the protein directly into the cell.

Three Common Transduction Vehicles Described

Protein transduction efficiency rests on the identification of domains in the protein that confer the ability to enter the cell and even the nucleus. The three most studied domains include the Drosophila antennapedia peptide, the herpes simplex virus VP22 protein and the HIV TAT protein [23, 27, 30, 85]. The antennapedia family of proteins recognize and bind DNA through a sixty amino acid region arranged in three α-helical sequences, called the homeodomain, AntpHD [23, 85]. Of interest is the third helix of the homeodomain, with sixteen amino acids, which can also move small molecules into living cells, the AntpHD peptide. The herpes simplex virus type 1 (HSV-1) VP22 protein forms a portion of the viral tegument between the envelope and capsid regions of the virion [23]. VP22 has been shown to introduce large proteins into various cells, and direct cellular uptake of the protein has been shown. The TAT protein,

encoded by the HIV, is a regulatory protein which trans-activates genes that are expressed from the HIV long terminal repeat (LTR) [36]. Currently, the most efficient PTDs at transduction include residues 47-57 of TAT, the third alpha helix (residues 43-58) of ANTP and 267-300 residues of VP22 [26]. Each PTD section listed has a great percentage of basic amino acids (arginine and lysine). Similar to the HIV TAT protein, the high arginine and lysine content of the AntpHD peptide supports the "inverted micelle" hypothesis of movement across the plasma membrane. While the mechanism of transduction across a lipid bilayer is unknown, it is clear that transduction doesn't occur with the classical receptor-, transporter- or classical endosome-mediated fashion [23, 30, 86]. Transduction into cells is a rapid, concentration-dependent process that targets the cells in a receptor independent fashion [29, 30, 87-89].

The TAT Protein History

The TAT protein is a promising vehicle to move proteins into cells. A product of the HIV regulatory gene, the TAT protein is 86 amino acids long. Made by transcription of the viral genome after it has been integrated into the host cell chromosomes, it normally attaches to the LTR region of the viral genome inside the nucleus and increases the transcription of the HIV genes. Green and Frankel, in 1988, independently discovered the HIV TAT protein's ability to cross cell membranes and trans-activate the HIV promoter [35, 36]. Alan Frankel and Carl Pabo discovered that the HIV-1 purified protein could be taken up by cells in culture and could trans-activate the viral promoter [35]. The TAT protein found in HIV, is a regulatory protein not found in other retroviruses. TAT trans-activates the HIV LTR and is essential for the viral replication *in*

vitro [35]. Frankel found that as little as 100 ng of the protein could cause trans-activation and the dose response was linear [35]. TAT protein produced in bacteria is active when introduced into mammalian cells [35, 86]. The TAT-responsive element (TAR) is a 60-80 nucleotide sequence at the 5' end of the viral RNA [36]. Green and Loewenstein, in 1988, synthesized amino acid mutant TAT peptides to establish the essentiality of functional domains of the protein on TAR [36]. Transactivation was specific to the TAT peptide [36]. Green suggested four regions, small domains, of the TAT protein affect LTR trans-activation autonomously. The 86 amino acid HIV-TAT protein contained a putative 11 amino-acid (residues 38-48) that was identified as the TAT activation domain [36]. HeLa cells were transfected with plasmids with various constructs to compare the control, TAT-only plasmid with various deletion plasmids and complete plasmids [36]. Mutant peptides of simply 21 to 41 amino acids of the protein exhibited significant activity. Green and Loewenstein found that only two regions were necessary for transactivation; these regions were described as an activation domain and a nucleic acid binding domain [36]. Data suggested that the basic amino acid region was essential for transactivation; substituting three of the basic amino acids with alanine eliminated most activity. The candidate nucleic acid binding domain and the TAT activation domain were named by Green and Loewenstein in 1988 [36].

Fawell, in 1994 showed that chemically cross-linking a 36-amino acid domain of TAT (residues 37-72) to four diverse heterologous proteins conferred the ability to transduce the proteins into cells [30, 35-37, 86]. It was reported that exogenously added TAT protein could be chemically cross-linked to peptides and delivered into cells in culture and *in vivo* tissues in mice. The possibility of TAT-mediated uptake for

therapeutic delivery of macromolecules was evident [37]. TAT peptides conjugated to the proteins were delivery independent of cell types [29, 37]. Using a chimeric protein with β-galactosidase-TAT, chemically crosslinked conjugates of the enzyme with either TAT-(1-72) or TAT-(37-72) were compared. TAT-(37-72) was consistently the most successful to retain essential full enzymatic activity, *in vitro* [37]. Mice injected intravenously with the 36-amino acid domain of TAT to heterologous proteins via the tail vein and subsequent histological staining showed high tissue-associated activity in the liver, spleen and heart [37].

Specific TAT Details

The HIV TAT is an 86 amino acid protein made from exons of 72 and 14 amino acids [23]. In infected cells, the TAT protein is one of the first viral products to be produced after the viral genome has been transcribed into DNA and integrated into the cell chromosomes. The TAT protein then passes back from the cytoplasm into the nucleus and attaches to the LTR region of the viral genome. This binding causes a marked increase in the rate of transcription of the HIV gene. This region of TAT that binds to the LTR is the same region responsible for the ability of the protein to transduce membranes [90]. Only eleven amino acids long, this region of the protein carries five arginines and three lysines, thus an exceptionally high positive charge in this basic region [90]. The most active region corresponds to aa 47-57 of TAT (YGRKKRRQRRR) and has a high net positive charge at physiological pH [23, 29]. A model of internalization is based on the formation of an inverted micelle; the positively charged peptide recruits membrane phospholipids which form a hydrophilic cavity and carries the protein to the

cytoplasm [23, 34]. The biological tool of TAT-fusion transduction presents the opportunity to treat intact living cells and gain access to the intracellular environment.

Specific pTAT-HA Details

A traditional full-length TAT fusion protein transduction method utilizes urea-denatured, shock-misfolded, genetic in-frame protein purification. Dr. Steven Dowdy of Washington University and Howard Hughes Medical Institute gave our lab the pTAT-HA bacterial expression vector. TAT-fusion proteins are constructed in an expression vector, pTAT/pTAT-HA. This vector contains an amino-terminal, in-frame 11 amino-acid, minimal transduction TAT domain. This vector also contains an ampicillin resistance marker, a T7 polymerase promoter, 6-histidine leader, glycine residues for free bond rotation, a hemagglutinin (HA) tag, and a polylinker or multiple cloning site [91-93].

Protein Transduction Domains as Biological Tools

Transduction is rapidly developing as a biological tool since Fawell demonstrated in 1994 that enzymes crosslinked to the PTD could transduce into cells [37]. The Antennapedia transduction molecules have been used to transduce antisense DNA [85]. The amyloid precursor protein (APP) is a transmembrane protein that is expressed by glial and neuronal cells and appears to have both a normal and pathological function. Amyloid βA4 peptide-containing deposits are found in Alzheimer's patients; while in normal tissue, the APP protein promotes neurite outgrowth and cell adhesion to substrate. Studies to determine the function of the APP molecule and aimed at blocking APP expression used a vector peptide to move APP antisense oligonucleotides inside the cell.

The AntpHD, the homeodomain of Antennapedia, linked to an APP antisense DNA could affect neurite outgrowth and decrease APP protein levels [85]. The decrease in APP neosynthesis provoked a distinct decrease in axon and dendrite outgrowth by embryonic cortical neurons developing *in vitro* [85]. DNA delivery by protein transduction regulated the cell transcription levels.

Steven Dowdy has shown that large proteins can be transduced into cells by attaching them to transcription factors [94]. Dowdy has developed the ability to transduce intermediate and large protein molecules (>5000 d) into cells by coupling them to the eleven residue PTD [94] . Dowdy is particularly interested in tumor-suppressor proteins, p16 and RB; the genetic pathway of these proteins is mutated in almost ninety percent of cancers [95]. Dowdy organized a team of investigators in a TAT study to include cancer research, the blood brain barrier and anti-HIV protein therapy. The following review of studies which include Lissy, Schwarze,Vocero-Akbani, Gius, Ezhevsky and Nagahara have all collaborated with Dr. Dowdy.

Nagahara and co-workers described a bacterial expression vector, pTAT-HA to produce genetic in-frame TAT full length fusion proteins [30]. Nagahara introduced the p27, a multifunctional, cyclin-dependent kinase inhibitor into Jurkat cells. The wild type transduction of the protein showed loss of Cdk2 kinase activity compared to the controls and arrested cells in the G_1 phase of the cell cycle in a dose-dependent trial. Transduction of this protein into human hepatocellular carcinoma cells induced cell scattering also. The production of energetically unstable, urea-denatured fusion proteins often found in bacterial inclusion bodies transduced inside 100% of the cells in a rapid concentration-dependent manner. The proteins refolded *in vivo* and retained known

biological activity [30]. Denatured proteins may transduce more efficiently into cells than low energetic, correctly folded proteins [30]. Once inside the cells, the protein may be correctly refolded by chaperones. Florescein FITC conjugated protein was added to the cell culture and then analyzed by fluorescence activated cell sorting (FACS) [30]. The TAT-p27-FITC protein transduced into ~100% of the cells, and achieved maximum intracellular concentration in less than ten minutes in a variety of cell types. The misfolded TAT-p27 protein resulted in a substantial G_1-phase cell-cycle arrest [30].

Another complex biological question was studied using the transduction of a full-length protein directly into cells by Ezhevsky and colleagues [87]. The cyclin-dependent kinase inhibitor, $p16^{INK4a}$ tumor suppressor gene negatively regulates cyclin complexes that phosphorylate the retinoblastoma tumor suppressor gene product (pRb). Inactivation of kinase inhibitors or pRb, and/or amplification of the cyclin complexes is found in many human malignancies; loss of negative regulation of G_1 phase cell cycling progression causes uncontrolled proliferation. Ezhevsky and co-workers transduced full length p16 kinase inhibitor proteins directly into cells to determine the cyclin complexes responsible for the pRB phosphorylation status with the transcription factors necessary for cell cycling [87]. When a TAT-p16 fusion protein was allowed to enter several cell types, it specifically bound to certain cyclin-dependent kinase complexes, prevented the pRb hypophosphorylation, and caused a G_1 specific cell-cycle arrest through hyperphosphorylation by activated cyclin E complexes [86, 87]. Bacterially produced wild-type TAT-p16 proteins of ~ 20 kDA efficiently transduced into 99% of cells and was able to bind to its cognate intracellular target [87]. Obviously, studies to restore

tumor suppressor function or to interfere with oncogenic pathways are an exciting aspect of this technology.

Yu and colleagues studied the roles of pRB and cyclin D kinases in melanocytes using a transducible TAT-p16^{INK4a} protein [96]. The major target of cyclin D:cdk4/6 kinase activity is believed to be the retinoblastoma tumor suppressor protein, and the current dogma of G_1 phase cell cycle regulation is alteration of the kinase activity in cancer that leads to the deregulated proliferation by the inactivated pRB. Injection of TAT-p16 was sufficient to block regeneration of the hair growth cycle in an *in vivo* hair follicle cycling mouse model [96].

Cell cycle regulatory mechanisms involved in receptor-mediated apoptosis has been studied by Lissy and co-workers [88]. These pathways may be involved in autoimmunity and malignancy. The results suggest that cell cycle regulation is integral in deciding cell fates in response to stimuli of peripheral negative selection and reestablishment of the immune context after an immune response [88]. Peripheral T cells must be able to activate their proteolytic caspases and DNA fragmentation after an immune response so that the patient doesn't suffer from an autoimmune-like syndrome. T cell receptor antigen induced death (AID) and the involvement of the cell cycle were studied. Since pRb is a negative regulator of the late G1 restriction point, Lissy *et al.* rescued the cells from AID by inactivating pRb through a TAT fusion protein that binds pRb [88].

Schwarz and colleagues and his associates fused a 120-kilodalton β-galactosidase protein to the TAT protein and determined the intraperitoneal delivery of the fusion protein to tissues in a mouse, including the brain. A 15-oligomer peptide was synthesized

containing the 11-amino acid TAT PTD, proceeded by an $NH_{2\text{-terminal}}$ fluorescein isothiocyanate (FITC)-Gly-Gly-Gly Gly motif that transduced into cells in culture and *in vivo* [97]. Murine blood, liver, kidney, heart and splenic cells showed an intracellular concentration of the transduced protein. The tissue samples were assayed by X-Gal staining and FACS transduction analysis [27]. Of particular interest is that all brain sections from the mice after ip injections of TAT-β-Gal showed strong activity, while the blood-brain barrier remained intact using the Evan's blue albumin test. [97].

An experimental anti-HIV protein therapy based on a transducible HIV protease-activated caspase-3 that causes apoptosis in HIV-infected cells, selectively was introduced by Vocero-Akbani [89]. Production of infectious viruses from HIV-infected cells, depends on an HIV protease for cleavage and maturation of viral structural proteins. Vocero-Akbani and co-workers engineered a modified caspase 3 protein, TAT-Casp3, with endogenous cleavage sites specifically activated by HIV protease in infected cells. The resulting apoptosis in infected cells would be coupled with the inactive zymogen Casp3 in uninfected cells [89]. In the HIV-infected cells, TAT-Casp3 becomes active by HIV protease, causing apoptosis. Caspase activates DNase which causes cell death. The 'Trojan horse' strategy depended on the substitution of endogenous cleavage sites for the HIV proteolytic cleavage sites. The TAT-Casp3 was activated by HIV protease in the infected cells, and apoptosis occurred. In the uninfected cells, the TAT-Casp3 remained in the inactive zymogen form. With the substitution of proteolytic cleavage sites, other pathogens encoding specific proteases could be targeted as evidenced by this landmark study of transduced TAT-fusion proteins fighting HIV [89].

Guis and colleagues were able to study the timing and duration of cyclin D complexes involved in phosphorylating pRB and the G_1 cell cycle progression [98]. By use of the $p16^{INK4a}$ fused with the TAT protein transduced into human keratinocytes, 100% of the cells were assayed for pRB phosphorylation and the kinetics of the cell cycle was studied. With this *in vivo* biochemical assay for pRb phosphorylation, entire cell populations were studied with precise timing intervals. It was determined that cyclin D activity is required for early G_1 phase progression and up to but not beyond the activation of cyclin E complexes inactivating hyperphosphorylation of pRb at the restriction point. Cyclin D complexes with activating hypophosphorylation of pRB in early G_1, were nonredundant with the cyclin E complexes in cell cycle progression [98].

Cu, Zn-superoxide dismutase (Cu,Zn-SOD) is an enzyme by which cells detoxify free radicals and protect themselves from damage of oxidative molecules [99]. Kwon and co-workers hypothesized that the TAT-SOD fusion protein could enter the membranes of HeLa cells and protect the cells from oxidative stress (determined through an addition of paraquat onto the cells) better than a control SOD-only protein [99]. This study compared the denatured TAT-SOD transduction rate to the native TAT-SOD and control SOD-only transduction rates. The scientists showed that unfolded proteins transduce at a greater rate than folded proteins. Also, through enzymatic studies, the group proved that transduced, unfolded proteins can regain their folded structure and restore their molecular functions. The confirmation of correct protein size was verified by both SDS-PAGE and Coomassie brilliant blue staining; the results demonstrated that TAT-SOD exhibited a protective function against oxidative stress [99].

TAT fusion proteins are powerful tools for the treatment of focal ischemia when delivered both before and after the ischemic insult; TAT fusion proteins may offer a future strategy in stroke therapy [100]. A glial line-derived neurotrophic factor (GDNF) and TAT fusion protein were intravenously applied either before or after intraluminal thread occlusion of the middle cerebral artery. Western blot analysis revealed a strong GDNF transduction with no transduction detectable in the control animals. The intravenous infusion of the fusion protein was able to transduce the blood brain barrier while requiring no surgical intervention. The TAT-GDNF prevented both apoptotic and necrotic injury after ischemia [100].

Snyder and co-workers reported of a transducible D-isomer RI-TATp53C' peptide that activated the p53 protein in cancer cells, but not in normal cells; TAT-mediated transduction may be a useful strategy for delivery of tumor suppressor molecules to malignant cells [101]. Mutation of genes in the p53 pathway is thought to be nearly universal in human cancer. In cancer cells, the p53C' peptide induces apoptosis by activating the wild-type p53 protein. Snyder and co-workers [101] synthesized a double inversion, thus RI (retro-inverso) D-peptide with the TAT PTD that represented a double inversion of the surface topology of the parental sidechains intact to stabilize the active peptide for *in vivo* application . This application often produces greater stability with increased potency. A single dose of the D-isomer peptide was sufficient to maintain a G_1 cell cycle arrest for greater than 7 days. Further studies indicated that the peptide induced a permanent growth arrest in the plated cells. In a terminal peritoneal carcinomatosis mouse model, the tumor-bearing mice lived on

average a greater than 6-fold increase in lifespan over mutant peptide- or vehicle-treated mice.

Possible Mechanisms of PTD Membrane Translocation

The exact mechanism of translocation of the proteins coupled to PTD has remained elusive. While fusing proteins to membrane-permeable PTDs is one of the main strategies for intracellular protein delivery, the membrane translocation properties have recently been questioned [102]. Studies in 2004 [101, 102] suggested that TAT-linked cargo is taken up by concentration-dependent, but receptor-independent, macropinocytosis.

Lundberg and colleagues [103] suggested that PTD membrane translocation was due to a fixation artifact and that PTDs were internalized by constitutive classical endocytosis. With the PTDs positively charged due to a high content of arginine or lysine residues, the positive charge mediates the electrostatic binding to the negatively charged nuclear DNA [103]. Lundberg also suggested that increased fluorescence verified through flow cytometry was due to cell surface adherence rather than actual translocation. While Lundberg also suggested the possibility of postfixation movement of proteins which would invalidate methods requiring fixation, the study did verify that several studies of PTD showed functional delivery such as $p16^{INK4a}$ [98] , $p27^{Kip1}$ [30], and an HIV protease activated caspase [89].

Ferrari and co-workers suggested that transduction did not occur in a fast and temperature-independent way as previously suggested but the internalization of the protein exploits a caveolar-mediated pathway that is inhibited at 4°C [104]. This

particular study also stressed the essential role of actin cytoskeletal elements in the displacement of TAT vesicles toward the nucleus. Caveolae are invaginated plasma membrane domains with the integral membrane protein caveolin-1 (Cav-1) involved with many endogenous cellular processes. Ferrari cites some evidence that the HIV-1 virus uses caveolae for transcytosis [104]. A TAT-EGFP with glutathione S-transferase was placed on cultured cells and the fluorescent signal was studied with laser irradiation. Also, when the cells were treated with heparin, no association of the protein with vesicle inclusions or cell membranes were detected; it was suggested that cellular heparin sulfates act as cellular receptors for anchorage of the fusion protein to the membrane. A positive marker of clathrin-mediated endocytosis did not colocalize with the fusion protein positive vesicles while a significant colocalization signal existed between the protein and a marker for caveolar endocytosis [104].

In February of 2004, Wadia and colleagues suggested that after an initial ionic cell-surface interaction, TAT-fusion proteins are internalized by a lipid raft-dependent macropinocytosis [102]. The transduction is independent of caveolar- and clathrin-mediated endocytosis and phagocytosis. This study group then enhanced the fusion protein by including a pH-sensitive peptide that allowed enhanced escape from the macropinosomes. The group removed cholesterol from the plasma membrane which would disrupt caveolae and macropinocytosis, both lipid raft-mediated endocytic pathways. Disruption of the cholesterol resulted in a dose-dependent inhibition of protein function. Several forms of endocytosis, including clathrin-, and caveolar- mediated endocytosis require dynamin GTPase activity to form vesicles. While expression of a dominant-negative mutant of dynamin blocked endocytic pathways, the blocked pathway

did not restrict the transduction of the protein into the cells. Also, treatment of the cells with macropinosome inhibitors resulted in dose-dependent reduction in transduction. An endosomal escape mechanism that takes advantage of the pH drop in mature endosomes involved the co-treatment of reporter cells (treated with macropinosome inhibitors) with the N-terminal region of the influenza virus hemagglutinin protein, a pH-sensitive fusogenic peptide that destabilizes lipid membranes at low pH [102]. The cotreatment (macropinosome inhibitors with the fusogenic peptide) resulted in a marked dose-dependent increase in functional transduced protein. The group concluded that the internalization of the fusion protein occurs through a lipid raft-dependent process that is exclusive of caveolar- and clathrin-mediated endocytosis [102].

Cationic PTD peptides with variable arginine residues entered cells exclusively through macropinocytosis, while no PTD peptide was found to enter at 4°C as previously reported [105]. This group designed an extensive washing system to remove any external cell surface bound PTD peptides to measure the transduction capabilities. Each time the cells were treated with the TAT peptide, the cells were treated with tyrpsin and heparin to remove all extracellular bound proteins. The cells were also treated with two selective inhibitors of macropinocytosis (cytochalasin D, an inhibitor of F-actin or EIPA, an inhibitor of the Na+/H+ exchange. The combination of trypsin and heparin treatment of the fusion protein/live cells at 4°C resulted in less than 5% association of the protein with the cells. It appears that little to no PTD peptide enters the cells at 4°C as previously reported. The cell surface cholesterol removal by β–cyclodextrin resulted in a dose-dependent inhibition of internalization. Both macropinosome inhibitors resulted in a dose-dependent reduction of the peptide uptake. Following the ionic interaction between

the positively charged fusion protein and the negatively charged cell surface proteoglycans, macropinocytosis is induced. These observations are consistent with a mechanism by which TAT-fusion proteins >30,000 Da and peptides (1000-5000 Da) enter cells by macropinocytosis [105].

Maternal to Zygotic Transition

The maternal to zygotic transition (MZT) is characterized by changes in both the origin and quantity of mRNA found in the developing embryo [106]. This period describes the change in control of embryonic development transferring from maternal stored transcripts to newly synthesized, embryonic-derived transcripts. Major activation of the embryonic genome at the MZT occurs during the porcine four-cell stage while in murine embryos the transition is at the two-cell stage. Bovine and ovine undergo the transition during the eight to sixteen cell stage [106-111], although some observations suggest that MZT starts as early as the two-cell stage in bovine embryos [111].

The cascade of events involved with MZT is gradual and complex. Murine maternal protein synthesis continues into the eight-cell stage while maternal mRNA degradation is triggered by meiotic maturation and is 90% completed in two-cell embryos [112]. Nothias and co-workers (1995) injected extrachromosomal plasmid DNA into the nuclei of murine oocytes and cleavage stage embryos and studied the endogenous gene expression with specific *cis*-acting regulatory sequences and *trans*-acting proteins in conjunction with the unique injected sequence expression [112]. Extrachromosomal DNA responds to the same molecular signals that regulate cellular DNA. The transition

from a one-cell to a two-cell murine embryo is marked by the appearance of chromatin-mediated repression that reduces the activity of any promoter. Chromatin-mediated repression can be overcome by enhancers; the repression ensures that genes are not expressed until the appropriate time in development when enhancers (positive factors) can relieve this repression. Position of nucleosomes in relation to DNA binding sites and histone acetylation determine the accessibility of the binding sites. Enhancers consist of transcription factor binding sites distal to the start site in either orientation upstream or downstream of the promoter while promoters consist of transcription factor binding sites located upstream and proximal to the transcription start site. Enhancers provide the means to impose tissue specificity on promoter activity; the enhancer stimulation of promoters is not observed until formation of a two-cell murine embryo. The ability to utilize enhancers does not appear until the two-cell embryo stage, and stimulation of murine promoters by an enhancer does not require a TATA box until cell differentiation is evident. Enhancer-mediated stimulation of TATA-less promoters allows for housekeeping gene expression early in development [112].

Porcine transition from maternal to embryonic control of development is a gradual event occurring during the third cell cycle or four-cell stage. The third cell cycle has a shortened G1 phase as DNA synthesis (S phase) begins within the first two hours after cleavage to the four-cell stage. The S phase is completed at 16 h after cleavage and the prolonged G2 phase results in a 50-hour cell cycle. Proteins derived from embryonic transcripts appear at 16 hours and, in particular, at 24 hours after cleavage. Embryonic protein synthesis is necessary for the down regulation of the maternally derived translation products and is essential for further embryonic development [109].

The major transcriptional activation often occurs in parallel with nucleolar formation evidenced through the transcription of ribosomal RNA genes. In swine embryos, functional ribosome-synthesizing nucleoli become recognizable toward the end of the third post-fertilization cell cycle (four-cell stage); localization of proteins to the nucleolar anlage is apparently completed at the onset of the fourth cell cycle [113-115]. Development of the nucleolus may serve as an indirect marker of embryonic genome activation through the three main ultrastructual components: fibrillar centers, dense fibrillar components and the granular component. The recent biosynthesis model of nucleolar formation includes: a fibrillar center with the transcriptional enzymatic apparatus; primary unprocessed transcripts in the dense fibrillar component; and the processed transcripts in the granular component. First signs of development of fibrillar centers in porcine embryonic nucleoli are displayed toward the end of the third cell cycle. At 20 and 30 hours after cleavage to the four-cell stage, different stages of nucleolar formation are evidenced which include fibrillar centers (FC), and dense fibrillar and granular components (DFC and GC, respectively). The nucleolus consist of the rRNA genes and their transcripts including all the proteins that play roles in rRNA transcription and processing [113-115]. Also, antibody labeling patterns used against six important nucleolar proteins are compatible with the formation of the fibrillo-granular nucleoli toward the end of the third cell cycle [109]. Embryonic nucleologenesis in the porcine embryo with FCs, DFC, and GC on the nucleolar anlage was more similar morphologically to murine embryo nucleologenesis than in the bovine embryo [113].

Bjerregaard and colleagues demonstrated that development of embryonic nucleoli requires *de novo* mRNA transcription [108]. Some of the key nucleolar proteins involved

in development of embryonic nucleoli are described as: RNA Pol I, polymerase bound to the rRNA; the RNA Pol I associated factor PAF53, polymerase association factor involved in the formation of the initiation complex at the promoter by mediating the interation between Pol 1 and UBF (upstream binding factor) for the active rRNA synthesis; and UBF which binds the RNA Pol I to the rRNA thereby activating actual transcription. These proteins are transcribed *de novo* as shown by specific inhibition with α-amantin on controls [108]. Bjerregaard and co-workers used the expression of these proteins to study the quality of porcine embryos [108].

In another study of porcine embryonic development, message levels of the cell cycle controller cdc25c during the MZT were studied in four-cell *in vivo*- and *in vitro*-derived porcine embryos. Quantitative reverse transcription-competitive polymerase chain reaction (RT-cPCR) measured the maternal and embryonic derived cdc25c transcripts. The essential positive regulator of mitotic entry, cdc25c, message post-4-cell cleavage (P4CC) shifted to embryo derived message production between 10- and 18-hour P4CC. The shift to embryonic cdc25c message was accompanied by degradation of the maternal transcripts [106].

Murine Implantation and Placentation

Implantation and development of the placenta occur in a stepwise manner with most of the major roadblocks to development in utero occuring during the major transitions in the development of the placenta [116, 117]. Initial developmental decisions in the mammal involve formation of three extraembryonic lineages that are precursors to

the placenta. First, trophoblast cells form the specialized epithelial cells of the placenta, and then the endodermal and mesodermal components of the placenta arise from the ICM cells. The first differentiation event occurs with the formation of the TE on the outside of the morula, still enclosed within the zona pellucida at murine day 3.5; this produces the blastocyst. Polar murine TE that overlie the ICM continue to proliferate, while the cells away from the ICM stop dividing and become primary trophoblast giant cells [116]. The transition from TE to trophoblast includes morphologic and behavioral transformations [118]. The trophoblast giant cells in mice such as the cytotrophoblast cells in humans regulate maternal physiological processes through the production of hormones [117]. Both implantation and early vasculogenesis are mediated by the trophoblast giant cells with the transformation of the TE into invasive trophoblast [118].

Implantation in the mouse occurs soon after the blastocyst hatches from the zona pellucida at day 4.5. Within a few hours of this implantation event, the murine decidual response, the transepithelial invasion of the trophoblasts and the apoptosis of the uterine epithelium occurs [116]. While the uterus undergoes developmental changes during preimplantation by action of the ovarian estrogen and progesterone from the follicles and corpora lutea respectively, a second surge of estrogen from the follicles induces implantation. An “exquisite synchrony” between the maternal cells and the blastocyst is required during implantation [116]. MUC-1 integral membrane protein expressed on the murine uterine epithelium is down-regulated; this possible barrier to blastocyst adhesion is removed. Ablation of the second surge of estrogen prevents attachment and the blastocysts may remain in diapause as long as 30 days before a single injection of estrogen will cause implantation [116].

In response to the estrogen, the uterine epithelium secretes cytokines such as epidermal growth factor (EGF) and leukemia inhibitory factor (LIF) [116]. EGF receptors (EGF-R) are also expressed on the TE of the murine conceptus. Implantation depends on maternal events to open the "window for implantation" but also on secondary events triggered by the blastocyst [116]. Blastocyst production of interleukin-1β (IL-1β) appears necessary for implantation.

Specific integrins binding to their extracellular matrix ligands mediate the binding of the trophoblasts to the murine uterine epithelium. Laminin receptors are up-regulated as uterine glycosaminoglycans such as chondroitin sulfate and hyaluronic acid participate in adhesion with the murine blastocyst [116].

The murine decidual response to the implanting embryo includes an initial, acute inflammatory response with the production of proinflammatory cytokines and a proliferation of a thickened uterine wall. Large numbers of macrophages and lymphocytes proliferate and exhibit a reduced alloreactivity. The pregnancy paradox is that the placenta, a semi-allograft of fetal tissue avoids maternal immune rejection [116, 119]. The TE forms the ectoplacental cone and trophoblast giant cells outside the placenta form the interface with the maternal cells [116]. The ectoplacental cone contains proliferating cells that supply the differentiating trophoblast giant cells [118]. Mouse trophoblast cells invade primarily by directed phagocytosis of apoptotic decidual cells [118]. In rodents, as in primates, trophoblasts are invasive making maternal blood in direct contact with the trophoblasts (hemochorial placentation).

The act of mating in rodents causes pulsatile prolactin release from the pituitary that sustains progesterone production; mating a nonfertile male induces pseudopregnancy

in a rodent. The trophoblasts produce prolactin-like hormones in the rodent, while the porcine antiluteolytic agent is estrogen and in ruminants the active factor is interferon-τ (IFN-τ) [116]. The embryonic secretory signals that sustain the function of the corpus luteum, is described as the maternal recognition of pregnancy [119].

Blastomeres of the four-cell morulae can each give rise to a mouse, while early eight-cell stage blastomeres cannot generate a mouse by themselves [120]. With cleavage to the 16-cell stage, a gradual restriction in the developmental potency of the cells exists due to the production of the TE and the ICM lineages [120]. The murine fully expanded blastocyst contains about 64 cells with approximately 20 in the ICM. During the fifth day of development, the blastocyst hatches from the zona and is ready for implantation [120].

Porcine Early Embryonic Development

Porcine embryonic development through morphogenesis has been documented since the late 1800's [121]. After fertilization in most mammals, the zygote undergoes several cleavage divisions; it compacts and then cavitates to form the blastocyst, and finally the blastocyst hatches. These early events are collectively called preattachement embryogenesis [122]. The first cleavage of the fertilized egg is usually accomplished within 3.5 hours following copulation in the pig. Blastocyst formation with fluid accumulation and morphological specialization of the trophoblast is described at the sixteen-cell stage. Inner cell masses have been photographed with 30 or more cells at the day four stage. By day 7 after copulation, the porcine trophoblast is growing and the zona pellucida, a mucopolysaccharide coat, disappears [123, 124]. The 0.2 to 0.3 mm

diameter egg contains a bilaminar blastocyst, while the 0.6 mm cell demonstrates an inner-cell mass that is sharply marked off from the overlying trophoblastic cells (referred to as Rauber's layer) [121].

Porcine Peri-implantation

Porcine peri-implantation development is marked by a rapid remodeling and elongation of the trophoblastic membrane. Generally, porcine conceptuses have a spherical morphology with diameters ranging from 0.3 to 8.0 mm on days 8, 9 and 10, respectively. Spherical blastocysts are bilaminar, with an external layer of TE cells and an inner layer of hypoblast cells [124]. The spherical blastocyst is transformed, over a period of 1 or 2 days, into a long thread of minute diameter, passing rapidly through a spherical, then oblong and finally filamentous shape accompanied by a rapid reduction in diameter [123]. These changes in spherical to tubular to filamentous forms occur between day 10 and 12 of pregnancy [121, 125, 126]. At day 10 or 11, the spherical conceptuses grow approximately 0.25 mm /hour in diameter up to 9 mm, followed by a faster increase in length of 30-45 mm /hour in the rapid transformation to tubular and filamentous stage [125]. The onset of blastocyst elongation occurs through changes in cellular organization rather than cellular hyperplasia, and the transition from spherical to tubular to filamentous results in a flattening of TE cells and an increase in microvilli [125].

Successful epitheliochorial placentation in pigs is dependent on rapid conceptus expansion throughout the uterine horns and release of estrogen, the "maternal recognition of pregnancy" to maintain the corpora lutea [127]. However, spherical as well as tubular and early filamentous conceptuses can be found within the same litter on day 11 [124]. A

large amount of variation exists in stage of conceptus development with day post coitus, therefore, often the data are analyzed with conceptus size within the uterine horn [128]. Following rapid expansion of the TE on day twelve of pregnancy, porcine conceptuses initiate attachment to the uterine lumenal surface. The rapid remodeling and elongation of the trophoblastic membrane within the uterine horns determine success of the epitheliochorial placentation [127]. Initial trophoblast attachment to the uterine surface begins on day thirteen of pregnancy with interdigitation of uterine surface and trophoblast occurring on day 15 and 16 [125, 129].

The uterine lumen mucosal surface is greatly folded, and the conceptus may attain a length of a meter or more while occupying only 20-30 cm of uterine horn [123]. Continuance of pregnancy beyond the duration of the estrous cycle depends on the fetal occupancy of the whole length of the uterine horns. In 1981, it was suggested by Perry and colleagues that this occupancy probably prevents the production of a prostaglandin which in the non-pregnant animal causes the corpora lutea to regress and stop the production of progesterone [123].

Integration describes the bringing together of cells in the right place at the right time with the control of their changing positional relations and the regulation of all histogenetic changes and functional activities; understanding the operation of the controlling factors is a fascinating challenge to experimental embryology [130]. Genes for steroidogenic enzymes, extracellular matrix receptors, estrogen receptors, growth factors and their receptors, as well as retinoic acid receptors are expressed during elongation in the pig [109].

Temporal associations with the developing conceptus within the uterine porcine lumen include ions, proteins, and enzymes produced by both the conceptus and endometrium. During elongation of the TE and differentiation of the conceptus, development is controlled by synchronized gene expression patterns. Conceptus synthesis of steroids and proteins may interact in a paracrine and/or autocrine fashion with the endometrium to prepare the uterine histotroph for trophoblastic elongation [131]. Mammalian uteri contain endometrial glands that secrete histotroph, which nourishes the conceptus, and produces pregnancy recognition signals, immunoprotection, attachment, implantation and placentation [132]. The histotroph includes enzymes, growth factors, cytokines, lymphokines, hormones and transport proteins [132]. A survey of the porcine uterine microenvironment with information gathered from some rabbit and bovine studies reviews the molecular biology foundation of this study.

Attachment of the conceptus to the uterine surface in polytocous species is of importance due to similarity of uterine environmental issues. Differentially expressed genes, specifically at the implantation sites in the rabbit endometrium were identified through subtraction/suppressive hybridization. Expression for particular genes is specific for epithelial cells at the implantation sites and is not detected in non-implant-site endometrium. Genes induced by the embryo, specifically at the implantation site are of particular importance to the success of pregnancy. Cell-surface proteins, including integrins and sulfated oligosaccharide selectin ligands, may function in the initial attachment of the embryo [133].

In domestic animals, the prereceptive stage describes the period between blastocyst hatching from the zona pellucida and conceptus attachment to the uterus.

Domestic animals have a prolonged preimplantation period characterized by migration of the embryo, spacing of the embryos, endometrial gland secretion and generation of the conceptus signal for maternal recognition of pregnancy [119]. The prereceptive, nonadhesive stage of the porcine uterus detects Muc-1 as a candidate for maintenance of the prereceptive state. Muc-1 staining is detected in day 0 pregnant gilts but was absent by day 10 [129]. The prereceptive uterine epithelial cells exhibit the apical glycocalyx of Muc-1, a glycosylated integral transmembrane glycoprotein, and the expression of Muc-1 was down-regulation during the implantation window. Porcine conceptuses are unattached in the uterus for almost a week from hatching at approximately day six to attachment on day thirteen [129]. Porcine trophoblast cells do not penetrate the uterine epithelium, but maintain an apical-apical cellular union throughout the implantation process [119]. Bowen also detected the presence of two extracellular matrix proteins, fibronectin and vitronectin (found in the uterine epithelium and conceptus TE) and four specific integrin heterodimers (found in the porcine conceptus TE) on day 11 to 15 of pregnancy [119]. Integrins are adhesion molecules implicated in the attachment of the conceptus to the uterine epithelium. Conceptus TE and uterine epithelium in pigs express integrins and these heterodimers can bind to the fibronectin and/or vitronectin matrix molecules [119]. Integrin β-1 was detected in spherical, tubular and filamentous conceptuses studied by Yelich and co-workers [134]. The integrin receptor-ligand complex spans the cell membrane and may have an important role in restructuring of the TE during elongation. Integrins serve as receptors for laminins and fibronectins: the integrin receptor-ligand complex spans the cell membrane and unites the extracellular matrix with the cytoskeleton [131, 134]. Together, these matrix molecules and integrin

heterodimers are available for supporting implantation during the window of implantation or period of recognition of pregnancy [129].

Between day 11 and 12, estrogen production by porcine conceptuses is initiated, which is the "signal" for maternal recognition of pregnancy [128, 135, 136]. Spherical conceptuses measuring 9-10 mm produce estrogens as compared to little or no detectable estrogen production by conceptuses that measure 2-4 mm [128]. Estrogen synthesis involves two key cytochrome enzymes: P450 17α-hydroxylase ($P450_{17\alpha}$) and aromatase ($P450_{arom}$). The gene expression pattern of both of these cytochrome enzymes increases just before elongation [127]. Day 10 to 12 of porcine pregnancy include several events critical for embryonic survival and maternal recognition of pregnancy. These factors are: rapid trophoblastic elongation, conceptus attachment to the uterine epithelium and inhibition of maternal immune rejection [127]. The porcine conceptuses provide the estrogen signal that prevents the decline of progesterone production to block regression of the corpus luteum (CL) on day 11 of pregnancy [119]. During normal cyclicity of the sow, prostaglandin $F_{2\alpha}$ ($PGF_{2\alpha}$) from the uterine endometrium provides the luteolytic stimulus that causes regression of the CL. During pregnancy, the conceptus and uterus secrete prostaglandin E (PGE) which has been shown to block the luteolytic $PGF_{2\alpha}$ effects [119]. Porcine embryonic estrogens are paracrine effectors of uterine secretion and exhibit an antiluteolytic signal that allows for the continued progesterone production by the corpora lutea to initiate and maintain pregnancy [137].

A known regulator of uterine IGF-I (insulin-like growth factor-I) secretion is estrogen, which is produced by porcine pre-implantation embryos. Ko and colleagues (1994) examined the conceptus steroidogenic enzyme gene, aromatase cytochrome P450

mRNA and protein with uterine concentrations of IGF-I [138]. Maximal concentrations of IGF-I at day 12 of porcine development parallel the relative higher levels of aromatase P450 protein in the conceptus. The growth factor, IGF-I, controlled by conceptus estrogen appeared critical to the uterine receptivity for embryonic implantation. Uterine IGF-I molecules modulate the embryonic functional expression of estrogen which, in turn, could modulate endometrial preparation of the uterus for implantation [138].

The estrogen biosynthetic capability in the perimplantation porcine conceptus is transient, coincides with trophoblast elongation, and is temporally associated with the maximal uterine release of insulin-like growth factor (IGF-I) into the uterine lumen [137]. The potential regulation by uterine IGF-I of the conceptus $P450_{17\alpha}$ and $P450_{arom}$ was studied through the *in vitro* addition of IGF-I to day twelve filamentous and spherical morphologies. Filamentous conceptuses exhibited increased amounts of $P450_{arom}$ mRNA and contrasted with decreased levels of $P450_{arom}$ mRNA in the spherical conceptuses. Thus, the complex biochemical dialogue between the endometrium and conceptus possibly involves the regulation of embryonic steroidogenesis through IGF-I [137].

Geisert and co-workers suggested that the appearance of uteroferrin was associated with the initiation of conceptus estrogen synthesis on day 12, while, estrogen later suppresses synthesis and/or secretion of uteroferrin, a progesterone-induced glycoprotein by day 14 [128]. Uteroferrin plays a role in iron transport throughout pregnancy, and may serve as a hematopoietic stem cell (HSC) growth factor during early development of the conceptus [127].

Increased estrogen content of uterine flushings occurred when conceptuses reached approximately 10 mm which corresponds to the late spherical stage at about day 11.5 of pregnancy [139]. The conceptus estrogens may stimulate the release of free calcium from the uterine epithelium with a subsequent increase in prostaglandin production and a release of secretory proteins into the uterine lumen [128]. Estrogen content increased almost 4-fold in flushings containing tubular compared to spherical conceptuses**.** Calcium, prostaglandin F and prostaglandin E_2 increased in association with the release of estrogen [128]. The calcium content had declined by day fourteen while the PGF and PGE_2 continued to increase to day fourteen. The estrogen-conceptus local effect would allow for maintenance of the corpora lutea, establishment of pregnancy and conceptus nourishment [128, 139]. Transmission electron microscopy also revealed a synchronized release of secretory vesicles from the glandular epithelium with the formation of tubular conceptuses and onset of conceptus estrogen production [128, 139]. It is postulated that the porcine estrogens stimulate uterine epithelial cell secretion through calcium mediated events and that an increase in prostaglandins cause calcium activation of phospholipase A2 and subsequently the arachidonic acid cascade [139]. This release of material from the glandular epithelium parallels a flattening of the surface epithelium (TE cells) observed by scanning electron microscopy. This flattening could increase the endometrial surface area between day twelve and eighteen of pregnancy [128]. It has been suggested that conceptus elongation may be essential to the establishment of pregnancy by increasing the uterine luminal surface area [125].

Yelich and co-workers [134] used RT-PCR to study a series of developmentally important proteins in individual pig embryos during day ten to twelve of preimplantation

development. Conceptuses having 2 to 4, 5, 6, 7, 8, 9, and 10 to 12 mm spherical, 13 to 25 mm tubular, and >100 mm filamentous morphologies were studied. The initial 17-alpha-hydroxylase was detected in early spherical conceptuses of 2-4 mm and increased through to the 7 mm conceptuses, while the aromatase gene expression increased in 6 to 7 mm conceptuses with the increased expression throughout development. The 8 mm spherical conceptuses, therefore, appear to be fully activated by 17α-hydroxylase and aromatase gene transcription to produce the increased amounts of estradiol needed for recognition of pregnancy. Initial expression of brachyury in the 6 mm conceptuses precedes the initial detection of 10 mm conceptus mesodermal outgrowth [134]. Leukemia inhibitory factor (LIF) is one of the most notable cytokines secreted by the porcine endometrium; LIF is a hematopoietic regulator involved in cellular differentiation and growth [134, 140]. LIF transcripts were detected in all stages of the conceptuses studied; leukemia inhibitory factor receptor (LIFR) gene expression increased dramatically after the 5 to 7 day spherical conceptus stage and endometrial LIF gene expression was maximal on day 11 to12 [134]. The increase of LIFR prior to elongation may indicate a binding to LIF that appears to be necessary for implantation in the mouse and may play a role in trophoblastic membrane remodeling of the porcine conceptus [109, 134].

Embryonic development is extremely sensitive to vitamin A as both an excess and deficiency of the morphogen can lead to bovine abortion and embryonic malformation [110, 131, 134]. A disappearance of the bovine transcript for retinol-binding protein and nuclear retinoic acid receptors between the eight to sixteen-cell and the subsequent elevation at the morula stage or the initiation of embryonic transcription suggests that RA

is likely to directly regulate gene expression during bovine preimplantation development [110, 131, 141]. Retinol is believed to serve as a potent morphogen in vertebrate embryonic development. It has been proposed that retinol binding protein (RBP) binds retinol and is involved in the systemic and intercellular transport of the retinol from the plasma to its target cell. Retinol is oxidized by dehydrogenases to its active form, RA. Retinoic acid binds with two subgroups of nuclear receptors, nuclear RAR and RXRs, and their various isoforms. These receptors together with RA and other proteins form complexes with retinoic acid response elements, or enhancer elements, on the DNA molecule and exert transcriptional control [110, 131, 134, 142]. Yelich and colleagues detected transcripts for retinoic acid receptors in both day 12 spherical and tubular conceptuses [131]. Individual conceptuses were used for the RNA extraction and subsequent RT-PCR such that gene expression events could be detected within a 2 to 3 hour period of transition of trophoblastic elongation. A RBP peak occurs just prior to the 10mm stage of rapid trophoblastic remodeling and elongation, and another dramatic increase in RBP occurs with the tubular to filamentous morphology [110, 131, 134, 142, 143]. The presence of RBP in the TE certainly suggests that the retinoid system plays a role in trophoblastic remodeling. Retinol supplementation enhanced embryo survival in swine, and vitamin A administration to sows before ovulation enhanced embryonal survival [143]. Bovine whole mount *in situ* hybridization and RT-PCR detected three retinoid X receptors and retinaldehyde dehydrogenase 2. The simultaneous expression of these molecular players in the retinoid signaling pathway suggests that the early bovine embryo may be competent to regulate gene expression during preattachment development through retinoic acid signaling [143].

OPN is an extracellular matrix protein that binds integrins and promotes cellular attachment and communication. The use of *in situ* hybridization localized OPN messenger RNA to specific regions of the porcine uterine luminal epithelium (LE) on day 15 of pregnancy and to the entire LE thereafter. OPN mRNA expression was located in discrete regions of the uterine LE adjacent to the conceptus beginning on day 12, increasing by day 15, and then throughout the luminal epithelium surface by day 20 of pregnancy. It is speculated that OPN, expressed by the uterine epithelium may interact with integrin receptors on the conceptus and uterus to promote conceptus development and signaling between the tissues for attachment and placentation [144]. Integrins are transmembrane heterodimeric glycoprotein ligand receptors that are associated with the cytoskeleton and signaling [129, 144]. Specific integrin subunits are expressed by the luminal epithelium during the maternal recognition of pregnancy and are localized to implantation sites [129]. The OPN expression gives evidence to the speculation that a paracrine factor from the conceptus may be responsible for the LE production of OPN mRNA, and the OPN binds conceptus and uterine integrins to initiate functional intracellular signals [129, 132, 144]. OPN is a cytokine of the extracellular matrix and a component of the histotroph [132]. As a substrate for cleavage by matrix metalloproteinases, the OPN fragments initiate adhesion and migration [132, 145].

The inter-α-trypsin inhibitor family of serine protease inhibitors is composed of a combination of two heavy chains and the light-chain member, bikunin [146]. Bikunin inhibits trypsin, cathepsin G, elastase and plasmin and could assist in the regulation of porcine conceptus proteolysis of the uterine cellular surface [146]. Hettinger and colleagues compared the bikunin protein production during the estrous cycle and early

pregnancy and quantified the expression of bikunin mRNA in the porcine endometrium [146]. Protease inhibitors possibly protect the uterine epithelium from the proteolytic activity of developing porcine conceptuses. Other inhibitors of the porcine endometrium include plasmin/trypsin inhibitor and tissue inhibitors of metalloproteinases. A 30- to 100-fold increase in endometrial bikunin gene expression between day ten and eighteen of the estrous cycle and pregnancy corresponded with the detection of free bikunin in the uterine flushings and localization of bikunin mRNA in glandular epithelium [146].

Maintenance of the corpora lutea and facilitation of the placental attachment are involved in the establishment of pregnancy. During day ten to day fifteen, pregnant sows exhibited a 3-fold increased activity of the serine protease, kallikrein from low activity on day 10 [147, 148]. Kallikrein, a serine protease, may cleave inter-α-trypsin heavy chain 4 (IαIH4) and play a role in extracellular matrix stabilization [147-149]. The heavy chains of IαI family possess a von Willebrand type A domain that targets integrins, proteoglycans and heparin for adhesion [127, 147-149]. With the previously described reduction in Muc-I, the conceptus can interact with adhesion molecules such as integrins and proteoglycans. Cleavage of endometrial IαIH4 could permit conceptus trophoblast adhesion to the uterine epithelium during conceptus elongation [127].

Kallikrein is a member of the kininogen-kallikrein-kinin system in which kininogen is cleaved with the release of bradykinin, a vasoactive peptide, with bioactive properties that cause a release of calcium and conceptus prostaglandins and an increase in blood flow [148]. Kinins are vasoactive peptides known to be involved in the inflammatory-associated effects such as increased blood flow, tissue prostaglandin synthesis, and induction of smooth muscle contraction [150]. Thus, kallikrein could assist

with opening sites for conceptus attachment through the cleavage of IαIH4 molecules and providing vascular support for the conceptus.

Kallikrein is also related to the insulin-like growth factor (IGF) system. Insulin-like growth factor binding proteins (IGFBPs) were present in days one to ten of pregnant porcine uterine flushings but these binding proteins were not present in the pregnant uterine flushings from day 12 or 15. Insulin growth factors (IGF-1 and IGF-II) were two to three times greater on day 12 of pregnancy in contrast to cyclic gilts [151]. When incubated with protease inhibitors, IGFBPs indicated that cleavage through serine proteases such as kallikrein could release IGF-I and IGF-II. The presence of IGFBPs can affect the ability of IGF-I to interact with its receptors [151]. The period of conceptus elongation exhibits the greatest uterine luminal content of IGF-I, while Geisert and co-workers [151] indicated that the loss of the IGFBPs was probably regulated by progesterone-stimulated kallikrein activity and activation of matrix metalloproteinases.

Allen and colleagues suggested the importance of the inflammatory kallikrein-kinin system in porcine implantation through the increase in bradykinin in the porcine uterine lumen and alteration of endometrial bradykinin receptor expression during porcine placentation [150]. Endometrial bradykinin β_2 receptor mediates the majority of physiological effects of kinins. The study compared the bradykinin content in the porcine uterine lumen and the alteration of endometrial bradykinin receptor expression during early pregnancy and the estrous cycle**.** Bradykinin uterine flushing concentrations were 5-fold greater in pregnant gilts than in cyclic gilts on day 12 with an 8- to 10-fold greater increase for bradykinin in the pregnant gilts uterine flushings on day 15 and 18, respectively. A 6-fold increase in expression of the endometrial gene expression of

bradykinin β_2 receptor on days 12 to 15 of the estrous cycle and pregnancy was indicated when compared to day 5 and 10. With the estrogen receptors in the uterine endometrium and glandular epithelium of the pig showing abundance on day 10 and 12 of pregnancy, estrogen may play a regulatory role in the release of bradykinin from the porcine endometrium [150].

Analysis of differential gene expression during trophoblastic elongation (day eleven to twelve of gestation) from spherical, ovoid, tubular to filamentous stages indicates the events necessary for successful implantation and embryonic survival [126]. During this period, conceptus release of estrogen causes the maternal recognition of pregnancy with a simultaneous acute phase response. Recently, using suppression subtractive hybridization, S-adenosylhomocysteine hydrolase (SAHH) and heat shock cognate 70KD (HSC70) protein were shown to produce an expression increase of approximately 7-fold and 10-fold, respectively, from spherical to filamentous porcine conceptuses [126]. Ross and co-workers suggested that SAHH serves as a biological regulator of transmethylation reactions by reducing SAH (S-adenosylhomocysteine) to homocysteine. The release of a methyl group from s-adenosylmethionine (SAM), a universal methyl donor, creates S-adenosylhomocysteine (SAH), while maintaining the SAM/SAH ratio for transmethylation reactions to occur could be necessary for optimal porcine conceptus development. The HSC70 has been associated with neural tube development and cytoskeletal conceptus remodeling [126].

In gestating sows, the number of major MHC class II-expressing cells were reduced on day nineteen of gestation in the surface epithelium [152]. This could reflect a suppression of the immune response during the implantation period to prevent embryo

rejection. Immunomodulation of the MHC class II expressing cells indicate that the porcine trophoblast influences the endometrium required for porcine embryonic attachment and survival. The effects of pregnancy on the day 19 endometrium demonstrated a significant reduction in T cells, natural killer cells, and cytotoxic T cells in the surface epithelium, and with no T helper cells compared with earlier stages studied. The MHC class II expressing cell number was low. This indicates that the porcine embryos may initiate at this stage some processes to suppress the immune response in the surface epithelium [152].

The presence of elongating conceptuses within the uterine lumen of pigs correlates directly with increased uterine release of the enzyme cathepsin. Cathepsins are a class of lysosomal cysteine proteases. A dramatic increase in cathespin L activity and the immunoreactive, epithelial location on day 15 of pregnancy in the gilt and a decline on day 18, corresponds to the initial formation of the allantochorionic membrane during placental attachment [140]. While the function of cathepsins during conceptus attachment is unclear, Cathepsin L possibly serves as a modulator of invasion, with limited proteolysis of the epithelium in the species that has an endothelial-chorial type of placentation, or cathepsin may function to hydrolyse small peptides for subsequent conceptus uptake [140].

Porcine Endothelialchorial Placentation

A glycocalyx on both the maternal and fetal epithelium before close contact is established with day thirteen and fourteen post coitus endometrium, exhibit protruding epithelial proliferation which work to immobilize the conceptus and keep the maternal

and fetal sides together so that cell to cell contact will develop [153, 154]. Subsequently the trophoblastic and uterine epithelium become partly depleted of microvilli on day 14 with the appearance of development of interdigitating microvilli on day 15 and 16 [135, 153, 154]. The luminal uterine epithelium is changed from a columnar epithelium to a dome-like epithelium devoid of microvilli [119]. The trophoblast cells play an important role in the relationship between maternal tissues and the developing embryos in animal with prolonged pre-implantation stages [124]. Trophoblastic initial attachment to the uterine epithelium begins on day 13 of pregnancy with completion of the epitheliochorial placenta occurring on day 18 [125]. With growth and fluid expansion of the allantosis between days thirteen and eighteen of pregnancy the full apposition and adhesion of the maternal and conceptus TE occurs [146].

Formation of Chorion and Amnion

Soon after elongation, the first mesodermal cells appear from the ectoderm of the embryonic disc. The sheet of tissue formed increases in area and soon extends beyond the margins of the embryonic disc. The central portion will be incorporated into the developing embryo; the 'extra-embryonic' portion splits with one layer overlying the endoderm and the other layer underlying the ectoderm. The extra-embryonic coelom is formed this way. The outer layer of mesoderm is raised with the covering ectoderm around the embryonic disc [123]. The outer layer of mesoderm and the overlying trophoblast make up the chorion [123]. The two amniotic folds fuse above the embryonic disc; this forms the amnion, and is separated from the chorion [123]. The amnion forms

by folds in the extra-embryonic portion of the somatopleure; these folds rise up and surround the embryo at the periphery of the embryonic plate. This folding occurs before the first somites appear [121]. The allanto-chorion in the pig has an outer single layer of ectodermal trophoblastic cells while the endoderm is also single layered and lines the allantois; the intervening tissue is mesoderm and contains extra-embryonic blood vessels [123].

The porcine chorion grows up to 1.4 meters in length by day 17. From the 13th to 17th day post coitus (p.c.) in the pig, while the ectoderm of the embryonic disc has formed the neural tube and the beginnings of a nervous system, the mesoderm has formed somites (or beginnings of the muscle system and vertebrae) [121, 123]. The allanto-chorion provides nutrition and respiration for the developing embryo.

CHAPTER III

DETECTION OF *Oct-4* GENE EXPRESSION IN PORCINE CONCEPTUSES DURING PERI-IMPLANTATION DEVELOPMENT

Need for Improved Porcine Reproductive Technology

A major problem in porcine reproductive efficiency is that porcine prenatal mortality incidence ranges from 20% to 46% at term [109]. Most of the loss occurs before day twenty of gestation including the period between day 11 and 12, when the conceptus is undergoing rapid differentiation and expansion of the TE [125, 131, 134]. About 30% of porcine conceptuses are lost between days 12 and 15 of gestation [136]. An understanding of the sequential activation of the embryonic genome *in vivo* is crucial to optimize the different embryological techniques [109].

Efficiency of all pig NT embryos is low [109]. The efficiency of animal production by cloning is very low following somatic cell NT. Reprogramming of the donor nucleus must occur to produce an embryonic profile of gene expression needed for development to proceed [155]. Daniels and colleagues (2000) described a detailed analysis of developmentally important genes, including bovine *Oct-4* in granulosa cell nuclear transfer (GNT) embryos as compared to IVF-derived bovine embryos. Patterns of gene transcription in cDNA of granulosa cells and in IVF-derived preimplantation

embryos were established through RT-PCR. In IVF-derived embryos, Oct-4 transcripts were found with a high PCR intensity in the oocyte and decreased intensity as development progressed to the 8-cell stage and then increased again to the blastocyst stage. Presumably, the degradation of maternally inherited mRNA was followed by an onset of embryonic transcription. Transcripts of Oct-4 were not detected in granulosa cell cDNA, and the onset of transcription of *Oct-4* in GNT embryos compared with that in IVF embryos was a critical factor when assessing the effects of nuclear reprogramming in cloned embryos. The GNT embryos displayed a similar pattern to that detected in preimplantation embryos for the *Oct-4* gene [155]. Although the reprogramming of the somatic cell nucleus was sufficient to produce the proper *Oct-4* expression, several other genes, IL6 (Interleukin-6), FGF4 (Fibroblast Growth Factor 4), and FGFr2 (Fibroblast Growth Factor receptor 2) exhibited a delayed or lack of expression.

Need for Porcine Conceptus/Uterine Gene Expression Patterns

A better understanding of stage-specific gene expression patterns is necessary. It is presumed that successful preimplantation and early fetal development is reliant on the temporal and spatial gene expression of approximately 10,000 genes [156]. In order to get healthy cloned animals, the restoration to nuclear totipotency in differentiated somatic cells following nuclear transfer remains remarkable but inefficient and prone to epigenetic errors [157]. The degree of donor cell differentiation affects cloning efficiency. The cloning efficiencies with blastomere donors are approximately one order of magnitude higher than the somatic cells (35% versus 0.6% in mice) [157]. Transferred cloned embryos reconstructed from murine ES cells derived from embryonic blastomeres

produce a higher proportion of transferred cloned embryos than somatic cell clones (10-20% of ES cell derived embryos reached adulthood, compared with only 1-3% in somatic donor cells) [157]. ES cell derived blastocysts express key embryonic genes such as *Oct-4* [157]. Bortvin and colleagues [158] suggested that the failure to reactivate the full spectrum of *Oct-4* and *Oct-4*-related genes may contribute to the embryonic lethality found in somatic-cell clones. Included in the study were the following genes: *Prame/4* (PRAME-like 4), *Ndp52a* (Nuclear domain 10 protein 52-like1), *Dppa3* (Developmental pluripotency associated 3), and *Dppa4* (Developmental pluripotency associated 4) [158]. Therefore, it has been hypothesized that the limited developmental potency of certain cloned embryos is a result of incomplete reactivation of certain pluripotency genes; a similar theme of developmental potency has been studied regarding different porcine breeds and genetic expression patterns found in the uterine environment.

Meishan-Landrace sows with a larger litter size were compared with conventional Landrace sows; the two different porcine breeds were compared through suppression subtractive hybridization (SSH) [136]. The differential expression of the endometrium and the conceptuses following SSH and cloning, transforming, sequencing and BLAST searches were compared. 62% of the endometrial tissue clones and 78% of the conceptus library clones showed homology with known genes. Of the cDNA sequences found in the subtracted libraries, 38% derived from the endometrial tissue and 22 percent of conceptus origins were described as novel genes with sequences having no identity to any GenBank entries or corresponding to hypothetical proteins and repetitive DNA elements. It is surprising that such a large number of cDNA clones remain unrecognized with the exponential growth in the database in recent years [136]. Information gleaned through

expression profiling of embryonic cells and the uterine environment is critical to understanding cell differentiation.

Oct-4: A Master Regulator of Embryonic Transcription

Oct-4, a Class V of the POU transcription factor family exhibits conservation in protein sequence, genomic organization and chromosomal localization [43]. Bovine and humans share a 90.6% overall sequence identity at the protein level [42, 43]. Interestingly, human Oct-4 expression was found in the heart, kidney, liver, placenta, spleen and pancreatic islets using RT-PCR technology [40], while the actual protein and activity of that protein in these tissues hasn't been demonstrated. The *Oct-4* gene was localized to the sixth, seventeenth, and twenty-third chromosomes in the human, murine and bovine species, respectively [40, 42, 61].

While embryos of the mouse, pig and cow all progress through compaction, cavitation and expansion transitions with hatching and implantation, some differences of the preimplantation embryos are evident. Timing of the MZT occurs at the 2-cell, 4-cell, and 8-cell stages in murine, porcine and bovine embryos, respectively [141]. Cells within the early murine embryo respond to their relative positions on the inside or outside of the cellular aggregate and then differentiate along different lineages according to their positions. Early during the 8-cell stage, murine cells develop a stable axis of polarity based upon the cell-cell adhesion that mediates intercellular flattening. This cell polarization gives spatial heterogeneity to each blastomere and to the embryo itself [159]. The segregation of inner and outer cells in porcine morulae follows a different pattern

compared to mouse embryos. Porcine segregation of inner and outer cells is less strictly regulated and is perhaps a random process [160].

In the search for pluripotency molecular markers, Van Eijk and co-workers [42] isolated and evaluated the bovine ortholog of *POU5F1* and followed its expression during early embryonic development. The gene was localized through segregation analysis of a PCR product to the MHC on bovine chromosome 23. Immunocytochemical evaluation of the Oct-4 expression in bovine oocytes and embryos revealed expression in the nucleus and cytoplasm of all stages until day 10 of development. A marked nuclear localization of Oct-4 existed during segmentation but a more diffuse distribution of Oct-4 was expressed upon formation of the blastocoel. Oct-4 was not found in bovine conceptuses at day 14 and 16. With the expression of Oct-4 in the trophoblast cells, expression is thus not limited to pluripotent cells of the early bovine embryo [42].

Kirchhof and co-workers investigated the potential of individual blastomeres to express the Oct-4 protein using a construct consisting of selected parts of the upstream region of the murine *Oct-4* gene [43]. The construct, an 18-kb fragment, GOF18-ΔPE EGFP, contained a modified promoter with the PE removed. The genomic *Oct-4* fragment (GOF), included the GC-box, hormone response elements and the DE. An EGFP factor was inserted in frame and introduced in front of the ATG of the *Oct-4* gene; the EGFP served as a reporter. Pronuclei of bovine, murine and porcine zygotes were microinjected with the gene construct. Of significance is the timing of the activation of the embryonic genome (MZT) transition from maternal to zygotic control of transcription [141]. Therefore, murine cells were examined at day 3 and porcine and bovine cells examined on day 5, with day of microinjection and the beginning of *in vitro* culture

defined as day 1. Fluorescence of embryos, both before and after major activation of the embryonic genome was checked. After transfection, positive blastomere expression of fluorescence was contrary to expectation as fluorescence wasn't restricted to ICM cells but also seen in bovine and porcine TE cells. Mice, cattle and pigs exhibited fluorescence in their embryonic cells after the three species were microinjected with the murine upstream region. The fluorescence of all three species seems to indicate that all three species have similar control mechanisms for this promoter [43].

Kirchhof and co-workers also included whole mount immunocytochemistryon *in vivo*-derived bovine, murine and porcine blastocysts [43]. Polyclonal antibodies raised in rabbits against the Oct-4 protein were purified and applied to the blastocysts. Secondary goat anti-rabbit antibodies incubated in propidium iodide were applied to the blastocysts mounted on slides and analyzed using confocal scanning laser microscopy. With maturation of the murine blastocysts, Oct-4 protein disappeared from the TE and was restricted to the ICM. The protein was localized in all cases to the murine nucleus. Bovine and porcine embryos showed a very different immunostaining pattern. Oct-4 was revealed in the blastocyst ICM as well as in TE cells with signal in the cytoplasm as well as in the nuclei of these cells [43]. Porcine day ten and day eleven Oct-4 mRNA was detected by RT-T7 RNA-dependent amplification in both the TE and the primitive ectoderm cells [43, 161] .

The Need for Porcine Peri-implantation Gene Expression

Kirchhof hypothesized that the delayed downregulation of the *Oct-4* gene in large mammals may be the consequence of the lengthened period of preimplantation [43].

Observations of porcine conceptus expression on day 8 to 15, is an important window to study the down regulation of *Oct-4* expression [43].

Murine, porcine and bovine species exhibit great differences following blastulation. Murine embryos form an egg cylinder stage with hatching and implantation occurring more or less simultaneously, while the livestock germinal disc-stage embryos exhibit a delayed implantation [43]. Expansion of the murine blastocyst is relatively modest with mitosis occurring only among the TE cells overlying the ICM [43]. Contrastingly, porcine trophoblast cells continue to divide and expand by several orders of magnitude prior to implantation; bovine trophoblast expansion isn't quite as extensive as the porcine but does increase more than the murine trophoblastic cells [43]. Kirchhof and co-workers established the necessity to measure Oct-4 activity quantitatively as the mere presence of Oct-4 protein does not define pluripotency [43]. The porcine model has not been previously studied, and further experiments are needed to confirm porcine Oct-4 expression. Through Real Time RT-PCR we will characterize the expression of the *Oct-4* gene and compare the stage-specific gene expression during porcine preimplantation development.

Materials and Methods

Conceptus Collection

Research was conducted in accordance with and approval by the Oklahoma State University Institutional Animal Care and Use Committee. Cyclic, crossbred gilts (Animal Science Department, Oklahoma State University) were checked for estrus behavior twice daily (0700h and 1800h) in the presence of intact boars and were bred

naturally at the onset of estrus (day 0) and twelve hours later. Gilts were hysterectomized through midventral laparotomy on day 10, 12, 13, 15 and 17 as previously described [162]. Conceptuses were recovered in sterile Petri dishes and classified as spherical, tubular or filamentous morphologies; conceptus diameters were also recorded [163]. Identical morphologies were transferred to cryogenic vials (Fisher Scientific, Pittsburgh, PA) snap-frozen in liquid nitrogen and stored at -80°C.

RNA Isolation

Total RNA was isolated from pools of similar individual conceptuses using an RNA isolation reagent, RNAwiz (Ambion, Inc., Austin, Texas). Using 1 ml of RNAwiz for every 100 mg of tissue, the samples were disrupted in a Virtishear polytron homogenizer (Virtis Co. Inc., Gardiner, NY). The homogenate was incubated at RT for five minutes to dissociate the nucleoproteins from the nucleic acids. A 0.2X starting volume of chloroform was added to the homogenate and vortexed for ~ 20 seconds. Following incubation at RT for 10 minutes, the mixture was centrifuged at 14,000 X g for 25 minutes at 4°C. The aqueous phase was transferred into a clean, 1.0 ml RNase-free tube without disturbing the interphase. A 0.5X starting volume of RNase-free water (Epicentre, Madison, WI) was added and mixed well. A 1X starting volume of isopropanol was added, mixed and incubated at RT for 10 minutes. Following centrifugation at 10,000 x g for 45 minutes, the samples were placed in –20°C for 45 minutes and then 10 minutes in –80°C. Finally, the samples were incubated at RT for 10 minutes. The supernatant was decanted and the pellets vortexed with cold 75% ethanol. The samples were centrifuged at 10,000 X g for 5 minutes at –20°C. The supernatant

was discarded. The pellet was air dried and then the RNA resuspended in RNase-free water, DNase I, and DNase buffer for 30 minutes at 37°C followed by a 70°C to heat inactivate the DNase I. The RNA was quantified spectrophotometrically, and the purity of RNA was determined based on absorbance at the 260nm wavelength using the 260:280 (RNA light absorbance to protein light absorbance) ratio. The concentration of RNA in each sample was determined using the equation: A_{260} X 40 (dilution factor) X 50 (extinction coefficient) / 1000 = ng/ul. The RNA samples were diluted to 25 ng/ul with 5 ul of each sample used in subsequent manipulations. A total of 24 conceptus pools representing: 4, day 10; 6, day 12; 3, day 13; 7, day 15; and 4, day 17 morphologies were assembled.

Porcine Oct-4 Primer Construction and cDNA Synthesis

Preparation of the porcine Real Time primers involved several steps. The first Oct-4 primer sets used by our lab were derived from murine Oct-4 sequences shared in papers by Vassilieva and Pesce [3, 164]. The oligonucleotide sequences are Oct-4 forward 5'-GGCGTTCTCTTTGGAAAGGTGTTC-3' and the Oct-4 reverse is 5'-CTCGAACCACATCCTTCTCT-3' (prepared by Oklahoma State University Recombinant DNA/Protein Resource Facility, Stillwater, Oklahoma). These sequences were verified as complementary on the murine Oct-4 cDNA (accession X52437) and referenced by Scholer in *Nature* [6].

Porcine conceptuses, both oblong and spherical, were gathered at Oklahoma State University in Stillwater, Oklahoma and reverse transcribed according to the directions for Cells-to-cDNA Kit from Ambion (Ambion, Inc., Austin, Texas). The kit contains Cell

Lysis Buffer, DNase I, RT Buffer M-MLV Reverse Transcriptase, RNase Inhibitor, dNTP Mix, Random Decamers and Nuclease-free water. Basically, cells were treated with a cell lysis buffer, gently centrifuged and covered with RNase and protease free mineral oil (Sigma-Aldrich, St. Louis, MO) to prevent evaporation and then placed in a 70°C water bath for 10 minutes. DNase I is then added to the samples to rid each sample of genomic contamination and incubated at 37°C for 30 minutes. The DNase I is inactivated at 75°C for 5 minutes. The 20 ul reverse transcription reaction includes 6 ul of cell lysate RNA, 4 ul dNTP Mix, 2 ul Random Decamers (50 uM) and up to 16 ul Nuclease-free Water. The mixture is centrifuged gently and heated 3 minutes at 70°C. The cell mass is placed on ice for 1 minute, centrifuged briefly and then placed back on ice. Two microliters of 10X RT Buffer and 1 ul of M-MLV (Moloney Murine Leukemia Virus) Reverse Transcriptase and 1 ul of RNase Inhibitor are added, gently mixed and centrifuged. A control sample with no reverse transcriptase is always included to check for genomic contamination. The contents are incubated at 42°C for one hour and then the transcriptase enzyme is stopped with an incubation at 95°C for 10 minutes. The reaction is then stored at –20°C or used immediately. The 20.0 ul PCR reaction is gently mixed and includes 2.5 ul of the RT reaction, 0.2-1 uM final concentration of each primer and 12.5 ul of "D" FailSafe PCR 2X PreMix (Epicentre, Madison, WI) with 0.5 ul of FailSafe PCR Enzyme Mix. Thermocycler conditions are as follows: initial denaturation at 2 minutes, 94°C; cycling conditions with denaturation at 94°C for 30 seconds, annealing 55°C for 30 seconds and extension at 72°C for 30 seconds with a total of 35 cycles. The products are extended at 72°C for 5 minutes in the Perkin Elmer 9600 thermocycler (PE Biosystems, Foster City, CA). The murine primer sequences

(described above) were used as primers on the porcine mRNA. Through touch prep and QiaQuick PCR Purification Kit (Qiagen, Valencia, CA), the porcine DNA amplification products were purified. The DNA was spectrophotometrically quantified and sequenced using the PCR amplification primers described above (Oklahoma State University Recombinant DNA/Protein Resource Facility).

The chromatograms of the raw sequences of the reverse porcine and forward porcine sequences were aligned with the BioEdit (www.mbio.ncsu.edu/BioEdit/bioedit.html) biological sequence alignment editor and then a consensus sequence was derived from the two traces. The porcine sequence was then entered into the TIGR Gene Indices program (http://tigrblast.tigr.org/tgi/), and a BLASTN search was performed. An 89% homology was found with the *Sus scrofa* (TC58938) octamer-binding transcription factor 3. This particular sequence was then compared with sequences in NCBI (http://www.ncbi.nlm.nih.gov/) database and a high homology with *Bos taurus* POU domain (NM_174580.1) and *Sus scrofa* MHC class I (SSC251914) were found. We were interested in finding homologous sequences for bovine and porcine *Oct-4* to design one primers/probe set for both species. The (TC58938) TIGR sequence which was homologous to the bovine sequence, was then imported into the ABI 7700 software to design *Taq*Man primers and probe. A *Taq*Man probe specific for porcine *Oct-4* was designed to contain a fluorescent 5' reporter dye (6-FAM) and a 3'quencher dye (TAMRA). The *Oct-4* forward primer is 5'-TGGTCCGCGTGTGGTTCT-3' and the reverse primer 5'-TCGTTGCGAATAGTCACTGCTT-3' with the fluorescent-labeled *Oct-4* probe

5’CAACCGTCGCCAGAAGGGCAAAC[Tamra~Q] (prepared by Qiagen, Valencia, CA).

Quantitative, Real-Time, One-step RT-PCR

Using Qiagen QuantiTect Probe RT-PCR Kit (Qiagen; Valencia, CA), both reverse transcription and PCR take place in a single tube. The RT mix contains Omniscript and Sensiscript Reverse Transcriptases with a HotStarTaq DNA Polymerase that remains completely inactive during the reverse transcription reaction (Qiagen, Valencia, CA). Conceptus *Oct-4* gene expression was evaluated by Real Time Polymerase Chain Reaction using a fluorescent reporter and 5’ exonuclease assay system. The RT-PCR took place in an ABI PRISM 7700 Sequence Detection System (PE/Applied Biosystems, Foster City, CA). First, reverse transcription was allowed to proceed for 30 minutes for 50°C; since RNA cannot serve as a template for PCR, the first step is to reverse transcribe the RNA template into cDNA. Then, the DNA Polymerase is activated by a 15 minute 95°C incubation step; this step also inactivates the reverse transcriptase enzymes and therefore, temporally separates the reverse transcription from the PCR. The two-step cycling also includes an annealing/extension of 60 seconds at 60°C with 45 cycles, followed by a final extension at 72°C. The *Taq*Man Ribosomal 18S RNA internal control was supplied by PE/Applied Biosystems (Foster City, CA). This normalization control corrects for loading discrepancies. Fifty nanograms of total RNA were tested for each morphology studied.

Using the products from the Real Time RT-PCR, the amplification efficiencies of the target sequence was prepared by a 10X dilution series in sterile, nuclease-free water

(Epicentre, Madison, WI). Each dilution was amplified by RT-PCR. The C_T values of the target gene, *Oct-4* were subtracted from the C_T values of the internal control 18S. The plot of the difference in C_T values against the logarithm of the template resulted in a line with a slope <0.1 (Data not shown). Amplification efficiencies were therefore, comparable. Confirmation of target and normalization genes was collected with continuous fluorescent data acquisition of the melting curve graph.

Relative Quantitation of *Oct-4* Expression

Gene expression was quantitated by the determination of the threshold cycle (C_T) number of the FAM fluorescence within the geometric region of the semi-log plot generated during Real Time PCR. Within the geometric region of the amplification curve, each difference of one cycle is equivalent to a doubling of the amplified product of the PCR. The relative quantitation of *Oct-4* expression across conceptus morphologies was evaluated using the comparative C_T method [165-167]. The ΔC_T value was determined by subtracting the ribosomal 18S C_T value for each sample from the Oct-4 C_T value of that sample. Calculation of the $\Delta\Delta C_T$ value is achieved by using the highest mean ΔC_T value as an arbitrary calibrator to subtract from all other mean ΔC_T morphology values. Fold changes comparing the various porcine morphologies were then determined by the expression, $2^{-\Delta\Delta CT}$.

Statistical Analysis

Quantitative RT-PCR ΔC_T values were analyzed using the Statistical Analysis System with the Mixed Procedure [168, 169]. The statistical model used in the analysis tested the fixed effect of Developmental Stage (day 10, 12, 13, 15, and 17) of conceptus development. Significance ($P<0.05$) was determined by probability differences of least squares means between conceptus day of development and gene expression of Oct-4. Results are presented as the arithmetic mean ± SEM.

Results

RT-PCR Quantitation Using Taqman PCR

Through the initial investigation of the porcine cDNA with the murine primers, it was discovered that the murine *Oct-4* primers could bind and amplify the porcine cDNA. Another indication of homology between species, found during the TIGR and NCBI database searches, is the fact that both the porcine and bovine *Oct-4* gene sequences are located near the MHC. While the pluripotent cells of the embryo appear to be expressing the Oct-4 transcript during early peri-implantation, the MHC class II cells of the uterine epithelium appear to suppress the immune response [152].

The present communication describes the use of Real Time RT-PCR. The target gene expression was evaluated using a dual-labeled probe on small pools of porcine conceptuses. The relative abundance of mRNA encoding Oct-4 was calculated using the comparative C_T method. Ribosomal 18S rRNA was used to normalize for RNA loading variation. The messenger RNA expression profile of the Oct-4 gene was generated using

the ABI PRISM 7700 Sequence Detection System (PE/Applied Biosystems, Foster City, CA). Following the amplification, C_T, ΔC_T and $\Delta\Delta C_T$ values were calculated and recorded in Table 3.1.

The ΔC_T measures the raw expression of the *Oct-4* gene based upon normalization. Based on normalization with 18S ribosomal RNA, day 12 to day 17 of conceptus development significantly affected ($P< 0.001$) Oct-4 mRNA expression. With a total of twenty-four observations, day 10, 12 and 13 of conceptus development varied significantly with day 15 and 17 of development ($P<0.05$). Conceptus expression of Oct-4 was approximately 2, 8, and 11-fold greater on day 10 and 12 of pregnancy compared to expression on day 13, 15, and 17, respectively. Placental differentiation is associated with the down regulation of *Oct-4* gene expression as described in Figure 3.1.

Embryonic Stage	Oct-4 Mean C_T	18S rRNA Mean C_T	ΔC_T	ΔC_T Mean	$\Delta\Delta C_T$	Fold Difference
Day 10	25.4	15.8	9.7			
	25.1	16.1	9.0			
	29.6	20.8	8.8			
	26.3	16.1	10.23	9.4 ± .66[a]	3.5	11.6
Day 12	25.6	16.4	9.2			
	26.1	16.0	10.1			
	26.4	15.9	10.4			
	26.1	16.1	10.0			
	24.1	16.2	7.9			
	25.2	16.2	9.0	9.4 ± .54[a]	3.5	11.6
Day 13	25.0	16.4	8.9			
	24.9	15.9	9.0			
	28.8	15.9	12.9	10.2 ± .76[a]	2.8	6.8
Day 15	28.1	16.7	11.4			
	31.2	16.7	14.4			
	28.9	16.3	12.6			
	29.7	16.1	13.6			
	27.1	16.4	10.7			
	27.2	16.3	10.9			
	29.5	16.3	13.2	12.4 ± .50[b]	0.6	1.5
Day 17	28.3	16.3	12			
	28.2	16.0	12.2			
	29.2	16.2	13.0			
	31.3	16.7	14.6	13.0 ± .66[b]	0.0	1.0

Table 3.1 Quantitative RT-PCR Analysis of Gene Expression During Rapid Trophoblastic Elongation for Oct-4.

ΔC_T = Cycle threshold: cycle number in which amplification crosses the threshold set in the geometric portion of amplification curve.

‡ΔC_T = Subtracted gene product of interest C_T – 18S rRNA C_T; normalization of PCR cycles for subtracted gene target with 18S rRNA.

¶$\Delta\Delta C_T$ = Mean ΔC_T – highest mean ΔC_T value: the mean value Day 17 Oct-4 expression (highest ΔC_T; lowest expression of Oct-4 in study) was used as a calibrator to set the baseline for comparing mean differences in values across all other groups.

§a-b Values with different superscripts differ significantly in expression of Oct-4 ($P < 0.05$).

Day 12 and Day 17 values for the target gene differed significantly ($P< 0.001$).

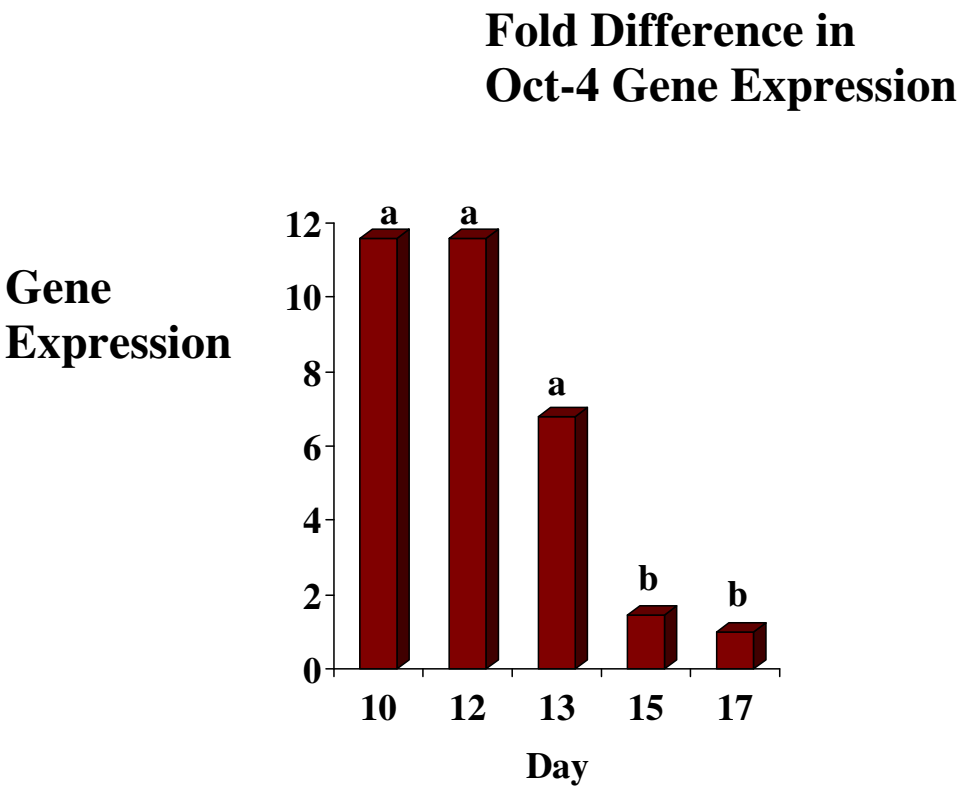

Figure 3.1 Results of RT-PCR Quantitation Using Taqman Probe. Based on normalization with 18S ribosomal RNA, Day 12 to Day 17 of conceptus development significantly affected (P< 0.001) Oct-4 mRNA expression. Different superscripts (a, b) differ significantly in expression of Oct-4 ($p<0.05$).

Discussion

The expression of *Oct-4* has not been characterized during this unique transitional stage of porcine development (days 10-17 of gestation). As a classical marker of ES cells and *in vivo* embryonic blastocyst cells the transcription factor, *Oct-4* is exclusively expressed by embryonic and germ cells and plays a critical role in the establishment and/or maintenance of pluripotent cells [1, 2].

Caution must be exercised in analysis as presence of the transcript does not necessarily result in protein expression. An interesting study would employ whole mount immunohistochemistry to detect the Oct-4 transcript in the TE and/or ICM of the porcine conceptuses.

Prudence is warranted as 18S rRNA has exhibited variability across developmental stages as a result of the dynamic nature of bovine embryonic cells. Preattachment embryos exhibit the dynamic nature of RNA populations [122]. While the comparative C_T method allows for the determination of the relative differences in transcripts, a disadvantage is the dependence on a normalizer expressed in the dynamic state of embryogenesis. However, the use of an absolute measurement would be difficult to interpret given the dynamic embryonic state [122].

It has been proposed that conceptus estrogen production stimulates the release of endometrial proteins and sequestration of histotroph. Autocrine and paracrine secretion of polypeptides by the conceptus may influence integrin/ fibronectin connections during

trophoblastic elongation. Clearly, the porcine uterine microenvironment must be analyzed during the critical stages of cellular differentiation.

During the period of porcine peri-implantation development when the length of the conceptus may grow 30-45 mm/hour, Oct-4 production is greatest. Indicated within this observation is the parallel of Oct-4 pluripotency marker proteins being expressed during this rapid growth phase. Porcine pregnancy days ten to twelve include rapid trophoblastic elongation and initiation of porcine production of estrogen. This signal for maternal recognition of pregnancy prevents the decline of progesterone production through continued uterine and conceptus production of Prostaglandin E_2 [119]. The critical maintenance of pluripotency through the Oct-4 transcription expression should coincide with conceptus estrogen production. The maximal uterine release of insulin-like growth factor (IGF-1) into the uterine lumen temporally coincides with conceptus estrogen biosynthesis and increased amounts of $P450_{arom}$ mRNA in filamentous conceptuses [137]. The data seem to indicate that Oct-4 expression corresponds temporally with the establishment of pregnancy in the pig. Leukemia inhibitory factor transcripts are maximal on days eleven to twelve [131, 134]. Similarly, the molecular players in the retinoid signaling pathway, retinol binding protein, RA, and the nuclear receptors are simultaneously expressed with the transition from tubular to filamentous morphology. While, LIF is involved in cellular differentiation and growth, perhaps this increase, immediately prior to trophoblastic elongation signals the subsequent down-regulation of Oct-4. Uterine epithelium produced OPNbegins on day 12 and increases to day 15; as Oct-4 transcripts begin a decline, the differentiation needed for attachment and placentation with the suggested conceptus increase in uterine and conceptus integrin

attachment through OPN [129]. Possibly, Oct-4 protein levels must decline for placentation to take place. The 30-to 100-fold increase in the serine protease inhibitor light chain member, bikunin during days 10 to 18 indicates the need for protection of the porcine uterine lining when the pluripotency marker, Oct-4 is declining and apposition of the conceptus to the uterine lining is necessary [146]. Similar comparisons can be made with the serine protease, kallikrein increase from day 10 to day 15 [147, 148]. In summary, the present study showed a significant down-regulation of the Oct-4 transcript from day 12 to day 17. Oct-4 expression in the developing conceptuses during the developmental period prior to and during early trophoblastic elongation (days 10 and 12) indicates active porcine embryonic pluripotent stem cells. The down regulation of the Oct-4 transcript (days 15 and 17) indicates differentiation inherent in transcripts which prepare the endometrium and conceptus for implantation.

CHAPTER IV

DETECTION OF *Oct-4* GENE EXPRESSION IN MURINE EMBRYOS DURING PREIMPLANTATION DEVELOPMENT

Introduction

The objective of this study was to compare the mRNA expression patterns of the *Oct-4* gene in early mouse embryos using Real Time polymerase chain reaction (PCR). Embryos at the four-cell, eight-cell and blastocyst stage were studied. Murine Oct-4 is expressed in the murine ICM but not in the pretrophectodermal cells [4, 42]. Oct-4 protein is found in the nuclei of two-cell embryos, and zygotic activation of Oct-4 expression occurs prior to the eight-cell stage [4, 14]. Expression of the gene is uniform in all cells of the embryo through the morula stage, however, as the outer cells differentiate intoTE, Oct-4 expression becomes restricted to the cells of the ICM in the blastocyst [10, 14, 39]. Expression of Oct-4 has not been characterized using individual whole murine embryos. Total RNA was extracted from whole individual embryos representing development from day two post coitus (2dpc) with four cell and eight cell embryos to day three post coitus (3dpc) with the developing blastocyst. Employing quantitative PCR, we assayed Oct-4 cDNA using 18S rRNA gene expression as a normalization control. Oct-4 expression differences between the embryonic stages were determined using the comparative C_T method. Embryonic stage significantly affected

($p<0.005$) *Oct-4* gene expression. Embryonic expression was greatest in the blastocyst being approximately 85 and 12-fold greater than the four-cell and eight-cell embryonic stages, respectively. Four-cell, eight-cell and blastocyst embryos have four, eight and approximately twenty pluripotent cells [120]. While these embryos (four-cell, eight-cell and blastocysts) exhibit a 1X, 2X and 5X increase in pluripotent cell number, within this study, the same embryos demonstrated a 1X, 7X and 85X increase in *Oct-4* gene expression, respectively.

The murine embryo generates the first two cell lineages (the TE and the hypoblast) which form the basis of the placenta and the extraembryonic yolk sacs required for successful interaction with the mother. The gestation period for the mouse is 19-20 days [120]. The murine two-cell egg is present on the first daypost coitus (dpc) with the 4-16 cell morula on the second dpc [120]. The blastocysts have hatched free of the zona by the fourth dpc with the implanting blastocyst and hypoblast on 4.5dpc [120]. The blastocyst contains two extraembryonic lineages, TE and hypoblast, and the embryo itself comprises a pool of pluripotent cells located within the ICM [47]. The murine ICM forms a second pluipotent cell population, the primitive ectoderm between 4.75 and 5.25 dpc. The outer primitive ectoderm cells proliferate and by 6.0-6.5 dpc have formed a pseudo-stratified epithelial layer of pluripotent cells. The germ cells arise from the primitive ectoderm and during gastrulation, the primitive ectoderm generates the primary germ layers of the embryo and the extra-embryonic mesoderm [47]. Pre-implantation development ends in the formation of a blastocyst with three layers: the trophoblast, the ICM or epiblast and the hypoblast that will form the embryo [170].

Undifferentiated stem cells of the ICM give rise to the whole of the embryo proper as well as the mesenchymal components of the placenta. The murine sixteen-cell stage with the radially oriented divisions of some of the blastomeres leads to segregation of the daughter blastomeres generating the outer TE layer of the blastocysts and the inner cohesive ICM. This segregation establishes the placental and embryonic progenitors [118]. A major question is how cellular polarization results in differential gene expression. The POU transcription factor, Oct –4 is required to maintain totipotent phenotype of ICM cells, while either loss of expression or over expression leads to differentiation [59]; deletion of *Oct-4* leads to loss of ICM with all blastomeres forming TE [15, 118]. The three germ layers of the embryo, ectoderm, mesoderm and endoderm form during gastrulation [117].

Blastomeres of the four-cell morulae can each give rise to a mouse, while early eight-cell stage blastomeres cannot generate a mouse by themselves [120]. With cleavage to the 16-cell stage, a gradual restriction in the developmental potency of the cells exists due to the production of the TE and the ICM lineages [120]. The murine fully expanded blastocyst contains about 64 cells with approximately 20 in the ICM. During the fifth day of development, the blastocyst hatches from the zona and is ready for implantation [120].

Materials and Methods

Embryo Collection

Four week old CD1 female mice (Charles River Laboratory, Boston, MA) were injected with 0.1ml (7.5U) of PMSG (Sigma-Aldrich, St. Louis, MO) then 48 hours later with 0.1ml (7.5U) of hCG (Sigma-Aldrich, St. Louis, MO) and placed with males. Vaginal plugs were checked thirteen hours post-hCG and positive bred females were placed in the maternity area. The *in vivo*-developed mouse embryos at the four-cell, eight-cell and blastocyst stages were flushed from either oviducts or uteri at 61, 69, and 97.5 hours post-hCG, respectively. Timings were derived empirically and through literature review [171, 172]. The flushing medium, BWW/Hepes (Irvine Scientific, Santa Ana, CA) with BSA (Irvine Scientific, Santa Ana, CA), was sterilized through a 0.2 micron filter (ISC, BioExpress, Kaysville, Utah) and warmed to 37°C. Zona pellucidae were removed by pipetting the embryos up and down through a fine bore pipet in acid tyrodes (Sigma-Aldrich, St. Louis, MO) medium (pH 2.5) [120]. The embryos were then washed with serum free BWW/Hepes.

Extraction of RNA

Complementary DNA (cDNA) from mouse embryos was extracted by the Cells-to-cDNA Kit (Ambion, Inc., Austin, Texas) according to the manufacturer's protocol. The kit contents have been previously described. In brief, the cDNA from mammalian cells can be extracted without specifically isolating RNA. A heat treatment in the Cell Lysis Buffer ruptures the cells, releasing the RNA and inactivating endogenous RNases.

The crude cell lysate is treated with DNase I to degrade the genomic DNA. Since DNA contamination will result in inaccurate quantification [173], DNase I is added to rid the sample of genomic DNA.

Specifically, each zona pellucida free embryo was pipetted into 5 ul of cold cell lysis buffer in a 0.2 ml nuclease free microfuge tube (United Scientific Products, SanLeandro, CA). The cells were gently centrifuged down into the lysis solution and the cell lysis/embryo mixture was covered with 1-2 drops of nuclease-free mineral oil to prevent evaporation (Sigma-Aldrich, St. Louis, MO). The embryos were incubated immediately for ten minutes in a 75°C water bath to lyse the cells, release the RNA, and inactivate the RNases. DNase I was then added at 0.8 ul/reaction tube (2U/ul) and incubated at 37°C for 30 minutes. The DNase I was inactivated at 75°C for five minutes.

Reverse Transcription

Previously, the porcine reverse transcription and polymerase chain reaction were conducted in a one-step reaction. The murine embryos were treated in two steps: reverse transcription and then polymerase chain reaction. The separation of the RT and PCR steps has the advantage of generating a stable cDNA pool that can be stored virtually indefinitely [174]. Using the Cells-to-cDNA kit (Ambion, Inc., Austin, Texas) in a nuclease free 0.2 ml microfuge tube (United Scientific Products, San Leandro, CA,) the 5 ul of cell lysate (RNA) was mixed with 4 ul of dNTPs, 2 ul of random decamers and 5 ul of nuclease-free water. The use of random primers maximizes the number of mRNA molecules that can be analyzed from a small RNA sample [174]. After gentle vortexing

and a brief centrifugation, individual microfuge tubes were heated for 3 minutes at 70°C, placed on ice for 1 minute, followed by a second brief centrifugation and replaced on ice. The remaining reagents were added to each cell lysate sample: 2 ul of reverse transcriptase buffer, 1 ul of M-MLV Reverse Transcriptase and 1 ul of the Rnase Inhibitor (10U/ul). Since the cell lysates may have contaminating genomic DNA, it is necessary to include a minus-reverse transcriptase control to demonstrate that the template for transcription was cDNA and not genomic DNA. The 20 ul samples were mixed gently, centrifuged briefly and incubated at 42°C for an hour. The reverse transcription was inactivated with a 10 minute, 95°C incubation. The samples can be stored at -20°C, or used immediately for amplification.

PCR Amplification

To analyze the extraction of reverse transcription of the mRNA an aliquot of several samples was used in PCR amplification in a thermocycler Perkin Elmer 9600 (PE Biosystems, Foster City, CA) to verify mRNA extraction and cDNA production before the Real Time trials were conducted. The primers sense 5'-GGC CCA GAG CAA GAG AGG TAT CC-3' and antisense 5'-AGC CAC GAT TTC CCT CTC AGC-3' for an endogenous 460 bp β-actin amplification was added as an internal control of the PCR reaction [3]. Also, primers sense 5'-CTC GAA CCA CAT CCT TCT CT-3' and antisense 5'-GGC GTT CTC TTT GGA AAG GTG TTC-3' were used to amplify Oct-4 cDNA [3] for a 312 bp product. Both sets of primers were synthesized by the Oklahoma State University Recombinant DNA/Protein Resource Facility. The PCR reaction was

performed using a 35-cycle program consisting of a 2 minute initial denaturation at 94°C, 30 seconds at 94°C, 55°C and 72°C each, with a final extension of 72°C for 5 minutes. To check for nucleic acid contamination, a negative control (minus template) was also prepared to contain all of the reagents except the template.

The polymerase chain reaction was set up using the FailSafe PCR System (Epicentre, Madison, WI) with a 1uM final concentration of each primer. Briefly, we prepared the FailSafe Master Mix by adding primers (final concentration of 1uM) and water to 9.5ul for each reaction tube. 12.5 ul of FailSafe PCR PreMix "D" was placed into individual microcentrifuge tubes and 2.5ul of template cDNA was added to the PreMix "D." 1.25 units/reaction FailSafe polymerase was added to the master mix and 10 ul of the final Master Mix was added to each tube for a total 25ul reaction. Samples of cDNA were electrophoresed on a 1.5% agarose gel stained with ethidium bromide and visualized to verify the PCR had produced the appropriately sized amplification product.

Real Time PCR Amplification

The relative changes in quantity of mRNA transcripts were determined using Real Time Polymerase Chain Reaction in the MJResearch Opticon 2 (Bio-Rad Laboratories, Inc., South San Francisco, CA). In brief, 3 ul from four-cell, eight-cell and blastocyst stage extracted and reverse transcribed cDNA products were Real Time PCR amplified in a reaction containing 12.5 ul of DyNAmo HS SYBR Green master mix (New England Biolabs, Beverly, MA) with a final primer concentration of 10uM of forward and reverse primer with nuclease free water up to 25 ul final reaction. Each sample was run with

primers (Invitrogen Corp., Carlsbad, CA) of Ribosomal 18S sense: 5'- TCA AGA ACG AAA GTC GGA GGT T-3' and Ribosomal 18S antisense: 5'-GGA CAT CTA AGG GCA TCA CAG-3,' and *Oct-4* Real Time sense: 5'-TGGAGGAAGCCGACAACAATGA-3' and *Oct-4* Real Time antisense: 5'-ACTCCACCTCACACGGTTCTCAAT-3'. The *Oct-4* primer set produces a 110 bp product and was derived through the oligo analyzer on the IDT web site (http://www.idtdna.com/biotools/primer_quest/primer_quest.asp) and Primer Select Oligonucleotide Design and Analysis tool suite (DNASTAR, Inc., Madison, WI). Duplicate samples of reverse transcribed samples were run with each primer pair. The PCR consumables were prepared as a mixture or master mix [175, 176].

Specific conditions of the Real Time reaction for Ribosomal 18S were 95°C for 15 minutes with 42 cycles of 94°C at 20 sec, 61°C at 45 sec and 72°C at 45 sec with fluorescence measured at 76°C and 78°C. The melt curve was run at 54°C to 90°C in one second, 0.2°C intervals; products were annealed with a ten minute final annealing temperature of 72°C. Products were held at 10°C. Specific conditions of the Real Time reaction for the murine *Oct-4* gene were 95°C for 15 minutes with 42 cycles of 94°C at 20 sec, 56°C at 20 sec and 72°C at 20 sec with fluorescence measured at 76°C and 78°C. The melt curve was run at 50°C to 90°C in one second, 0.2°C intervals; products were annealed with a ten minute final annealing temperature of 72°C.

Statistical Analysis

Quantitative PCR ΔC_T values were analyzed using the analysis of differences in the means between the three embryonic populations with a one-way ANOVA. The one-way ANOVA was followed by multiple pairwise comparisons among the means using Tukey's Multiple Comparison Test. These tests were performed using GraphPad Prism version 4.00 for Windows, GraphPad Software, (SanDiego, CA).

Results

The amplification efficiencies of the target and reference must be approximately equal in order for the $\Delta\Delta C_T$ calculation to be valid [166]. An assessment to determine if the two amplicons have the same efficiency is to look at the variation in the ΔC_T with template dilution**.** A 10x dilution series in sterile, nuclease-free water (Epicentre, Madison, WI) was performed and each dilution was amplified by RT-PCR. The results of an experiment in which the cDNA preparation was diluted over a 100-fold range are found in Figure 4.1. The log cDNA dilution versus the ΔC_T were added as data points and a line plotted by linear regression analysis. The efficiency of amplification of the target gene (Oct-4) and internal control (18S rRNA) was examined using Real Time PCR and SYBR green detection. The serial dilutions of cDNA were amplified by Real Time PCR. The absolute value of the slope of the line did not significantly deviate from zero. Thus, the efficiencies of the target (*Oct-4*) and the reference gene (18S rRNA) are similar and the $\Delta\Delta C_T$ calculation for the relative quantification of the target could be used.

When replicate PCRs are run on the same sample, it is appropriate to average the ΔC_T data of each target and internal control values. Samples that did not amplify, did not show the exact melt curve peak, or did not demonstrate the appropriately sized amplification product after agarose gel electrophoresis and staining were not used during analysis. Specificity and RT-PCR product verification were achieved by plotting fluorescence as a function of temperature to generate a melting curve of the amplicon. The temperature was slowly increased above the T_m (melting temperature) of the amplicon and fluorescence measured. Since SYBR Green binds to the minor groove of the DNA double helix, a characteristic melting peak at the melting temperature of the amplicon will distinguish it from amplification artifacts. The DNA sequence of the target amplicon contributes significantly to the melting profile [174, 177, 178]. Specificity of the desired product was also documented by staining and visualization after high-resolution gel electrophoresis. Data sets from four-cell, eight-cell and blastocyst embryos are presented in Tables 4.1, 4.2, and 4.3, respectively. Table 4.4 demonstrates the calculations necessary to derive the $\Delta\Delta C_T$ of the Oct-4 gene, normalized with 18S rRNA in the various murine embryos.

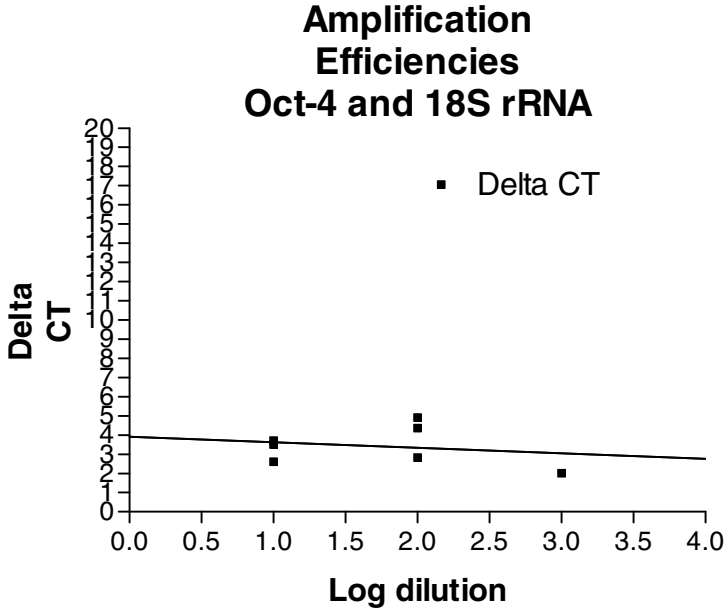

Figure 4.1: Validation of the $2^{\Delta\Delta CT}$ method. Amplification of the cDNA diluted over a 100-fold range.

Table 4.1: Quantitative PCR Analysis of Gene Expression During Murine Embryonic Development

Four Cell Embryonic Analysis

Murine Four Cell Oct-4 Mean C_T[†]	Murine Four Cell 18S Mean C_T[†]	Murine Four Cell ΔC_T[‡¶]
29.705	21.3275	8.3775
30.0395	22.77	7.2695
29.526	21.512	8.014
34.1865	31.19	2.9965
28.902	22.1045	6.7975
29.322	20.3465	8.9755
30.9815	21.0155	9.966
29.285	22.1905	7.0945
33.6065	25.9625	7.644
31.222	26.392	4.83
33.1635	24.087	9.0765
31.0585	22.59	8.4685
31.122	23.706	7.416
31.0465	24.9245	6.122
31.9665	25.383	6.5835
33.926	26.946	6.98
34.748	23.2825	11.4655
31.0475	25.0475	6
32.526	24.153	8.373
30.75	22.507	8.243
35.4585	27.812	7.6465
31.232	30.3705	0.8615
32.9155	30.421	2.4945

C_T[†] = Cycle threshold: cycle number in which amplification crosses the threshold set in the geometric portion of amplification curve
ΔC_T[‡¶] = Subtracted gene product of interest C_T – 18S rRNA C_T ; normalization of PCR cycles for subtracted gene target with 18S rRNA

Table 4.2: Quantitative PCR Analysis of Gene Expression During Murine Embryonic Development

Eight Cell Embryonic Analysis

Murine Eight Cell Oct-4 Mean C_T[†]	Murine Eight Cell 18S Mean C_T[†]	Murine Eight Cell ΔC_T[‡¶]
28.6575	23.576	5.0815
29.2345	25.0975	4.137
27.2735	22.0165	5.257
28.2695	25.356	2.9135
27.632	26.7865	0.8455
29.9805	26.0155	3.965
28.1375	19.4555	8.682
25.695	26.085	-0.39
28.668	23.461	5.207
28.881	20.1205	8.7605
29.5355	21.753	7.7825
28.463	24.7115	3.7515
28.234	24.281	3.953
28.483	26.797	1.686
28.077	21.9295	6.1475
28.6955	21.7975	6.898
27.8835	22.339	5.5445
28.5525	30.7235	-2.171
27.62	22.701	4.919
28.636	25.918	2.718
28.3535	27.1475	1.206

C_T[†] = Cycle threshold: cycle number in which amplification crosses the threshold set in the geometric portion of amplification curve
ΔC_T[‡¶] = Subtracted gene product of interest C_T – 18S rRNA C_T ; normalization of PCR cycles for subtracted gene target with 18S rRNA

Table 4.3: Quantitative PCR Analysis of Gene Expression

During Murine Embryonic Development

Blastocyst Embryonic Analysis

Murine Blastocyst Oct-4 Mean C_T †	Murine Blastocyst 18S Mean C_T †	Murine Blastocyst ΔC_T ‡¶
27.4993	26.4057	1.0937
27.9827	26.7017	1.2810
29.1270	28.4063	0.7207
29.0667	28.1010	0.9657
31.7027	31.8110	-0.1083
31.3100	31.0827	0.2273
30.0650	29.3393	0.7257
30.6690	30.4423	0.2267
28.9510	27.9110	1.0400
27.9190	26.8240	1.0950
30.3793	30.4383	-0.0590
28.6897	27.7857	0.9040
32.4303	31.9757	0.4547
28.6773	27.6243	1.0530
32.4867	34.8563	-2.3697
29.5330	28.3607	1.1723
27.9650	27.0200	0.9450
28.7530	27.9297	0.8233
28.2823	27.6743	0.6080
28.4513	27.2463	1.2050
29.8863	28.7463	1.1400
31.6660	30.8383	0.8277
31.4213	31.7947	-0.3733
30.2557	29.5973	0.6583
29.2680	28.0287	1.2393
30.4363	29.5027	0.9337
31.6267	31.1667	0.4600
30.8577	30.1517	0.7060
30.3897	30.0197	0.3700
30.8393	30.1737	0.6657
31.2703	30.6757	0.5947

Table 4.4: Quantitative PCR Analysis of Gene Expression in Murine Embryos

Baseline Results	Mean Δ C_T	Standard Deviation	ΔΔ C_T[§]	Fold Difference
Blasts (n = 31)	0.620± 2.405[a]	0.693	6.410	85.039
8 cell (n = 21)	4.138± 2.849[b]	2.849	2.892	7.425
4 cell (n = 23)	7.030±.6932[c]	2.405	0.000	1.000

ΔΔ C_T[§] = Mean Δ C_T – highest mean Mean Δ C_T value: the mean value of 4 cell murine embryos Oct-4 expression (highest Δ C_T; lowest expression of Oct-4 in study) was used as a calibrator to set the baseline for comparing mean differences in values across all other groups.

[a-c] Values with different superscripts differ significantly in expression of Oct-4 ($P<0.005$). Statistics were determined using GraphPad PRISM with a 1way ANOVA analysis of the ΔCT Mean. 4 cell, 8 cell and blastocyst embryonic values for the target gene differed significantly ($P<0.005$).

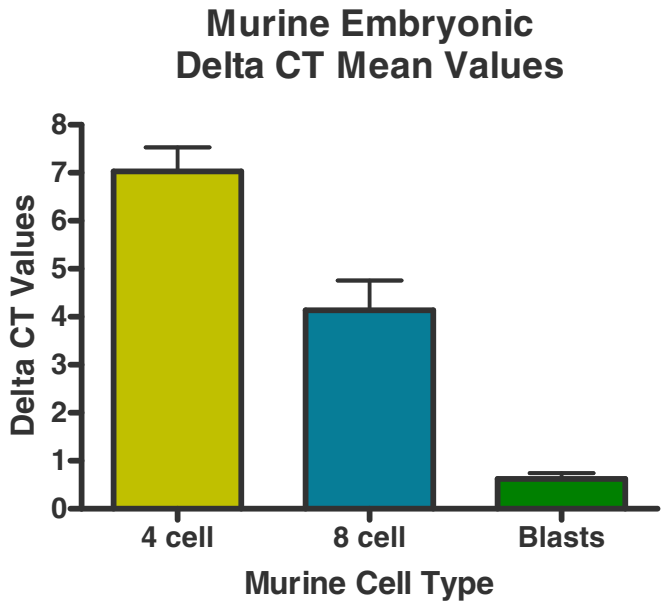

Figure 4.2: ΔCT Mean values of the 4-cell, 8-cell and blastocyst embryos.

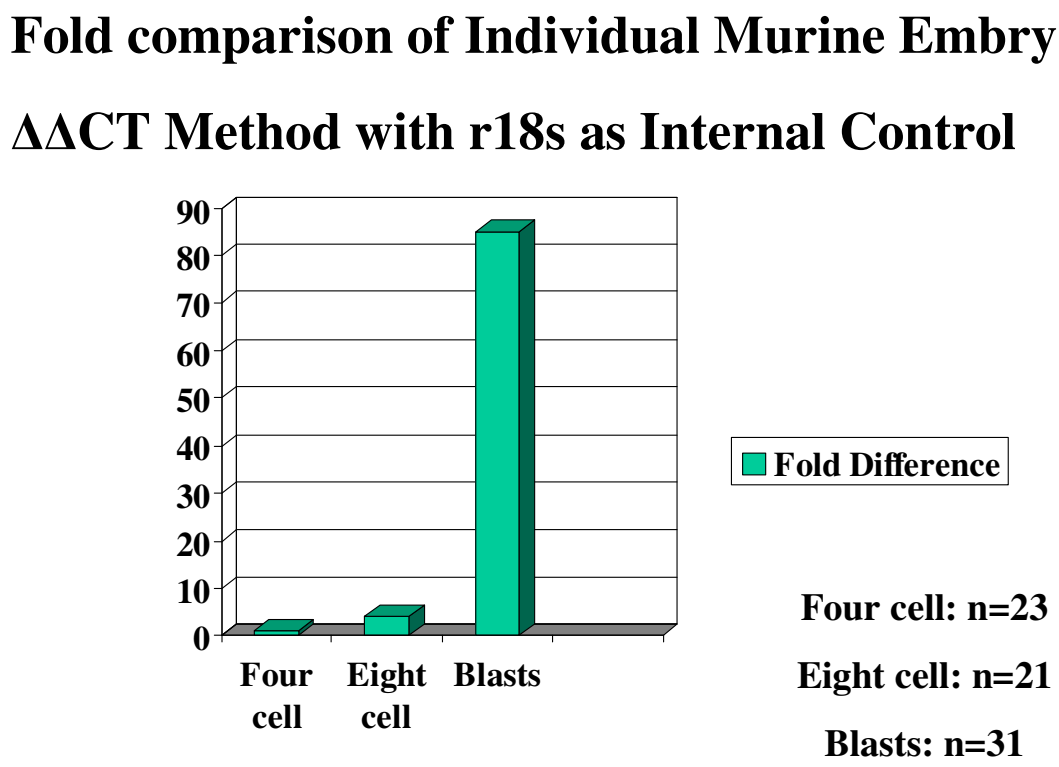

Figure 4.3: Results of Quantitative PCR Using SYBR Green Technology based on Oct-4 expression and normalization with 18S ribosomal RNA.

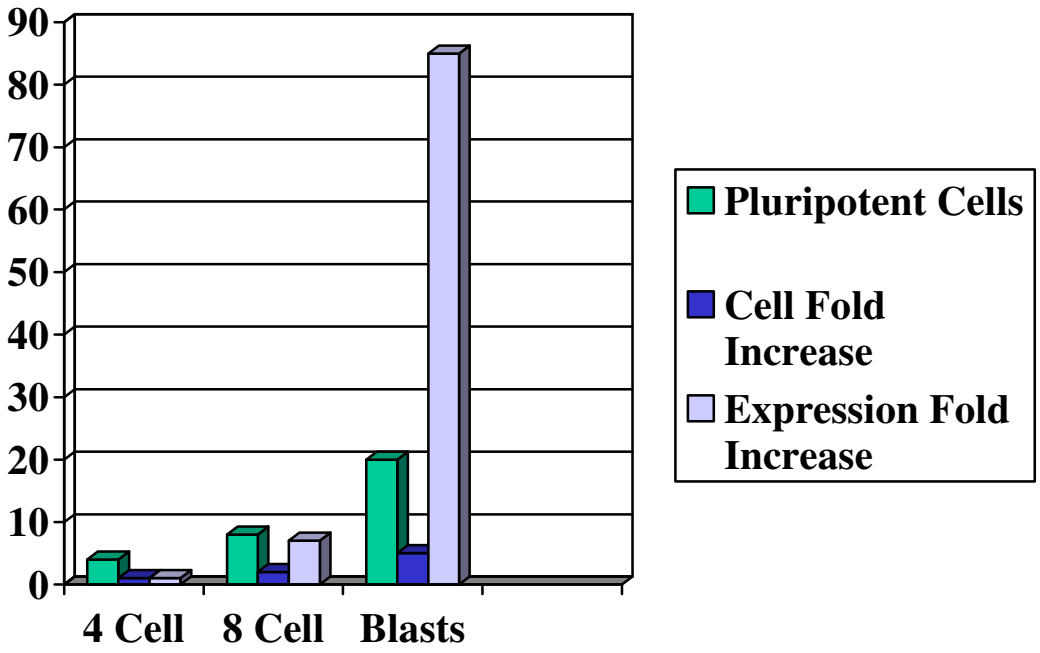

Figure 4.4: Up-regulation of the murine Oct-4 transcript per pluripotent cell in embryonic stages with a comparison of the number of pluripotent cells found in each embryo and the comparison of expression fold increase in Oct-4 expression levels. Four cell and eight cell embryonic pluripotent cells were identified through microscopy. The ~20 pluripotent cells in expanded blastocysts was derived from Hogan and co-workers [120].

Quantitative PCR ΔC_T values were analyzed using analysis of differences in the means between the three embryonic populations with a one-way ANOVA. The three murine populations, 4-cell (n = 23), 8-cell (n = 21), and blastocysts (n =31), demonstrated a median and standard error of the mean of 7.4 ± 0.5, 4.1± 0.6, and 0.7± 0.1, respectively, as shown in Figure 4.2. Since the one-way ANOVA allowed us to reject our null hypothesis that no difference existed between the three populations of murine embryos in Oct-4 gene expression, we knew at least one of the means varied significantly. When the ANOVA indicates that at least one of the means isn't the same as the other means, the determination of where the differences exist is performed by a post test. The one-way ANOVA with a significance of $P<0.005$ was followed by multiple pairwise comparisons among the means using Tukey's Multiple Comparison Test. This test showed pairwise comparisons with each P value <0.005. The one-way ANOVA with Tukey's post test was performed using GraphPad Prism version 4.00 for Windows, GraphPad Software, (SanDiego, CA).

Embryonic development stage significantly affected *Oct-4* mRNA expression. Blastocyst expression of Oct-4 was approximately 85 and 12-fold greater than the four-cell and eight-cell embryonic stages, respectively, and is shown in Figure 4.3. Four-cell, eight-cell and blastocyst embryos have 4, 8 and ~20 pluripotent cells [120]. The 1X, 2X and 5X increase in pluripotent cell number coincides with a 1X, 7X and 85X increase in Oct-4 gene expression, respectively and is illustrated in Figure 4.4. The increase in Oct-4 mRNA is not due to the increase in cell number.

Discussion

Oct-4 is a mammalian transcription factor exclusively expressed in embryonic and germ cells. Expression of Oct-4 has not been characterized using individual murine embryos. More than seventy embryos were compared for the mRNA expression pattern. The blastocysts and 8-cell embryos produced 85-fold and 7-fold more Oct 4, respectively than the four cell embryos (Fig. 3). A fully expanded blastocyst contains approximately 20 cells in the ICM [120] compared to the four and eight totipotent cells found in the comparison embryos. Certainly, the increase in cell number by approximately 5-fold more totipotent cells in the blastocyst and 2-fold more totipotent cells in an eight celled embryo cannot account for an 85 and 7-fold expression increase in Oct-4 expression, respectively (Fig. 4). The present study not only showed a significant up-regulation of the Oct-4 transcript from the four-cell to eight-cell and blastocyst embryos, but it indicates an up-regulation of the Oct-4 transcript per totipotent cell.

With the amplification efficiencies of the target gene and the normalization gene verified, and this preliminary study comparing number of pluripotent cells found in each embryo with the expression fold increase in Oct-4 expression levels, the groundwork is prepared for technologies which influence transcription levels of individual murine embryos. This study of Oct-4 transcription levels in individual murine embryos with the suggested up-regulation of the Oct-4 transcript is the basis for a protein transduction study of individual murine embryos.

CHAPTER V

PURIFICATION AND PROTEIN TRANSDUCTION OF TAT-HA FUSION PROTEINS

The Proteins of Interest: Oct-4, GCNF, BMP8b

Oct-4 establishes the murine pluripotent condition. Oct-4 expression is equal in all cells until cavitation of the embryo, when Oct-4 is confined to the cells of the ICM; after implantation, Oct-4 is expressed in the epiblast and downregulated during gastrulation [4, 179]. Primordial germ cells are the only embryonic cells that continue to express Oct-4 after gastrulation [59]. It is of primary importance to understand how Oct-4 creates pluripotency and to identify the signals upstream of the Oct-4 expression in this founder population of embryonic primary germ cells. A brief study of the upstream gene regulators of Oct-4, GCNF and BMP8b, is necessary.

Germ cell nuclear factor (GCNF) functions as a repressor of gene transcription and is involved in murine preimplantation embryonic development [180]. GCNF was first designated in 1994 by Chen and co-workers and its function as regulator of gene expression in germ cell development suggested [181]. GCNF is an ophan nuclear receptor with an unidentified ligand. Orphans are receptors for which the ligands and functions have not yet been identified [182]. GCNF has a well-defined DNA-binding domain (DBD) or hormone responsive element (TCAAGGTCA); this element contains one or more half-site sequences (such as AGGTCA) which can be arranged as direct

repeats, inverted or everted repeats [181, 182]. Described as an orphan member of the nuclear receptor superfamily [183], GCNF is a putative ligand-activated transcription factor and binds to DNA on a hexad sequence AGGTCA with zero-base pair spacing [183, 184]. While the direct repeat with zero base pair spacing suggests that GCNF binds the DNA as a homodimer, Cooney and co-workers raised the possibility that it could bind DNA as a monomer [185]. The residues, EGCKG, (glutamic acid, glycine, cysteine, lysine, and glycine) in the DBD sequence convey binding to the AGGTCA half-site by GCNF [186]. GCNF can repress transcription through competition for binding and through interactions with co-repressors [186].

While GCNF is expessed as early as the murine egg cylinder stage, its repression function is mediated by co-repressors that recruit histone deacetylases that deacetylate promoters and repress the gene expression [182]. One proposed model for GCNF is that it represses expression of genes in the absence of a signal and then activates the genes upon binding ligand [187, 188]. A "generic" mechanism of action was described by Cooney and co-workers [184] in which the absence of a ligand causes recruitment of corepressors which recruit histone deacetylase complexes and cause net deacetylation of the histones in the promoter region and the repression of the target gene expression. With cognate ligand binding, the nuclear receptor undergoes a conformational change that displaces the corepressors and recruits coactivators and histone acetyltransferases. The net histone acetylation of the promoter region causes expression of the target gene [184].

The nuclear receptor superfamily of ligand-dependent transcription factors regulate gene expression involved in development, cellular proliferation and differentiation [189]. P19 cells that are stimulated to differentiate though exposure to

RA exhibit a transient upregulation of GCNF, then a down regulation and finally no GCNF detectable in fully differentiated cells; these results suggest a connection of GCNF with developmental stages during cellular differentiation [182].

Gene targeting used to generate a mouse model lacking GCNF showed that knockouts of the *Gcnf* gene were embryonically lethal [184]. Based upon relatedness in the DBD, GCNF is placed in a separate branch of the nuclear receptor superfamily [184]. A unique description expression pattern is exhibited by GCNF with both embryonic and adult expression; GCNF is expressed in germs cells as well as neuronal cells [185]. GCNF is named based upon its restricted expression pattern in the adult [186]. The GCNF message was detected in mouse embryos at E8.5 and was barely detectable at E10 [185, 190].

The first studies to suggest that GCNF repressed *Oct-4* gene activity was presented by Fuhrmann in 2001 [191]. GCNF specifically binds to the *Oct-4* proximal promoter and to extended half-sites of the AGGTCA core motif [187, 190, 191]. Through transfected GCNF plasmids, the GCNF expression was shown to inversely correlate with the Oct-4 expression in mouse embryogenesis and the relationship appeared as a functional link [186, 191]. GCNF homozygous null mutant mice express Oct-4 more widely than just the primodial germ cells after gastrulation. It was suggested that GCNF necessarily repressed Oct-4 *in vivo* [186, 191, 192].

Bone morphogenetic proteins (BMPs) are members of the transforming growth factor type β superfamily of growth factors that function as heterodimers or homodimers [193]. Embryonic cells communicate with each other using just a few conserved families of signaling molecules and one of these families is that of the bone mophogenetic

proteins [194]. BMP as a name is misleading because much genetic and experimental evidence shows that these molecules regulate biological processes as diverse as apoptosis, cell proliferation, differentiation, cell-fate determination, and morphogenesis [194, 195]. BMP4 and BMP8B are often coexpressed in tissues or cell types during embryongenesis; while the two proteins have an overlapping expression in the extraembryonic ectoderm, both are required for primary germ cell generation. BMP4 and BMP8B belong to different classes (Dpp and 60A, respectively) of the transforming growth factor type β superfamily and appear to function through a two-pathway model with synergistic signaling but separate receptor complexes to elicit the biological process [193, 196]. The *Bmp4* and *Bmp8b* genes are expressed in the extraembryonic ectoderm and the suggested function is induction of primary germ cells [193]. Through transfections of COS cells with pIRES or pIRES with *Bmp4/Bmp8b* insertions, murine embryos with removed extraembryonic ectoderm and proximal epiblast (containing PGC precursors) were cultured on top of the COS cells. A 54-fold increase in the number of PGCs with the *Bmp4/Bmp8b* COS cells of the murine embryonic portions over the control COS cells with the murine embryonic portions demonstrate a positive relationship between BMP8b and PGC production [193, 197]. Generation of the PGCs from the epiblast requires the expression of BMP8b in the extraembryonic ectoderm in the pregastrula and gastrula murine embryonic stages [198]. Proximity of the epiblast cells to the extraembryonic ectoderm is also required for generation of the PGCs suggesting that the signals from the epiblast are critical for PGC development [198-200]. Moreover, antisense RNA probes against murine Oct-4 exhibited clusters of Oct-4 positive cells in the epiblasts cocultured with the bone morphogenetic protein gene-containing COS cells

[193]. A signaling link has been suggested between the extraembryonic ectodermal production of BMP8B and the production of Oct-4 [201].

Our goal in this study was to construct plasmids within a prokaryotic expression system capable of expressing our particular genes, *GCNF*, *Bmp8b*, and *Oct-4*, fused to the TAT transduction domain and test the recombinant proteins on somatic and pluripotent cells. Techniques involved in this study would include 5' restriction site mutagenesis, cloning of PCR products, protein expression, purification through FPLC and verification of protein acquisition through SDS-PAGE and Western Blotting. The production of these proteins will allow subsequent transduction studies.

Materials and Methods

Traditional TAT-HA Fusion Protein Purification Method: An Overview

The expression vector into which a gene of interest has been cloned, is transformed into a bacterial strain, such as DH5α; individual clones are analyzed for the correct insert size by standard molecular biology techniques and then sequenced to confirm that the construct has been made through automated sequencing [91-93, 202]. Next, the desired expression plasmid is transformed into a high-expressing bacterial strain such as Gold(DE3)LysS, and the fusion protein is expressed in a 200-ml overnight culture. The bacteria are collected by centrifugation and the pellet is washed in a buffer. The fusion protein is then isolated by sonication of the bacterial pellet in 8M urea, as these hexahistidine-fused recombinant proteins are often found as inclusion bodies in the host bacteria. The urea sonication helps to disaggregate the insoluble proteins [91-93].

These insoluble recombinant proteins, expressed as inclusion bodies, are dense aggregates that consist mainly of the desired product in the nonnative state [203]. The clarified sonicate is then applied at room temperature to an immobilized metal affinity column for purification. A series of buffers of increasing imidazole concentrations (100mM, 250mM, 500mM and 1M) is applied to the column in subsequent steps, and start and flow-through fractions are saved. The start, flow-through and all fractions are then analyzed by SDS-polyacrylamide gel electrophoresis [91-93].

To treat culture cells and animal models with TAT-fusion proteins, the denaturant, 8M urea, must be rapidly removed. The proteins are added to a desalting column for this purpose. While this strategy to remove the urea produces purified protein and is more susceptible to precipitation and freeze-thaw problems; it is rapid and inexpensive. A PD-10 column, which is a prepacked Sephadex G-25 M resin (Amersham Pharmacia, Piscataway, NJ), is often used. One-milliliter fractions are collected in microcentrifuge tubes, and the pooled factions are analyzed by SDS-PAGE. The proteins are flash-frozen in 100 ul volumes in 10-20% glycerol and stored at–80 °C for further use [91-93].

Acquisition of the pTAT-HA plasmid

We were mailed the plasmid, pTAT-HA (gift from Dr. Steven F. Dowdy at Washington University, St. Louis, MO and Howard Hughes Medical Institute); using established methods we transformed the plasmids [204] into *E. coli* Top10 F' cells (Invitrogen Corp., Carlsbad, CA). We grew the transformed cells on Luria Bertani Medium with agarose [204] and with 50 ug/ml ampicillin. The TAT-HA plasmid

encodes ampicillin resistance. The TAT-HA expression vector encodes an N-terminal 6-histidine leader sequence followed by the 11-amino-acid TAT PTD flanked by glycine residues (GYGRKKKRRQRRRG), a hemagglutinin tag (GYPYDVPDYAG) flanked by glycine residues, and a polylinker [30]. An isolate bacterial colony from this LB-ampicillin selective plate was used to inoculate a starter culture of 5 ml LB medium containing ampicillin (50 ug/ml) and incubated for 8 hours at 37°C with vigorous shaking (~300 rpm). The starter culture was diluted 1/500 into the LB medium (50 ug/ml ampicillin) and grown at 37°C for 14 hours with vigorous shaking (~300rpm). Two ml of this culture were stored at –80°C. Plasmid DNA was purified from the remainder of the culture on a Qiagen midiprep column according to manufacturers instructions (Qiagen, Valencia, CA). The DNA was redissolved in 100 ul of TE, pH 8.0 and the plasmid DNA concentration was determined by UV spectrophotometry. The purified plasmid DNA was stored at –20°C.

5' Restriction Site-Directed Mutagenesis of *Oct-4*

The cDNA of the *Oct-4* gene was supplied by Hans Scholer [6]. This cDNA was digested by a BamHI and XhoI digestion protocol by standard means [204]. This purified fragment was ligated into a BamHI-XhoI digested plasmid vector, pBluescriptSKII(+) (Stratagene, LaJolla, CA). The ligation reaction was transformed into *E. coli* Top 10F' cells and grown overnight on LB agar plates with 50 ug/ml of ampicillin. White colonies were selected, and the individual clones of the construct were purified using established methods [204]. The clones were isolated and analyzed for the correct insert size by restriction enzyme digestion and gel electrophoresis. The DNA was

sequenced to confirm the existence of the *Oct-4* insert using pTAT-HA F: 5'-CCCGCGAAATTAATACGAC-3' and a Universal Forward Primer, (M13-20) and the resulting construct named pOct-4 (Applied Biosystems, Model 373A Automated Sequencer, Oklahoma State University Recombinant DNA/Protein Resource Facility).

The 5' untranslated region needed to be removed from the *Oct-4* cDNA insert and an NcoI restriction site added in order to obtain a genetic N-terminal in-frame fusion with the TAT leader in the pTAT-HA vector [91]. This was performed through 5'restriction site-directed mutagenesis as shown in Figure 5.1 and Figure 5.2. The pOct-4 was linearized by digestion with one unit of Sac I enzyme at 37°C in SuRE/Cut Buffer A (Boehringer Mannheim, Germany). The enzyme was denatured at 65°C for 20 minutes and the DNA purified through phenol extraction, precipitation and washing [204]. *Oct-4* NcoI F: 5'-cata**ccatgg**ATCCTCGAACCTGG-3' was designed (Sigma Genosys, The Woodlands, TX). The AUG is recognized efficiently as an initiation codon only when it is embedded in a suitable sequence with the optimum being: GCC**Pu**CC*AUG***G** with the most important determinants in the sequence including the G following the AUG codon and a purine, preferably adenine, preceding it by three nucleotides [205]. The linearized pOct-4 was amplified by a polymerase chain reaction using the 5'mutagenic primer and the universal forward primer. The thermocycler conditions (Perkin Elmer 9600) (PE Biosystems, Foster City, CA) include denaturation at 94 °C for 2 minutes followed by cycling conditions of 94°C, 55°C and 72°C at 30 seconds each for 35 cycles with a final extension of 72°C for 5 minutes.

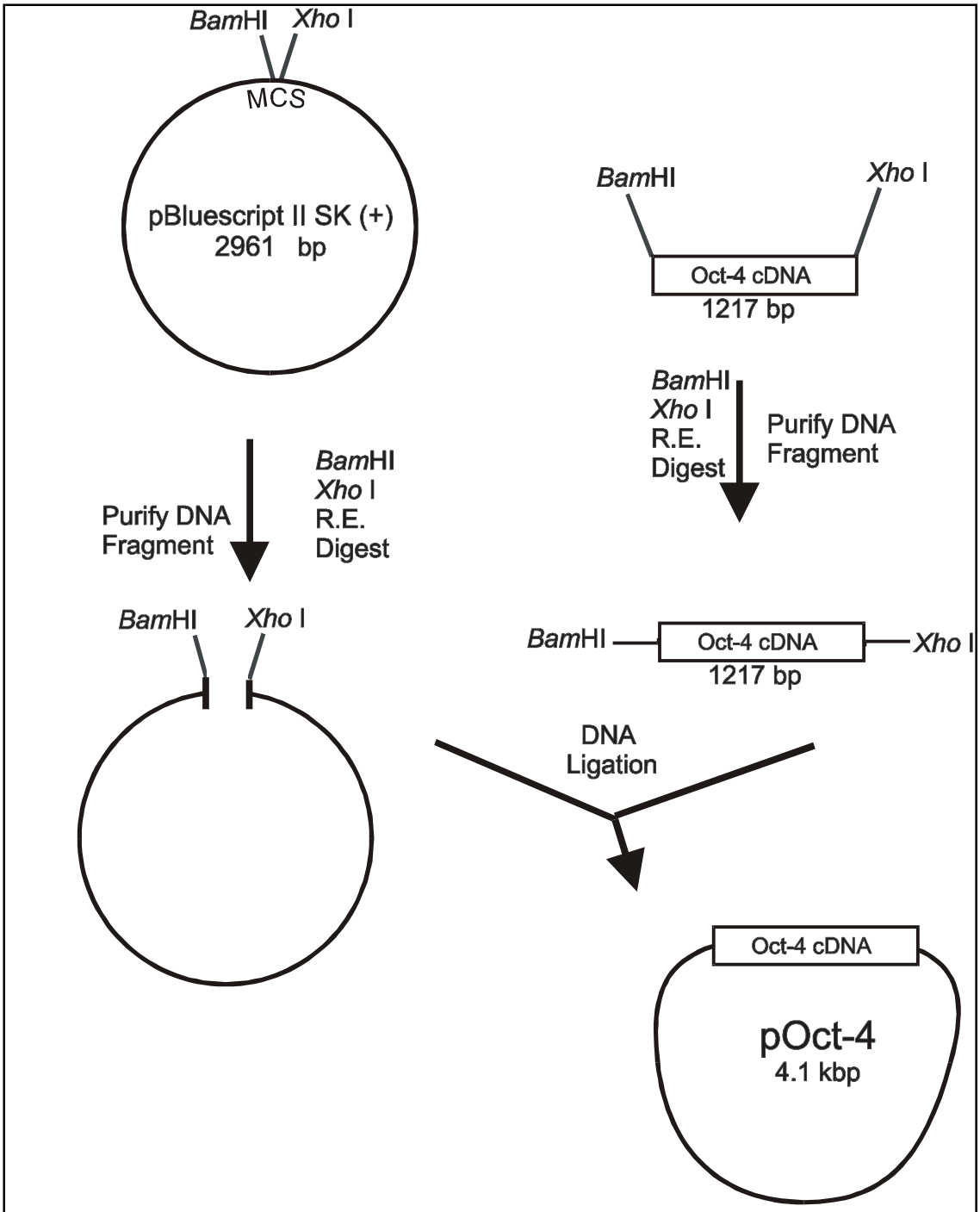

Figure 5.1 Generation of pOCT-4, the plasmid containing the *Oct-4* gene

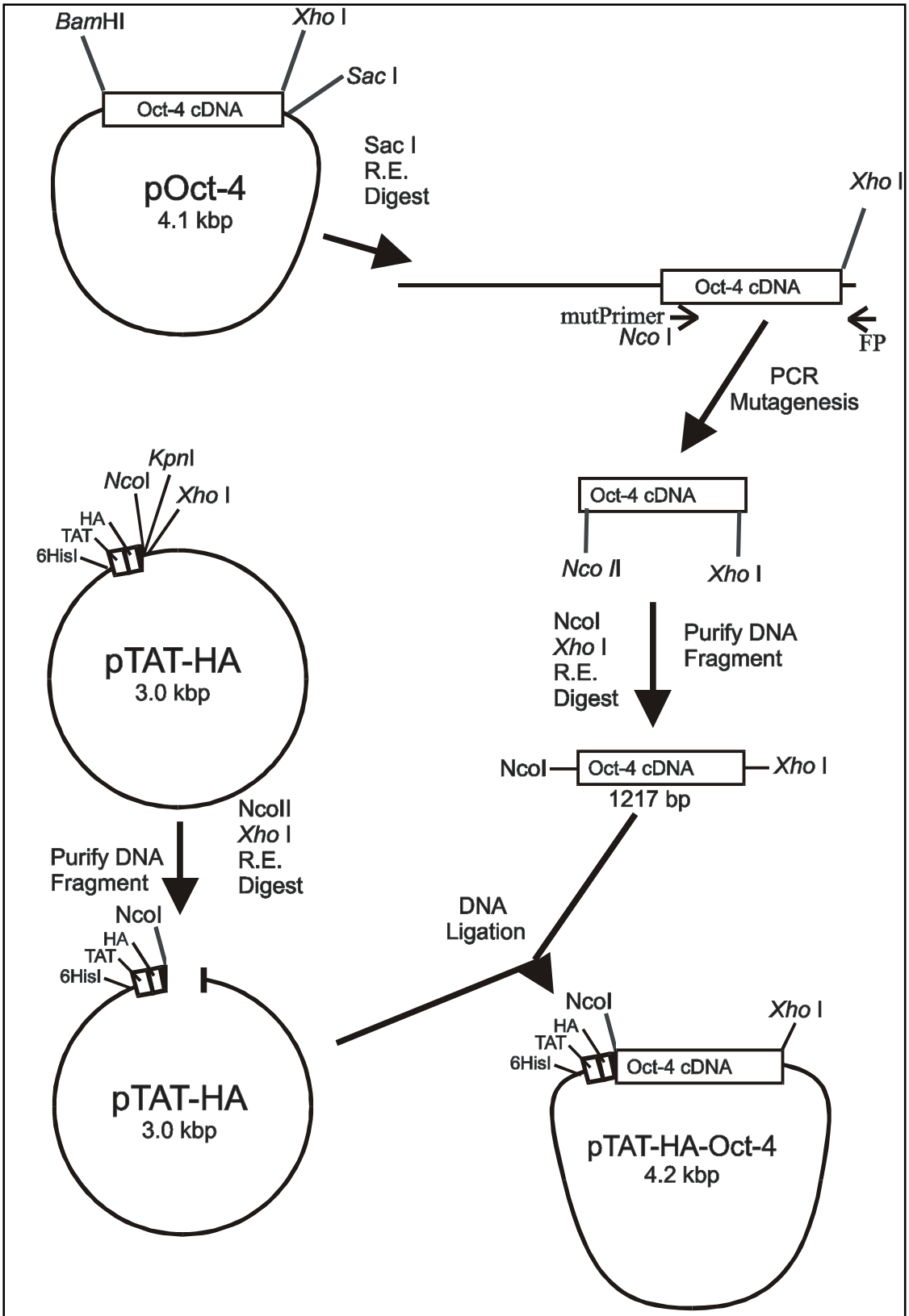

Figure 5.2 Generation of pTAT-OCT-4, the expression plasmid containing the *Oct-4* gene

A.

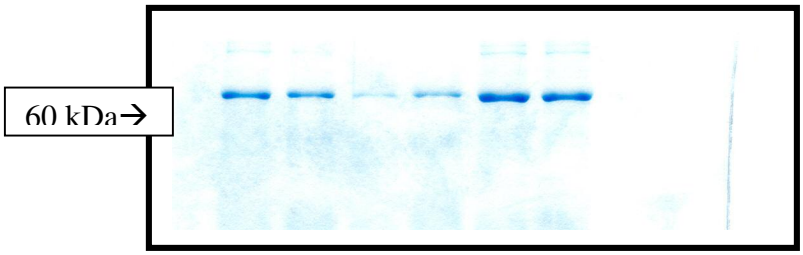

B.

Figure 5.3. GCNF-TAT-HA: Following FPLC and desalting, the GCNF-TAT-HA fusion purified protein as it appeared in two SDS-PAGE gels. (A) One gel was stained with Coomassie Blue, and the other SDS-PAGE gel (B) was stained with Invision His-tag In-gel Stain that consists of Ni^{2+} that binds specifically to oligohistidine, or the domain of His-tagged fusion proteins. 60 kDa area of gels are shown.

A.

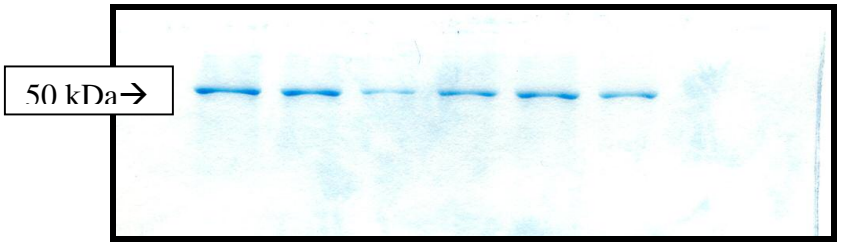

B.

Figure 5.4. BMP8b-TAT-HA: Following FPLC and desalting, the BMP8b-TAT-HA fusion purified protein as it appeared in two SDS-PAGE gels. (A) One gel was stained with Coomassie Blue, and the other SDS-PAGE gel (B) was stained with Invision His-tag In-gel Stain that consists of Ni^{2+} that binds specifically to oligohistidine the domain of His-tagged fusion proteins. 50 kDa area of gels are shown.

A.

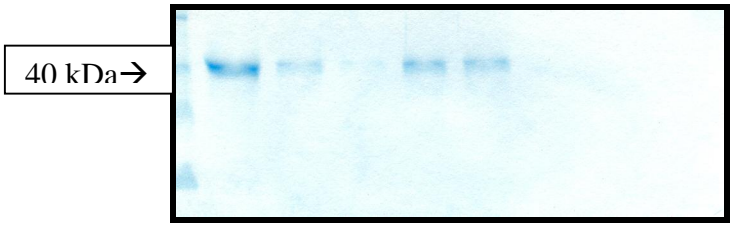

B.

Figure 5.5. Oct-4-TAT-HA: Following FPLC and desalting, the Oct-4-TAT-HA fusion purified protein as it appeared in two SDS-PAGE gels. (A) One gel was stained with Coomassie Blue, and the other SDS-PAGE gel (B) was stained with Invision His-tag In-gel Stain that consists of Ni^{2+} that binds specifically to oligohistidine the domain of His-tagged fusion proteins. 40 kDa area of gels are shown.

A.

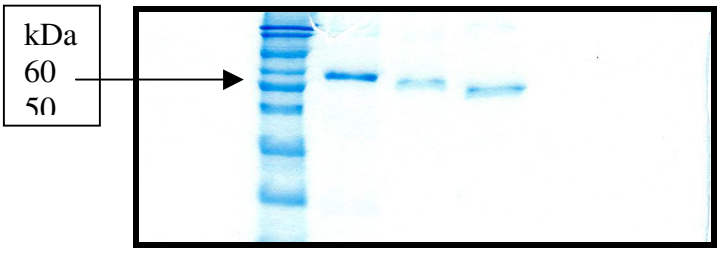

B.

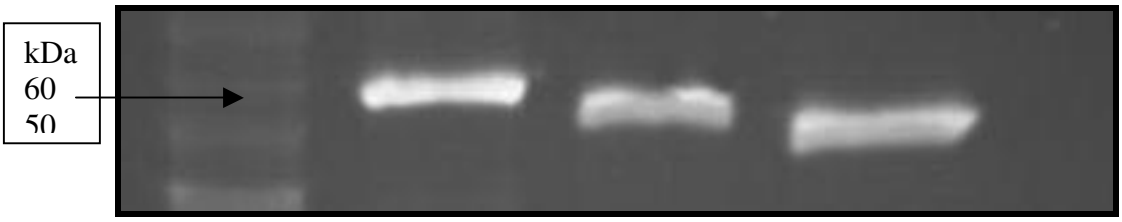

Figure 5.6. The three fusion proteins in (A) Coomassie Blue and (B) Invision His-tag In-gel Stain. The GCNF, BMP8b, and Oct-4 proteins were estimated at 60, 50 and 40 kDA, respectively, based upon the estimation that amino acids average 0.11kDA (http://www.promega.com/biomath).

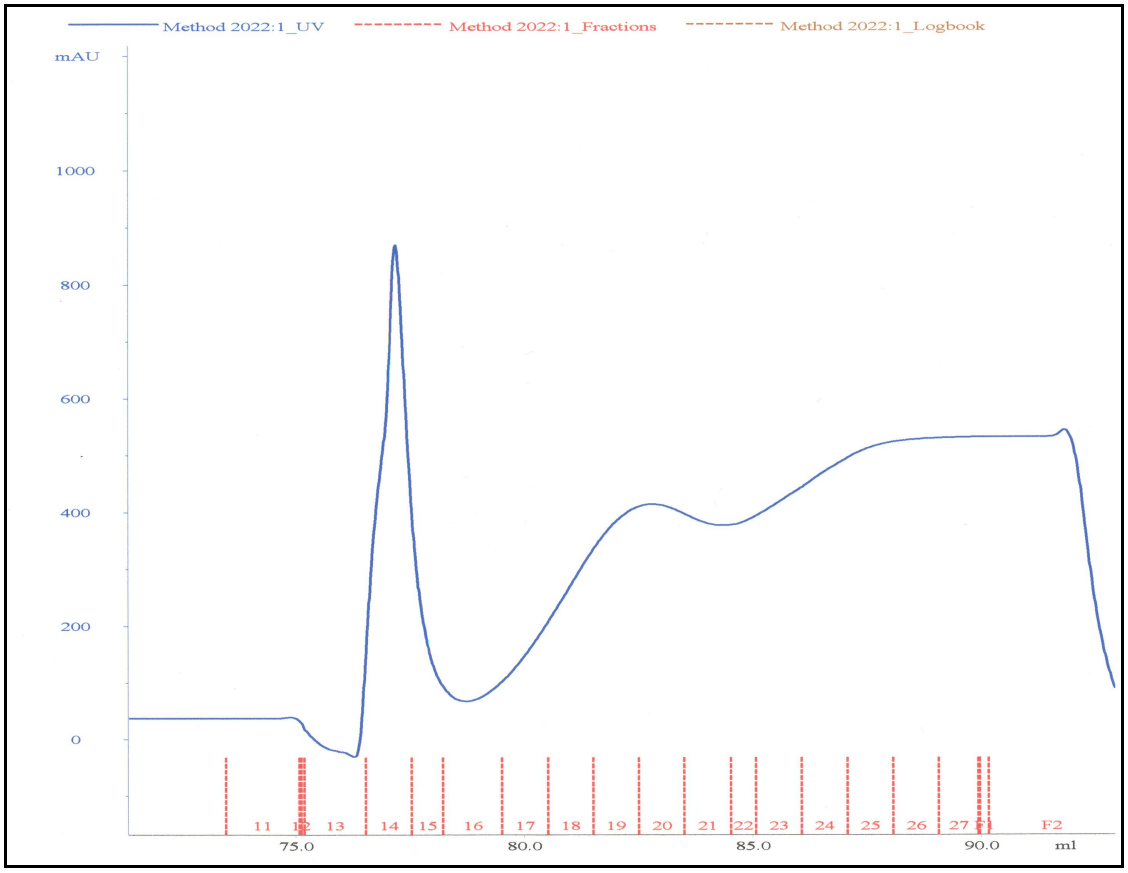

Figure 5.7. FPLC isolation of the GCNF-TAT fusion protein. Abcissa is ml of flow and fractional elutions; ordinate is absorbance. The protein is evident through the peak A_{280} absorbance.

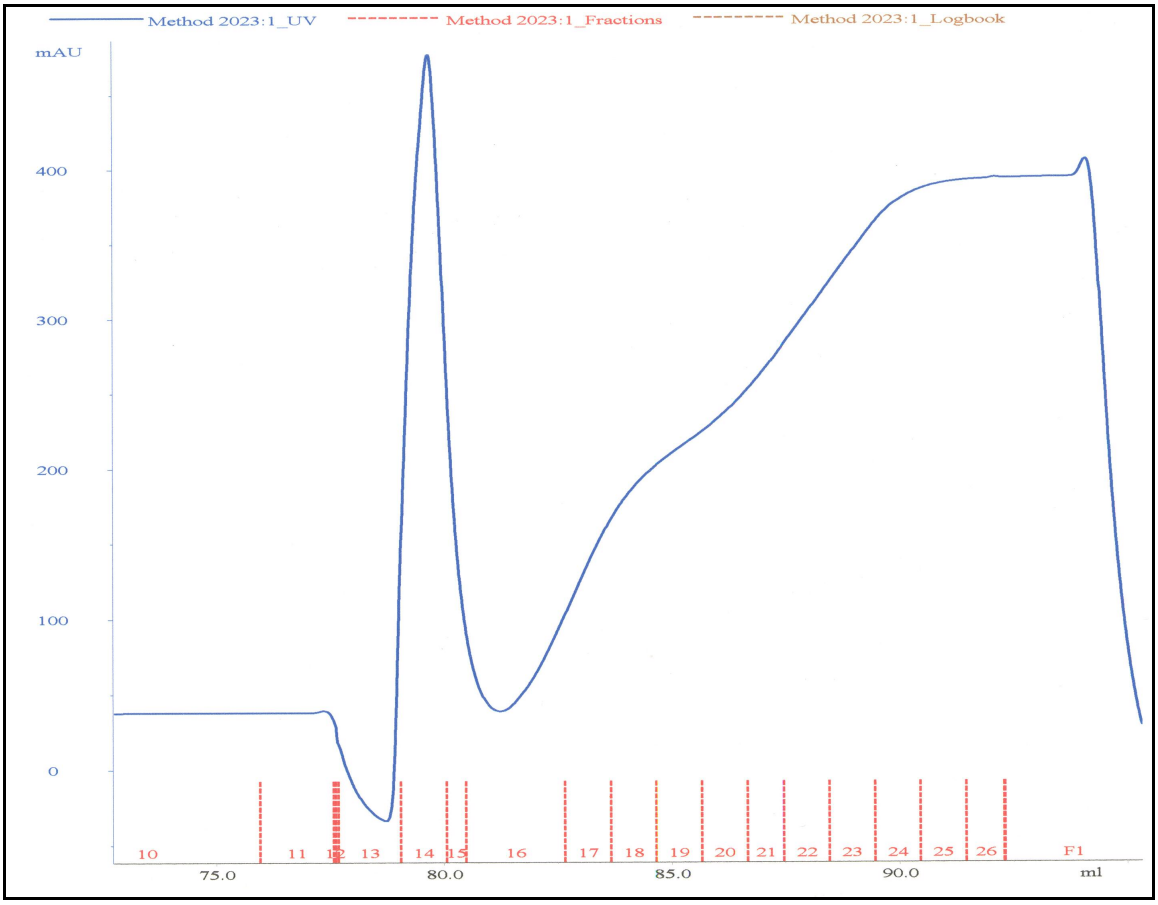

Figure 5. 8. FPLC isolation of the BMP8b-TAT fusion protein. Abcissa is ml of flow and fractional elutions; ordinate is absorbance. The protein is evident through the peak A_{280} absorbance.

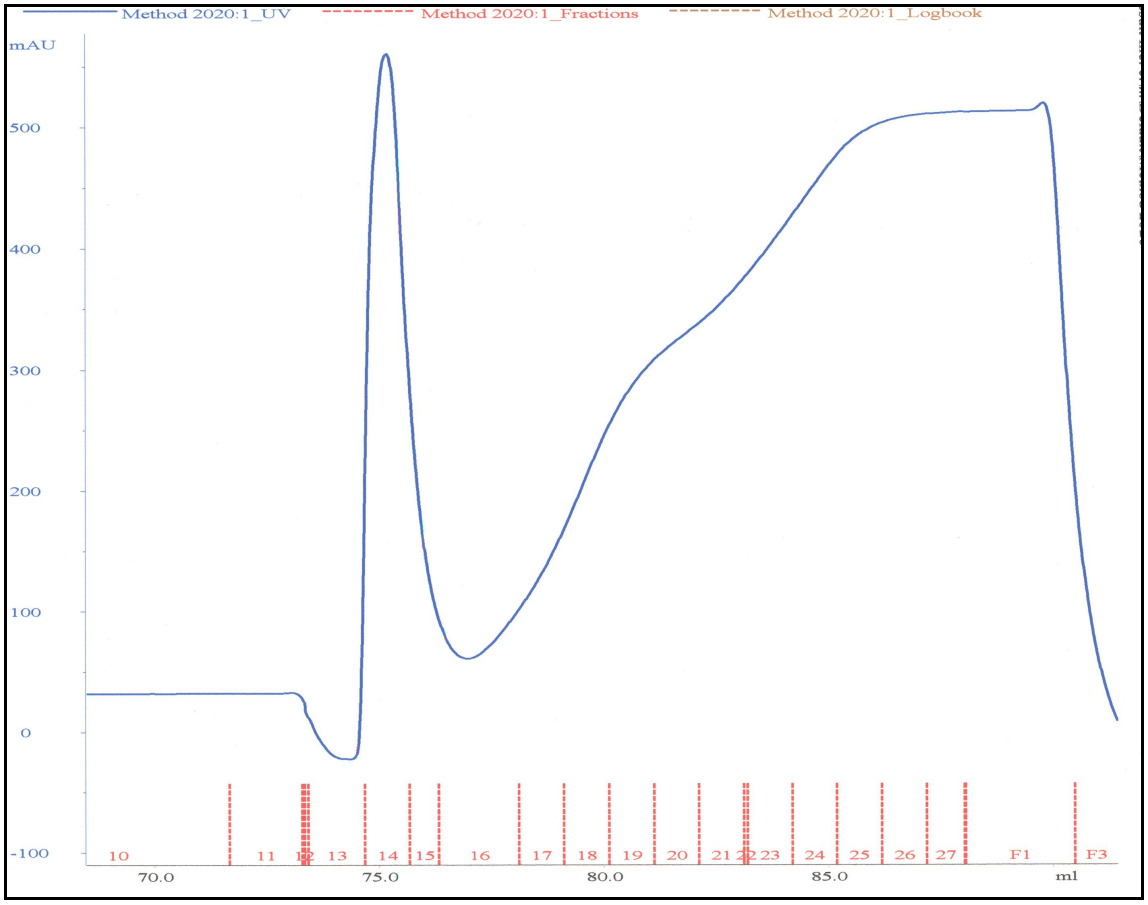

Figure 5.9. FPLC isolation of the Oct-4-TAT fusion protein. Abcissa is ml of flow and fractional elutions; ordinate is absorbance. The protein is evident through the peak A_{280} absorbance.

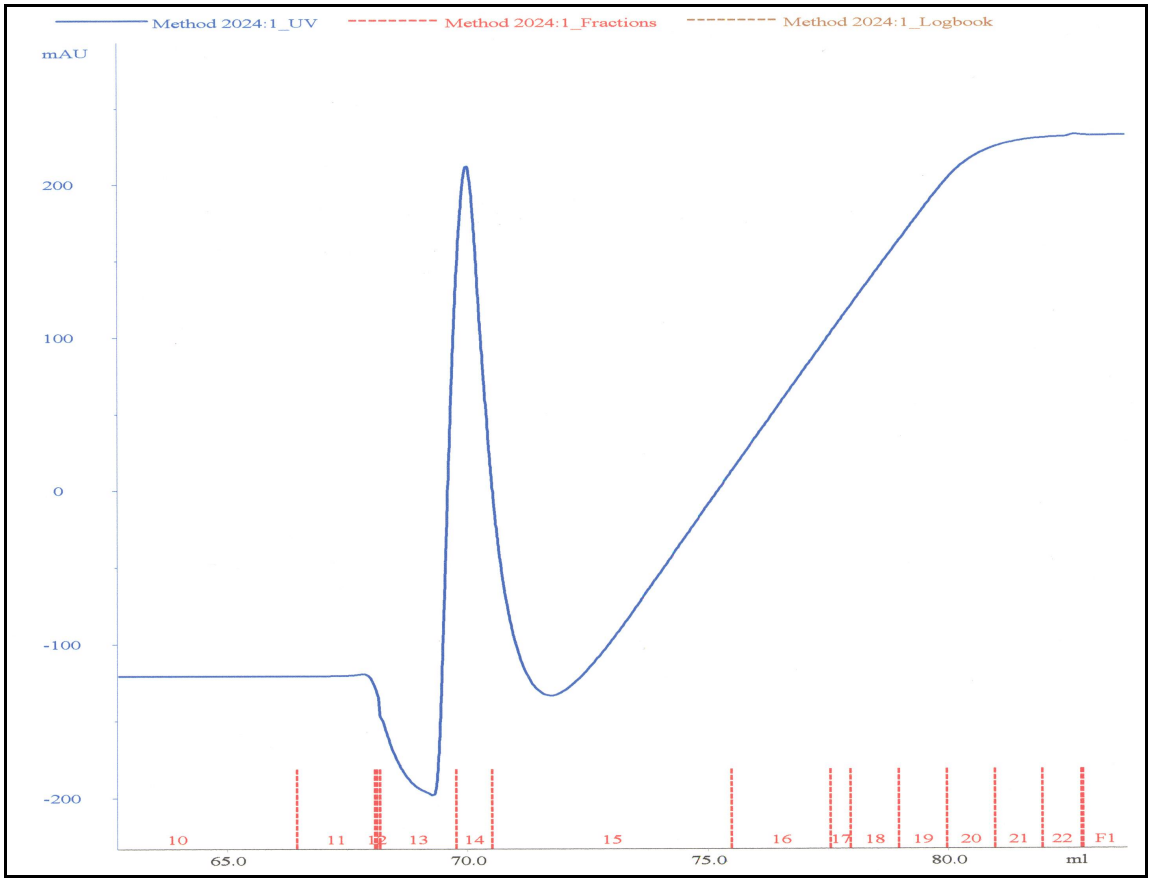

Figure 5.10. FPLC isolation of the TAT-HA fusion protein. Abcissa is ml of flow and fractional elutions; ordinate is absorbance. The protein is evident through the peak A_{280} absorbance.

5' Restriction Site-Directed Mutagenesis of *GCNF*

Similar to manipulations with the *Oct-4*, the 5'untranslated region (UTR) of the GCNF had to be deleted and a proper restriction site cloned into the gene of interest in order to obtain a genetic N-terminal in-frame fusion with the TAT leader. With the use of PCR site-directed mutagenesis, the complementary strands are separated in the denaturing step and then efficient polymerization of the PCR primers carrying specific restriction endonuclease sites are incorporated in the double-stranded plasmid. With the *GCNF* gene, we chose to ligate into the KpnI restriction site in the multiple cloning site as there were several NcoI sites within the coding region of the gene. The designed primers include: GCNF KpnI F: 5'-**ggtacc**atggCCTGTCTCATCTGTGGGG-3' and GCNF XhoIR: 5'-**ctcgag**CATCTTGGTCTCTGGCTCTTTC-3' (Sigma Genosys, The Woodlands, TX) with the KpnI and XhoI sites in bold and mutagenic bases in lower case. *Mus musculus* Germ Cell Nuclear Factor (accession U14666) was obtained from an insert of pBSSK(-)ΔNGCNF and had been confirmed through sequencing [181]. The plasmid was a gift from the lab of Austin Cooney at Baylor College of Medicine. In-frame cloning of the target *GCNF* insert was achieved through study of the deduced amino acid sequence from the Open Reading Frame (ORF) provided by Chen *et al.* [181] and verified through BioEdit translation of the nucleic acid sequence and through the description of Hummelke *et al.* [183]. Since the construct had a fragment with NcoI on both ends, a restriction site other than NcoI was required. The primers amplify a region from 421 to 1776 bp (Accession U14666) of the complete coding sequence that encodes the DNA binding domain and the ligand binding domain of GCNF [181].

5' Restriction Site-Directed Mutagenesis of *Bmp8b*

The designed primer for the *Bmp8b* gene include: Bmp8b NcoI F: 5'-cata**ccATGG**CTGCGCGTCCGGGACTCC-3' and Bmp8b XhoI R: 5'tac**ctcgag**GGACTCAGTGGCAGCCACAGGCC-3' (Sigma Genosys, The Woodlands, TX) with the NcoI and XhoI sites in bold and mutagenic bases in lower case. *Mus musculus* bone morphogenetic protein 8b (*Bmp8b*) (accession U39545) was obtained from an insert of pIRESBmp8b. The plasmid was a gift from the lab of Guang-Quan Zhao from the University of Texas Southwestern Medical Center [193]. The primers amplify a region from 187 to 1892 base pair (accession U39545) and with the mutated ends, generate an amplification product of 1218 base pair.

PCR products

Each PCR product was purified through a phenol/chloroform/isoamyl alcohol protocol [206]. The aqueous phase containing the DNA was removed following the addition of an equal volume of phenol/chloroform/isoamyl alchohol to the DNA solution. A 1/10 the volume of 7.5M ammonium acetate was added to the solution of DNA and mixed by vortexing briefly. 2.5 volumes of ice-cold 100% ethanol was added, vortexed and placed in a –70°C freezer for 15 minutes. The contents were then spun in a fixed-angle microcentrifuge for 5 minutes and the resultant supernatant aspirated with a pipetting device. The DNA pellet was washed with 750 ul of 70% ethanol, gently mixed and microcentrifuged. This supernatant was also removed, and the DNA pellet was dried. The DNA pellet was resuspended in 15 ul TE buffer [206].

Cloning of PCR Products Through the KKL Strategy

The cloning of the PCR products was achieved through a self-ligation of the linear PCR product which then generated multimeric DNA substrates for the complete cleavage of the restriction enzymes [207]. A concurrent incubation of the Klenow, T4 polynucleotide kinase and T4 DNA ligase created concatemeric DNA substrates by polishing, then phosphorylating and then ligating the PCR termini in a single step. Described briefly, 2 ul of 10X ligase buffer was added to the 15 ul of the purified PCR product DNA. dNTPS were added to 0.2 mM with 5 units of Klenow, 4 units of T4 polynucleotide kinase, 2 units of T4 DNA ligase to achieve a 25 ul final volume. The reaction was incubated at 25°C for 2 hours and the heat inactivated at 70°C for 10 min. These concatemeric ligated PCR products were then diluted to a double volume of restriction enzyme buffer and cut with 40 units of RE for 2 hours. Specifically, the BMP8b and Oct-4 PCR insert products were restriction digested with NcoI (10U/ul) and XhoI (20U/ul) with the appropriate restriction buffer (NEB Buffer 2 with BSA) for two hours at 37°C. The GCNF PCR insert products were restriction digested with XhoI (10U/ul) and KpnI (10U/ul) in the appropriate restriction buffer (NEB Buffer 1 with BSA) for two hours at 37°C. The individual digested PCR products were recovered and purified through the Microcon Centrifugal Filter Unit (Millipore, Billerica, MA).

Vector Preparation

On a 3% TAE agarose gel, we ran 15 ul of the pTAT-HA vector (.47ug/ul). The DNA fragment was recovered using a spin column [208]. The column purified DNA was

then treated with a phenol: chloroform extraction and ammonium acetate alcohol precipitation as described previously [204]. The DNA was washed with 750 ul of 70% ETOH and centrifuged to a pellet, dried and resusupended in 15 ul TE.

Five microliters of the TAT-HA extracted and purified vector was restriction digested with 1 ul of NcoI (10U/ul) and 1 ul of XhoI (20U/ul) in the appropriate restriction enzyme buffer (NEB Buffer 2 with BSA) in a total volume of 25 ul. After incubation overnight at 37°C, the DNA was electrophoresed on a 3% agarose gel for the BMP8b and Oct-4 PCR products. A similar restriction digest was performed for the *GCNF* gene with KpnI (10U/ul) and XhoI (20U/ul) with NEB Buffer 1 with BSA. The "cut" vector DNA was extracted, purified as described above and hydrated with 20ul DDI (distilled deionized) water.

Ligation and Transformation

Using the Promega BioMath Calculator (http://www.promega.com/biomath/default.htm), the dsDNA in micrograms was calculated to picomoles of both the vector and insert. Using a 1:3 ratio of vector to insert for the ligation, T4DNA ligase (Invitrogen Corp., Carlsbad, CA) and the appropriate buffer with the cohesive ended vector and insert were incubated at 14°C for 20 hours. The reaction was inactivated with 1 ul of EDTA (ethylenediaminetetraacetic acid).

BL21-Gold(DE3)LysS cells and BLR (Stragagene, La Jolla, CA) cells were made competent by treating the cells with $RbCl_2$ and $CaCl_2$ to modify the cell wall and membrane. These particular *E.coli* strains were chosen due to their lack of particular proteases (such as Lon and OmpT) which degrade recombinant proteins [209]. Five ul

of the ligation reaction with 25 ul DDI water were added to 50 ul of the competent cells and placed on ice for 30 minutes with gentle agitation every 10 minutes. The transformation mixture was placed in a 42°C waterbath for 2 minutes to heat shock the cells. The transformation reaction was added to 400 ul of 2YT broth and incubated in a 37°C waterbath for 30 minutes. One hundred ul of the transformation reaction was grown on LB (with 50 ug/ml ampicillin) plates and grown in a 37°C incubator overnight.

Miniprep Purification and Selection of Plasmid DNA

Plasmid DNA was extracted from the bacterial DNA using a Qiagen Miniprep protocol or through a traditional alkaline extraction [204]. The purified miniprep DNA was then digested with restriction enzymes, electrophoresed on an agarose gel and visualized by ethidium bromide staining to confirm the identity of the appropriate sized inserts in the recombinant plasmids. The purified plasmid DNA was subjected to dideoxy chain termination sequencing (Applied Biosystems, Model 373A Automated Sequencer, Oklahoma State University Recombinant DNA/Protein Resource Facility) to verify proper insert alignment in frame with the reading frame and containing no mutations in the constructs. The oligonucleotide sequences for the primers used are pTAT-HA forward 5'-CCCGCGAAATTAATACGAC-3' and the pTAT-HA reverse 5'-GTCCCATTCGCCATTCAGG-3' (Sigma Genosys, The Woodlands, TX).

Protocol for Protein Expression and Purification with FPLC

The pTAT-HA-GCNF, pTAT-HA-Bmp8b and pTAT-HA-Oct-4, were previously transformed into BLR, BL21-Gold(DE3)pLysS, and BLR (Stragagene, La Jolla, CA)

cells respectively, and the recombinant protein products were expressed, purified and assayed as described below. Two hundred ml of 2YT overnight culture of the isolates were grown with ampicillin at 50ug/ml. The following morning, the entire volume was inoculated into 1 L of 2YT plus 400 uM IPTG and shaken (225 rpm) for 8 hours at 37°C. The cell pellet was harvested via centrifugation (6000g X 15 min, 4°C). The pellets were frozen for 30 minutes @-20°C or overnight to maximize the cell breakage during the subsequent thaw. The cells were then thawed at 37°C for 15-20 minutes and resuspended in 30 mls of Buffer 1 (20mM Tris-HCl, pH8.0). The sample is highly viscous and requires repeated vortexing and pipetting until resuspended. We sonicated the cells on ice (4 X 15 sec) with the Fisher Scientific 550 Sonic Dimembrator (Fisher Scientific, Pittsburgh, PA) and centrifuged at 6000 X G for 15 minutes at 4°C in a Beckman Avanti 30 Centrifuge (Beckman Coulter, Inc., Fullerton, CA). The pellet was resuspended with 25 ml of 20 ml of Buffer 2 (20mM Tris-HCl, 0.5M NaCl, 2M urea and 2% Triton X-100). We continued washing with Buffer 2 by resuspending the pellet and centrifugation at 6000 X G for 15 minutes at 4°C in a Beckman Avanti 30 Centrifuge until the supernatant was clear. A final wash with Buffer 1 removed the Triton X-100. The pellet was resuspended in 5-20 ml of Buffer A1 (20 mM Tris-HCl, 0.5 M NaCl, 20 mM Imidazole, 6 M Guanidine-HCl, 5 mM Mercaptoethanol, pH 8.0). The GCNF recombinant protein was resistant to clearing, and we added the sample to a sterile microcentrifuge tube and spun it at 13,500 rpm at 4°C for 30 minutes. Then we filtered the GCNF protein through a 0.45 um filter to sterilize the solution (ISC, BioExpress, Kaysville, Utah).

The TAT-HA recombinant proteins were produced in a fusion form to include the hemagluttinin tag for identification and the hexahistadine region to facilitate purification by affinity chromatography. The chromatography was achieved by binding of the protein to an immobilized metal ion adsorbent with a subsequent specific elution chemistry [203]. The metal-chelate affinity chromatography is a highly selective method that relies on the binding affinity of the polyhistidine to nickel chelates tethered to the chromatographic matrix [203].

In preparation of use of the AKTA FPLC (Amersham Pharmacia, Piscataway, NJ), we washed the HisTRAP (Amersham Pharmacia, Piscataway, NJ) column as described in the literature with autoclaved millipore water. The column, packed with chelating Sepharose, allows for binding and elution of histidine-tagged fusion proteins. Since our proteins were expressed as inclusion bodies, the purification required the 6 M guanidine hydrochloride, or purification under denaturing conditions, with four elution steps of increasing imidazole concentrations. The protein sample (5-10 ml) was loaded and the flow rate was 0.1-1 ml/minute. The column was washed with Buffer A1 (described above) and then 10 ml of Buffer A2 (20mM Tris-HCL, 0.5M NaCl, 20 mM Imidazole, 6 M Urea, 5 mM Mercaptoethanol, pH 8.0). Refolding of the bound protein is performed by the linear 6-0 M urea gradient, starting with Buffer A2 and finishing with 100% Buffer B1 (20mM Tris-HCl, 0.5 M NaCl, 20 mM Imidazole, 5 mM Mercaptoethanol, pH 8.0). Elution of the refolded recombinant protein begins with Buffer B1 and ends with Buffer B2 (Buffer B1 plus 500 mM Imidazole). The flow rate for the elution was 1 ml/minute. Following use of the FPLC apparatus, the desalting or PD-10 column removed the imidazole and continued the refolding of the $(His)_6$-tagged

protein. The GCNF, BMP8b, and Oct-4 proteins were estimated at 60, 50 and 40 kDA, respectively, based upon the estimation that amino acids average 0.11 kDA (http://www.promega.com/biomath).

Quantitation, SDS-PAGE and His-tag Staining

Quantitation of the amount of the protein was accomplished using the BCA Protein Assay Kit (Pierce Biotechnology, Inc. Rockford, IL). The assay is based on the reduction of copper ions by protein coupled with the colorimetric detection of the cuprous cation using bicinchoninic acid, and then comparing the results to the binding of different amounts of a standard protein, usually BSA. The BCA protein assay with BSA standards was run to determine the concentrations of the three purified proteins. The purple-colored reaction product of this assay is formed by the chelation of the two molecules of BCA by the cuprous ion. Using the MultiImage Light Cabinet with the AlphaImager 2200 (Alpha Innotech, San Leandro, CA), BCA concentrations were determined. With concentrations of proteins determined, we added glycerol to prepare a final 10% glycerol concentration. The proteins were then flash frozen.

We used one-dimensional gel electrophorectic separation of the proteins under denaturing conditions, SDS-PAGE, to determine the size of each recombinant protein [210-212]. Following the FPLC, we ran two 10% SDS-PAGE gels of each study. One gel was stained with Coomasie Blue (EM Science, Germany) and the other gel was stained to detect the histadine tag through use of the Invision His-tag In-gel Stain and BenchMark His-tagged protein standard (Invitrogen Corp., Carlsbad, CA).

.

Immunocytochemistry of TAT Fusion Proteins

We grew Vero cells in a humidified CO_2 incubator until confluent in a 24-well plate and washed the cells with 1 ml of cold PBS (pH~7.5). We then added 0.5 ml of media with 2 ug of one of the TAT fusion proteins to each well. We added 0.5 ml of 3.7% Formaldehyde fixation solution and incubated for 30 minutes with a subsequent wash with PBS. We then permeabilized the cells with 0.5 ml of 0.5% Triton X/PBS and incubated at room temperature for 30 minutes followed with a wash of PBS. We added 0.5 ml of blocking buffer (PBS with 1% final concentration of FBS and 0.1% final concentration of Tween-20) to each well tested. We then added 0.5 ml of primary hemagglutinin antibody (HA) (1:1000 dilution in PBS) (Covance Research Products, Berkeley, CA) and incubated for 1 hour. This antibody recognizes the influenza hemagglutinin epitope. We then added 48 ul of the secondary FITC-labeled (fluorescein isothiocynate) antibody to 12 ml of 1X PBS. This secondary antibody is goat, anti-mouse IgG (heavy and light chain reactive) from Covance Research Products. Finally we washed the cells with 1 ml of PBS, and analyzed the cells for transduction using immunofluorescence microscopy.

Results

FPLC isolation of the proteins are found in Figure 5.7 (GCNF-TAT-HA), Figure 5.8 (BMP8b-TAT-HA), Figure 5.9 (Oct-4 TAT-HA) and Figure 5.10 (TAT-HA). Specific fractions were chosen from the chromatogram for further study on SDS-PAGE

gels. Verification of protein size and oligohistidine tag were verified through Coomassie staining and His-tag In-gel staining. Fractions containing the eluted proteins were pooled and subjected to buffer exchange using a Hi-Trap Desalting or PD-10 column before the flash freezing and storage of the protein.

Fractions 13, 14, 15, 16, 17, 19, and 20 were selected from the GCNF-TAT-HA chromatogram (Figure 5.7) and electrophoresced on two SDS-PAGE gels. GCNF-TAT-HA Coomassie stained fractions of the 14, 15, 16, 17, 19 and 20 are found in Figure 5.3A, and the same fractions stained with Invision His-tag In-gel Stain are found in Figure 5.3B. The presence of the oligohistidine tag and the proper size (60 kDa) of the GCNF-TAT-HA protein were therefore, verified. Fractions 19 and 20 were chosen for the desalting process and flash freezing.

BMP8b-TAT-HA FPLC fractions 13, 14, 15, 16, 17, 18 and 19 (Figure 5.8) were selected from the chromatogram and electrophoresced on two SDS-PAGE gels. The BMP8b-TAT-HA fractions (14-19) are found in Figure 5.4A with Coomassie stain and the His-tag In-gel Stain fractions are found in Figure 5.4B. The proper size (50 kDa) of the BMP8b-TAT-HA protein was verified. Fractions of BMP8b-TAT-HA 14, 15 and 18 were selected for the desalting process and flash freezing.

Oct-4-TAT-HA fractions 14, 15, 16, 19 and 20 were selected from the Oct-4-TAT-HA chromatogram (Figure 5.9). These fractions are found in Figure 5.5A with Coomassie stain on the SDS-PAGE gel, and the same fractions are shown in Figure 5.5B with the His tag In-gel Stain. The presence of the oligohistidine tag and the proper size (40 kDa) of the Oct-4 TAT-HA protein were verified. Fractions 14, 19 and 20 were selected for the desalting process and flash freezing. Figure 5.10 is the TAT-HA control

chromatogram. Figure 5.6 demonstrates the three TAT fusion proteins of interest in Coomassie Blue stain and Invision His-tag In-gel stain.

Following the immunocytochemistry protocol described, the fluorescence of GCNF-TA-HA, BMP8b-TAT-HA and Oct-4-TAT-HA was evident inside cells of the separate wells of Vero cells (Data not shown). This data indicates protein transduction of the recombined proteins. It also indicates that the influenza hemagglutinin epitope was present in the recombinant protein and it was bound to the secondary FITC-labeled (fluorescein isothiocynate) antibody.

Discussions

The goal of this project was to produce three TAT-HA fusion proteins, verify proper insertion of the target genes and verify protein transduction of those proteins. The fusions proteins were purified through FPLC technology and verification of the proteins were conducted through Coomassie staining and His-tag staining of SDS-PAGE gels. Immunocytochemistry verified protein transduction into the Vero cells and the presence of the hemagglutinin epitope on the recombined protein.

One of the original goals of the project was to use these fusion proteins for subsequent studies of pluripotency. Separate trials were conducted on both murine embryos and Vero cells using both the GCNF-TAT-HA and the BMP8b-TAT-HA fusion proteins. Results seem to indicate an up-regulation of the Oct-4 gene through the transduction of the BMP8b-TAT-HA fusion protein. Results, however were inconsistent within the assay trials and between trials.

While other TAT-HA fusion proteins in our lab have been successful in protein transduction trials, we must consider variables that cause the BMP8b-TAT-HA and GCNF-TAT-HA protein to not function consistently in cellular trials. These proteins are in imidazole (approximate pH of 8) when eluted from the FPLC column. When the salt is removed with cell culture media (approximate pH of 7-7.5) these proteins tend to precipitate due to their high hydrophobic residue content. Even when these proteins were diluted and slowly dialyzed, we consistently got a precipitate. The limiting factor of the protocol seems to be the desalting component of these specific proteins. Another limiting factor could possibly be that the recombinant proteins are toxic to living cells; we've experienced that the higher concentrations of some of the proteins seem to have deleterious effects on the life span of the cells in culture or living murine embryos being tested. While we were successful in achieving pure fusion proteins with transducible properties, we were not able to record a consistent TAT-mediated protein delivery of functional full-length proteins.

The effort to exploit the therapeutic capabilities of a TAT-mediated protein delivery with these particular proteins (GCNF-, BMP8b-, Oct-4-TAT-HA) provide several interesting future goals. The Oct-4-TAT-HA vector was produced for subsequent use in murine ES cells to increase the percent viability of the ICM cells; embryonic blastocyst ICM's could be isolated and ES cell cultures established and treated with the Oct-4-TAT-HA protein. GCNF-TAT-HA and BMP8b-TAT-HA vectors were produced to act as repressors and promoters, respectively, of the DE for Oct-4 production. The BMP8b purified protein could be used to up-regulate Oct-4 in somatic cells such as murine fetal fibroblast (MFF) cells to move differentiated cells to a more pluripotent

state. The GCNF vector and purified protein could be used to verify transduction and act as a negative control in this reprogramming of adult somatic differentiated cells. GNCF-TAT-HA protein could also positively regulate differentiation; several genes up-regulated during differentiation could be quantitatively measured. In the future, scientists could use these constructs to produce the fusion proteins necessary to regulate pluripotency in somatic and stem cells.

REFERENCES

1. Donovan, P.J. and J. Gearhart, *The End of the Beginning for Pluripotent Stem Cells.* Nature, 2001. **414**: p. 92-97.
2. Pesce, M., Gross, M.K. and Scholer, H.R., *In Line with our Ancestors: Oct-4 and the Mammalian GERM.* BioEssays, 1998b. **20**(9): p. 722-732.
3. Pesce, M., Wang, X., Wolgemuth, D. and Scholer, H.R., *Differential Expression of the Oct-4 Transcription Factor During Mouse Germ Cell Differentiation.* Mechanisms of Development, 1998a. **71**: p. 89-98.
4. Palmieri, S.L., et al., *Oct-4 Transcription Factor is Differentially Expressed in the Mouse Embryo during Establishment of the First Two Extraembryonic Cell Lineages Involved in Implantation.* Developmental Biology, 1994. **166**(No. 1): p. 259-267.
5. Herr, W., Cleary, M., *The POU Domain: Versatility in Transcriptional Regulation by a Flexible Two-in-One DNA-binding Domain.* Genes and Development, 1995. **9**: p. 1679-1693.
6. Scholer, H.R., et al., *New type of POU domain in germ line-specific protein Oct-4.* Nature, 1990a. **344**: p. 435-439.
7. Pan, G.J., et al., *Stem cell pluripotency and transcription factor Oct4.* Cell Res, 2002. **12**(5-6): p. 321-9.
8. Yeom, Y.I., Fuhrmann, G., OVitt, C.E., Brehm, A., Ohbo, K., Gross, M., Hubner, K. and Scholer, H., *Germline Regulatory Element of Oct 4 Specific for the Totipotent Cycle of Embryonal Cells.* Developmental Biology, 1996. **122**: p. 881-894.
9. Yoshimizu, T., et al., *Germline-specific expression of the Oct-4/green fluorescent protein (GFP) transgene in mice.* Dev Growth Differ, 1999. **41**(6): p. 675-84.
10. Ovitt, C.E., Scholer, H.R., *The Molecular Biology of Oct-4 in the Early Mouse Embryo.* Molecular Human Reproduction, 1998. **4**(11): p. 1021-1031.
11. Brehm, A., Ovitt, C.E., Scholer, H.R., *Oct-4: more than just a POUerful marker of the mammalian germline?* APMIS, 1998. **106**: p. 114-126.
12. Nordhoff, V., Hubner, K., Bauer, A., Orlova, I., Malapetsa, A., Scholer, H.R., *Comparative Analysis of Human, Bovine, and Murine Oct-4 upstream Promoter Sequences.* Mammalian Genome, 2001. **12**(4): p. 309-317.
13. Scholer, H.R., Hatzopoulos, A.K., Balling, R., Suzuki, N. and Gruss, P., *A family of octamer-specific proteins present during mouse embryogenesis: evidence for germline-specific expression of an Oct factor.* EMBO Journal, 1989b. **8**: p. 2543-2550.
14. Yeom, Y.I., et al., *Structure, Expression and Chromosomal Localization of the Oct-4 Gene.*Mech. Dev., 1991. **35**: p. 171-179.
15. Nichols, J., Zevnik, B., Anastassiadis, K., Niwa, H., Klewe-Nebenius, D., Chambers, I., Scholer, H., and Smith, A., *Formation of Pluripotent Stem Cells in the Mammalian Embryo Depends on the POU Transcription Factor Oct 4.* Cell, 1998. **95**: p. 379-391.
16. Moldovan, N.I., *Functional adaptation: the key to plasticity of cardiovascular "stem" cells?* Stem Cells Dev, 2005. **14**(2): p. 111-21.

17. Rajpert-De Meyts, E., et al., *Developmental expression of POU5F1 (OCT-3/4) in normal and dysgenetic human gonads.* Hum Reprod, 2004. **19**(6): p. 1338-44.
18. Gidekel, S., et al., *Oct-3/4 is a dose-dependent oncogenic fate determinant.* Cancer Cell, 2003. **4**(5): p. 329-30.
19. Reubinoff, B.E., et al., *Embryonic stem cell lines from human blastocysts: somatic differentiation in vitro.* Nat Biotechnol, 2000. **18**(4): p. 399-404.
20. Niwa H., M.J., Smith A.G., *Quantitative Expression of Oct-3/4 Defines Differentiation, Dedifferentiation or Self-Renewal of ES Cells.* Nature Genetics, 2000. **24**(4): p. 372-376.
21. Boiani, M., et al., *Oct4 Distribution and Level in Mouse Clones: Consequences for Pluripotency.* Genes and Development, 2002. **16**: p. 1209-1219.
22. Zhang, H., et al., *Effect of nicotine on Oct-4 and Rex-1 expression of mouse embryonic stem cells.* Reprod Toxicol, 2005. **19**(4): p. 473-8.
23. Ford, K.G., et al., *Protein Transduction: An Alternative To Genetic Intervention?* Gene Therapy, 2001. **8**(1): p. 1-4.
24. Hawiger, J., *Noninvasive Intracellular Delivery of Functional Peptides and Proteins.* Current Opinion Chemical Biology, 1999. **3**: p. 89-94.
25. Lindgren, M., Hallbrink, M., Prochiantz, A., and Langel, U., *Cell-penetrating peptides.* Trends Pharmacological Sciences, 2000. **21**: p. 99-103.
26. Schwarze, S.R.D., Steven F., *In vivo Protein Transduction: Intracellular Delivery of Biologically Active Proteins, Compounds and DNA.* Trends in Pharmacological Sciences, 2000. **21**(2): p. 45-8.
27. Schwarze, S.R., Ho, A., Vocero-Akbani, A., Dowdy, S.F., *In Vivo Protein Transduction: Delivery of a Biologically Active Protein into the Mouse.* Science, 1999. **285**(5433): p. 1569-1572.
28. Schwarze, S.R. and S.F. Dowdy, *In vivo protein transduction: intracellular delivery of biologically active proteins, compounds and DNA.* Trends in Pharmacological Sciences, 2000. **21**(2): p. 45-8.
29. Wadia, J.S. and S.F. Dowdy, *Modulation of cellular function by TAT mediated transduction of full length proteins.* Curr Protein Pept Sci, 2003. **4**(2): p. 97-104.
30. Nagahara, H., et al., *Transduction of full-length TAT fusion proteins into mammalian cells: TAT-p^{27kipl} induces cell migration.* Nature Medicine, 1998. **4**: p. 1449-1452.
31. Fuchs, E., Segre, J.A., *Stem Cells: A New Lease on Life.* Cell, 2000. **100**: p. 143-155.
32. Hansis, C., Tang, Y., Grifo, J., Krey, L., *Analysis of Oct-4 Expression and Ploidy in Individual Human Blastomeres.* Molecular Human Reproduction, 2001. **7**(2): p. 155-161.
33. *National Institutes of Health (NIH) Update on Existing Human Embryonic Stem Cells*. 2001, U>S> Department of Health and Human Services National Institutes of Health.
34. Derossi, D., G. Chassaing, and A. Prochianta, *Trojan Peptides: The Penetratin System for Intracellular Delivery.* Trends in Cell Biology, 1998. **8**: p. 84-87.
35. Frankel, A.D. and C.O. Pabo, *Cellular uptake of the tat protein from human immunodeficiency virus.* Cell, 1988. **55**: p. 1189-1193.

36. Green, M., Loewenstein, Paul M., *Autonomous Functional Domains of Chemically Synthesized Human Immunodeficiency Virus Tat Trans-Activator Protein.* Cell, 1988. **55**: p. 1179-1188.
37. Fawell, S., et al., *TAT-mediated delivery of heterologous proteins into cells.* Proceedings of National Academy of Sciences USA, 1994. **91**: p. 664-668.
38. Scholer, H.R., Balling, R., Hatzopoulos, A.K., Suzuki, N. and Gruss, P., *Octamer Binding Proteins Confer Transcriptional Activity in Early Mouse Embryogenesis.* EMBO Journal, 1989a. **8**: p. 2551-2557.
39. Scholer, H.R., Dressler, G.R., Balling, R., Rohdewohld, H. and Gruss, P., *Oct-4: A Germline -Specific Transcription Factor Mapping to the Mouse T-Complex.* EMBO Journal, 1990b. **9**: p. 2185-2195.
40. Takeda, J., Seino, S. and Bell, G.I., *Human Oct-3 Gene Family: cDNA sequences, Alternative Splicing, Gene Organization, Chromosomal Localization, and Expression at Low Levels in Adult Tissues.* Nucl. Acids Res., 1992. **20**: p. 4613-4620.
41. Okamoto, K., Okazawa, H., Okuda, A., Sakai, M., Muramatsu, M., Hamada, H., *A Novel Octamer Binding Transcription Factor Is Differentially Expressed in Mouse Embryonic Cells.* Cell, 1990. **60**: p. 461-472.
42. van Eijk, M.J.T., et al., *Molecular Cloning, Genetic Mapping, and Developmental Expression of Bovine POU5F1.* Biology of Reproduction, 1999. **60**: p. 1093-1103.
43. Kirchhof, N., et al., *Expression Pattern of Oct-4 in Preimplantation Embryos of Different Species.* Biological Reproduction, 2000. **63**(6): p. 1698-1705.
44. Fuhrmann, G., Sylvester, I., Scholer, H.R., *Repression of Oct-4 During Embryonic Cell Differentiation Correlates with the Appearance of TRIF, A Transiently Induced DNA-Binding Factor.* Cellular and Molecular Biology, 1999. **45**(5): p. 717-724.
45. Rosner, M.H., et al., *A POU-domain transcription factor in early stem cells and germ cells of the mammalian embryo.* Nature, 1990. **345**(6277): p. 686-92.
46. Scholer, H.R., *Octamania: The POU Factors in Murine Development.* Trends in Genetics, 1991b. **7**: p. 323-329.
47. Rathjen, J., Lake, J., Bettess, M.D., Washington, J.M., Chapman, G., Rathjen, P., *Formation of a Primitive Ectoderm like Cell Population, EPL cells, from ES Cells in Response to Biologically Derived Factors.* Journal of Cell Science, 1999. **112**: p. 601-612.
48. Adjaye, J., Bolton,k V., Monk, M., *Developmental Expression of Specific Genes Detected in High-Quality cDNA Libraries from Single Human Preimplantation Embryos.* Gene, 1999. **237**(2): p. 373-383.
49. Hansis, C., Grifo, J., Krey, L., *Oct-4 Expression in Inner Cell Mass and Trophectoderm of Human Blastocysts.* Molecular Human Reproduction, 2000. **6**(11): p. 999-1004.
50. Bhattacharya, B., et al., *Gene expression in human embryonic stem cell lines: unique molecular signature.* Blood, 2004. **103**(8): p. 2956-64.
51. Ramalho-Santos, M., et al., *"Stemness": transcriptional profiling of embryonic and adult stem cells.* Science, 2002. **298**(5593): p. 597-600.

52. Mitalipov, S.M., et al., *Oct-4 expression in pluripotent cells of the rhesus monkey.* Biol Reprod, 2003. **69**(6): p. 1785-92.
53. Sturm, R.A., G. Das, and W. Herr, *The ubiquitous octamer- binding protein Oct-1 contains a POU domain with a homeo box subdomain.* Genes Dev, 1988. **2**(12A): p. 1582-99.
54. Herr, W., et al., *The POU domain: a large conserved region in the mammalian pit-1, oct-1, oct-2, and Caenorhabditis elegans unc-86 gene products.* Genes Dev, 1988. **2**(12A): p. 1513-6.
55. Ryan, A.K. and M.G. Rosenfeld, *POU domain family values: flexibility, partnerships, and developmental codes.* Genes Dev, 1997. **11**(10): p. 1207-25.
56. Pesce, M., Anastassiadis, K., Scholer, H.R., *Oct-4: Lessons of Totipotency from Embryonic Stem Cells.* Cells Tissues Organs, 1999. **165**: p. 144-152.
57. Twyman, R.M. and W. Wisden, *Advanced Molecular Biology: A Concise Reference*. 1998, New York, New York: Osford: BIOS Scientific Publishers.
58. Ben-Shushan, E., Pikarsky, E., Klar, A. and Bergman, Y., *Extinction of Oct-3/4 Gene Expression in Embryonal Carcinoma X Fibroblast Somatic Cell Hybrids is Accompanied by Changes in the Methylation Status, Chromatin Structure and Transcriptional Activity of the Oct-3/4 Upstream Region.* Mol. Cellular Biology, 1993. **13**: p. 891-901.
59. Pesce M., S., H.R., *Oct-4: Control of Totipotency and Germline Determination.* Molecular Reproduction and Development, 2000. **55**: p. 452-457.
60. Sylvester, I., Scholer, H.R., *Regulation of the Oct-4 Gene by Nuclear Receptors.* Nucleic Acids Res., 1994. **22**: p. 901-911.
61. Okazawa, H., Okamoto, K., Ishino, F., Ishino-Kaneko, T., Takeda, S., Toyoda, Y., Muramatsu, M., Hamada, H., *The Oct3 Gene, A Gene for an Embryonic Transcription Factor, is Controlled by a Retinoic Acid Repressible Enhancer.* EMBO Journal, 1991. **10**(10): p. 2997-3005.
62. Ben-Shushan, E., Sharir, H., Pikarsky, E., Bergman, Y., *A Dynamic Balance Between ARP-1/COUP-TFII, EAR-3/COUP-TFI, and Retinoic Acid Receptor:Retinoid X Receptor Heterodimers Regulates Oct- 3/4 Expression in Embryonal Carcinoma Cells.* Molecular Cellular Biology, 1995. **15**(2): p. 1034-48.
63. Minucci, S., et al., *Retinoic acid-mediated down-regulation of Oct3/4 coincides with the loss of promoter occupancy in vivo.* Embo J, 1996. **15**(4): p. 888-99.
64. Buehr, M., et al., *Rapid Loss of Oct-4 and Pluripotency in Cultured Rodent Blastocysts and Derivative Cell Lines.* Biology of Reproduction, 2003. **68**: p. 222-229.
65. Ben-Shushan, E., et al., *Rex-1, a gene encoding a transcription factor expressed in the early embryo, is regulated via Oct-3/4 and Oct-6 binding to an octamer site and a novel protein, Rox-1, binding to an adjacent site.* Mol Cell Biol, 1998. **18**(4): p. 1866-78.
66. Pikarsky, E., Sharir, H., Ben-Shushan, E. and Bergman, Y., *Retinoic acid Represses Oct-3/4 Gene Expression Through Several Retinoic-acid Responsive Elements Located in the Promoter-Enhancer Region.* Molecular Cellular Biology, 1994. **14**: p. 1026-1038.

67. Du, Z., H. Cong, and Z. Yao, *Identification of putative downstream genes of Oct-4 by suppression-subtractive hybridization.* Biochem Biophys Res Commun, 2001. **282**(3): p. 701-6.
68. Ezashi, T., D. Ghosh, and R.M. Roberts, *Repression of Ets2- induced transactivation of the tau interferon promoter by Oct-4.* Mol Cell Biol, 2001. **21**(23): p. 7883-91.
69. Botquin, V., et al., *New POU Dimer Configuration Mediates Antagonistic Control of an Osteopontin Preimplantation Enhancer by Oct-4 and Sox-2.* Genes and Development, 1998. **12**: p. 2073-2090.
70. Scholer, H.R., Ciesiolka, T. and Gruss, P., *A Nexus Between Oct-4 and E1A: Implications for Gene Regulation in Embryonic Stem Cells.* Cell, 1991a. **66**: p. 291-304.
71. Scholer, H.R., *EMBL Gene Expression Scholer Group1996 Research Report: Oct-4 and the molecular biology of germline and early development of mammals*. 1996.
72. Pesce, M., Scholer, H.R., *Oct-4: Gatekeeper in the Beginnings of Mammalian Development.* Stem Cells, 2001. **19**(4): p. 271-278.
73. Yuan H, C., N., Basilico, C., Dailey, L., *Developmental-specific activity of the FGF-4 Enhancer Requires the Synergistic Action of Sox2 and Oct-3.* Genes Development, 1995. **9**(21): p. 2635-45.
74. Rappolee, D.A., Basilico, C., Patel, Y. and Werb, Z., *Expression and Function of FGF-4 in Peri- Implantation Development in Mouse Embryos.* Development, 1994. **120**(2259-2269).
75. Okuda, A., et al., *UTF1, a novel transcriptional coactivator expressed in pluripotent embryonic stem cells and extra-embryonic cells.* Embo J, 1998. **17**(7): p. 2019-32.
76. Nishimoto, M., et al., *The gene for the embryonic stem cell coactivator UTF1 carries a regulatory element which selectively interacts with a complex composed of Oct-3/4 and Sox-2.* Mol Cell Biol, 1999. **19**(8): p. 5453-65.
77. Hay, D.C., et al., *Oct-4 knockdown induces similar patterns of endoderm and trophoblast differentiation markers in human and mouse embryonic stem cells.* Stem Cells, 2004. **22**(2): p. 225-35.
78. Kim, M.H., et al., *Successful inactivation of endogenous Oct-3/4 and c-mos genes in mouse preimplantation embryos and oocytes using short interfering RNAs.* Biochem Biophys Res Commun, 2002. **296**(5): p. 1372-7.
79. Munsie, M., C. O'Brien, and P. Mountford, *Transgenic strategy for demonstrating nuclear reprogramming in the mouse.* Cloning Stem Cells, 2002. **4**(2): p. 121-30.
80. Boiani, M., et al., *Pluripotency Deficit in Clones Overcome by Clone-Clone Aggregation: Epigenetic Complementation?* EMBO J., 2003. **22**: p. 5304-5312.
81. Jin, T., Branch, D.R., Zhang, X., Qi, S., Youngson, B., Goss, P.E., *Examination of POU Homeobox Gene Expression in Human Breast Cancer Cells.* Int. J. Cancer, 1999. **81**: p. 104-112.
82. Monk, M. and C. Holding, *Human Embryonic Genes Re-Expressed in Cancer Cells.* Oncogene, 2001. **20**: p. 8085-8091.
83. Wender, P.A., Mitchell, Dennis J., Pattabiraman, K., Pelkey, Erin T., Steinman, Lawrence, Bothbard, Jonathan B., *The design, synthesis, and evaluation of*

molecules that enable or enhance cellular uptake: Peptoid Molecular transporters. Proceedings of National Academy of Science, USA, 2000. **97**(24): p. 13003-13008.
84. Ball, P., *Old Tat Teaches Drug Smugglers New Tricks*, in *Nature Science Update*. 2000.
85. Allinquant, B., Hantraye, P., Mailleux, P., Moya, K., Couillot, C., Prochiantz, A., *Downregulation of Amyloid Precursor Protein Inhibits Neurite Outgrowth In Vitro.* The Journal of Cell Biology, 1995. **128**(5): p. 919-927.
86. Schwarze, S.R., Dowdy, S.F., *In vivo Protein Transduction: Intracellular Delivery of Biologically Active Proteins, Compounds and DNA.* Trends in Pharmacological Sciences, 2000. **21**(2): p. 45-8.
87. Ezhevsky, S.A., Nagahara, H., Voceero-Akbani, A., Gius, D.R., Wei, M.C. and Dowdy, S.F., *Hypo-phosphorylation of the Retinoblastoma Protein (pRb) by Cyclin D:Cdk4/6 Complexes Results in Active pRb.* Proceedings of National Academy of Sciences USA, 1997. **94**: p. 10699-10704.
88. Lissy, N.A., VanDyk, L., Becker-Hapak, M., Vocero-Akbani, A., Mendler, J.H., and Dowdy, S.F., *TCR Antigen-Induced Cell Death Occurs From a Late G1 Phase Cell Cycle Check Point.* Immunity, 1998. **8**: p. 57-65.
89. Vocero-Akbani, A., Heyden, N.V., Lissy, N.A., Ratner, L., and Dowdy, S.F., *Killing HIV infected cells by Direct Transduction of an HIV protease-activated Caspase-3 Protein.* Nat. Med, 1999. **5**: p. 29-33.
90. Blakeslee, D., *JAMA HIV/AIDS Information Center - Special Reports - A Killer Strategy Against HIV*. 1999.
91. Vocero-Akbani, A., et al., *Protein transduction: delivery of Tat-GTPase fusion proteins into mammalian cells.* Methods in Enzymology, 2001. **332**: p. 36-49.
92. Vocero-Akbani, A., Lissy, N.A., Dowdy, S.F., *Transduction of Full-Length Tat Fusion Proteins Directly into Mammalian Cells: Analysis of T Cell Receptor Activation-Induced Cell Death.* Methods in Enzymology, 2001. **322**: p. 503-521.
93. Becker-Hapak, M., McAllister, S., Dowdy, S., *TAT-mediated Protein Transduction into Mammalian Cells.* METHODS, 2001. **24**(3): p. 247-256.
94. Dowdy, S.F., *Protein Transduction: Delivery of Biologically Active Proteins in Vivo.* Journal of Vascular Surgery, 2001. **33**(6): p. 1315.
95. *Howard Hughes Medical Institute Research News: AIDS Virus Fragment Delivers Protein Payload*. 2000.
96. Yu, B.D., et al., *Distinct and nonoverlapping roles for pRB and cyclin D:cyclin-dependent kinases 4/6 activity in melanocyte survival.* Proc Natl Acad Sci U S A, 2003. **100**(25): p. 14881-6.
97. Schwarze, S.R., et al., *In Vivo Protein Transduction: Delivery of a Biologically Active Protein Into the Mouse.* Science, 1999. **285**(5433): p. 1569-72.
98. Gius, D., Ezhevsky, S.A., Becker-Hapak, M., Nagahara, H., Wei, M.C. and Dowdy, S.F., *Transduced $p16^{INK\ 4a}$ peptides Inhibit Hypo-Phosphorylation of the Retinoblastoma Protein and Cell Cycle Progression Prior to Activation of cdk2 Complexes in late G_1.* Cancer Research, 1999. **59**: p. 2577-2580.
99. Kwon, H.Y., et al., *Transduction of Cu,Zn-superoxide dismutase mediated by an HIV-1 Tat protein basic domain into mammalian cells.* FEBS Letters, 2000. **485**(2-3): p. 163-7.

100. Kilic, U., et al., *Intravenous TAT-GDNF is protective after focal cerebral ischemia in mice.* Stroke, 2003. **34**(5): p. 1304-10.
101. Snyder, E.L., et al., *Treatment of terminal peritoneal carcinomatosis by a transducible p53-activating peptide.* PLoS Biol, 2004. **2**(2): p. E36.
102. Wadia, J.S., R.V. Stan, and S.F. Dowdy, *Transducible TAT-HA fusogenic peptide enhances escape of TAT-fusion proteins after lipid raft macropinocytosis.* Nat Med, 2004. **10**(3): p. 310-5.
103. Lundberg, M., S. Wikstrom, and M. Johansson, *Cell surface adherence and endocytosis of protein transduction domains.* Mol Ther, 2003. **8**(1): p. 143-50.
104. Ferrari, A., et al., *Caveolae-mediated internalization of extracellular HIV-1 tat fusion proteins visualized in real time.* Mol Ther, 2003. **8**(2): p. 284-94.
105. Kaplan, I.M., J.S. Wadia, and S.F. Dowdy, *Cationic TAT peptide transduction domain enters cells by macropinocytosis.* J Control Release, 2005. **102**(1): p. 247-53.
106. Anderson, J.E., et al., *Degradation of maternal cdc25c during the maternal to zygotic transition is dependent upon embryonic transcription.* Mol Reprod Dev, 2001. **60**(2): p. 181-8.
107. Betteridge, K.J. and J.E. Flechon, *The Anatomy and Physiology of Pre-Attachment Bovine Embryos.* Theriogenology, 1988. **29**: p. 155-186.
108. Bjerregaard, B., et al., *Expression of Nucleolar Related Proteins in Porcine Preimplantation Embryos Produced in Vivo and in Vitro.* Biology of Reproduction, 2003. **70**: p. 867-876.
109. Maddox-Hyttel, P., et al., *Gene expression during pre- and peri-implantation embryonic development in pigs.* Reprod Suppl, 2001. **58**: p. 175-89.
110. Mohan, M., et al., *Expression of retinol-binding protein messenger RNA and retinoic acid receptors in preattachment bovine embryos.* Mol Reprod Dev, 2001. **60**(3): p. 289-96.
111. Memili, E., T. Dominko, and N.L. First, *Onset of Transcription in Bovine Oocytes and Preimplantation Embryos.* Molecular Reproduction and Development, 1998. **51**: p. 36-41.
112. Nothias, Y.-Y., et al., *Regulation of Gene Expression at the Beginning of Mammalian Development.* Journal Biological Chemistry, 1995. **270**(38): p. 22077-22080.
113. Hyttel, P., et al., *Activation of ribosomal RNA genes in preimplantation cattle and swine embryos.* Anim Reprod Sci, 2000. **60-61**: p. 49-60.
114. Hyttel, P., et al., *Activation of ribosomal RNA genes in preimplantation cattle and swine embryos.* Anim Reprod Sci, 2000a. **60-61**: p. 49-60.
115. Hyttel, P., et al., *Nucleolar proteins and ultrastructure in preimplantation porcine embryos developed in vivo.* Biol Reprod, 2000b. **63**(6): p. 1848-56.
116. Cross, J.C., Z. Werb, and S.J. Fisher, *Implantation and the placenta: key pieces of the development puzzle.* Science, 1994. **266**(5190): p. 1508-18.
117. Cross, J.C., *Genes regulating embryonic and fetal survival.* Theriogenology, 2001. **55**(1): p. 193-207.
118. Sutherland, A., *Mechanisms of implantation in the mouse: differentiation and functional importance of trophoblast giant cell behavior.* Dev Biol, 2003. **258**(2): p. 241-51.

119. Bowen, J.A. and R.C. Burghardt, *Cellular mechanisms of implantation in domestic farm animals.* Semin Cell Dev Biol, 2000. **11**(2): p. 93-104.
120. Hogan, B., F. Costantini, and E. Lacy, *Manipulating the Mouse Embryo: A Laboratory Manual*. 1986, Cold Spring Harbor, New York: Cold Spring Harbor Laboratory.
121. Heuser C.H. and Streeter G.L., *Early Stages In The Development Of Pig Embryos, From The Period Of Initial Cleavage To The Time Of The Appearance Of Limb-Buds.* Contributions to Embryology, 1929. **20**: p. 3-229.
122. Mohan, M., et al., *Analysis of gene expression in the bovine blastocyst produced in vitro using suppression-subtractive hybridization.* Biol Reprod, 2002. **67**(2): p. 447-53.
123. Perry, J.S., *The Mammalian Fetal Membranes.* Journal of Reproduction and Fertility, 1981. **62**: p. 321-335.
124. Stroband, H.W.J., N. Taverne, and B. M., *The Pig Blastocyst: Its Ultrastructure and the Uptake of Protein Macromolecules.* Cell and Tissue Research, 1984. **235**: p. 347-356.
125. Geisert, R.D., et al., *Establishment of Pregnancy in the Pig: II. Cellular Remodeling of the Porcine Blastocyst During Elongation on Day 12 of Pregnancy.* Biology of Reproduction, 1982. **27**: p. 941-955.
126. Ross, J.W., et al., *Analysis and characterization of differential gene expression during rapid trophoblastic elongation in the pig using suppression subtractive hybridization.* Reprod Biol Endocrinol, 2003. **1**(1): p. 23.
127. Geisert, R.D. and J.V. Yelich, *Regulation of conceptus development and attachment in pigs.* J Reprod Fertil Suppl, 1997. **52**: p. 133-49.
128. Geisert, R.D., et al., *Establishment of Pregnancy in the Pig: I. Interrelationships Between Preimplantation Development of the Pig Blastocyst and Uterine Endometrial Secretions.* Biology of Reproduction, 1982. **27**: p. 925-939.
129. Bowen, J.A., F.W. Bazer, and R.C. Burghardt, *Spatial and Temporal Analyses of Integrin and Muc-1 Expression in Porcine Uterine Epithelium and Trophectoderm in Vivi.* Biology of Reproduction, 1996. **55**: p. 1098-1106.
130. Patten, B.M. and B.M. Carlson, *Foundations of Embryology*. 1974, New York: McGraw-Hill Book Company.
131. Yelich, J.V., D. Pomp, and R.D. Geisert, *Detection of transcripts for retinoic acid receptors, retinol-binding protein, and transforming growth factors during rapid trophoblastic elongation in the porcine conceptus.* Biol Reprod, 1997a. **57**(2): p. 286-94.
132. Johnson, G.A., et al., *Osteopontin: Roles in Implantation and Placentation.* Biology of Reproduction, 2003. **69**: p. 1458-1471.
133. Melner, M.H., et al., *Differential expression of genes in the endometrium at implantation: upregulation of a novel member of the E2 class of ubiquitin-conjugating enzymes.* Biol Reprod, 2004. **70**(2): p. 406-14.
134. Yelich, J.V., D. Pomp, and R.D. Geisert, *Ontogeny of elongation and gene expression in the early developing porcine conceptus.* Biol Reprod, 1997b. **57**(5): p. 1256-65.

135. Pomp, D., et al., *Sex identification in mammals with polymerase chain reaction and its use to examine sex effects on diameter of day-10 or -11 pig embryos.* J Anim Sci, 1995. **73**(5): p. 1408-15.
136. Vallee, M., et al., *Isolation of differentially expressed genes in conceptuses and endometrial tissue of sows in early gestation.* Biol Reprod, 2003. **69**(5): p. 1697-706.
137. Green, M.L., R.C.M. Simmen, and F.A. Simmen, *Developmental Regulation of Steroidogenic Enzyme Gene Expression in the Periimplantation Porcine Conceptus: A Paracrine Role for Insulin-Like Growth Factor-I.* Endocrinology, 1995. **136**(9): p. 3961-3970.
138. Ko, Y., et al., *Transient Expression of the Cytochrome P450 Aromatase Gene in Elongating Porcine Blastocysts Is Correlated With Uterine Insulin-Like Growth Factor Levels During Peri-Implantation Development.* Molecular Reproduction and Development, 1994. **37**: p. 1-11.
139. Geisert, R.D., et al., *Establishment of Pregnancy in the Pig: III. Endometrial Secretory Response to Estradiol Valerate Administered on Day 11 of the Estrous Cycle.* Biology of Reproduction, 1982. **27**: p. 957-965.
140. Geisert, R.D., et al., *Characterization and proteolytic activity of a cathepsin L-like polypeptide in endometrium and uterine flushings of cycling, pregnant and steroid-treated ovariectomized gilts.* Reprod Fertil Dev, 1997. **9**(4): p. 395-402.
141. Telford, N.A., A.J. Watson, and G.A. Schultz, *Transition from maternal to embryonic control in early mammalian development: a comparison of several species.* Mol Reprod Dev, 1990. **26**(1): p. 90-100.
142. Yelich, J.V., D. Pomp, and R.D. Geisert, *Detection of Transcripts for Retinoic Acid Receptors, Retinol-Binding Protein, and Transforming Growth Factors During Rapid Trophoblastic Elongation in the Porcine Conceptus.* Biology of Reproduction, 1997. **57**: p. 286-294.
143. Mohan, M., et al., *Expression Patterns of Retinoid X Receptors, Retinaldehyde Dehydrogenase, and Peroxisome Proliferator Activated Receptor Gamma in Bovine Preattachment Embryos.* Biology of Reproduction, 2002. **66**: p. 692-700.
144. Garlow, J.E., et al., *Analysis of Osteopontin at the Maternal-Placental Interface in Pigs.* Biology of Reproduction, 2002. **66**: p. 718-725.
145. Agoulnik, I.Y., et al., *Cloning, expression analysis and chromosomal localization of the human nuclear receptor gene GCNF.* FEBS Lett, 1998. **424**(1-2): p. 73-8.
146. Hettinger, A.M., et al., *Presence of the acute phase protein, bikunin, in the endometrium of gilts during estrous cycle and early pregnancy.* Biol Reprod, 2001. **65**(2): p. 507-13.
147. Vonnahme, K.A., et al., *Porcine endometrial expression of kininogen, factor XII, and plasma kallikrein in cyclic and pregnant gilts.* Biol Reprod, 2004. **70**(1): p. 132-8.
148. Vonnahme, K.A., et al., *Detection of kallikrein gene expression and enzymatic activity in porcine endometrium during the estrous cycle and early pregnancy.* Biol Reprod, 1999. **61**(5): p. 1235-41.
149. Geisert, R.D., et al., *Expression of an inter-alpha-trypsin inhibitor heavy chain-like protein in the pig endometrium during the oestrous cycle and early pregnancy.* J Reprod Fertil, 1998. **114**(1): p. 35-43.

150. Allen, M.R., et al., *Detection of bradykinin and bradykinin-beta(2) receptors in the porcine endometrium during the estrous cycle and early pregnancy.* Biol Reprod, 2002. **66**(3): p. 574-9.
151. Geisert, R.D., et al., *Possible role of kallikrein in proteolysis of insulin-like growth factor binding proteins during the oestrous cycle and early pregnancy in pigs.* Reproduction, 2001. **121**(5): p. 719-28.
152. Kaeoket, K., E. Persson, and A.-M. Dalin, *Influence of pre-ovulatory insemination and early pregnancy on the distribution of CD2, CD4, CD8 and MHC class II expressing cells in the sow endometrium.* Animal Reproduction Science, 2003. **76**: p. 231-244.
153. Dantzer, V., *Electron Microscopy of the Initial Stages of Placentation in the Pig.* Anatomy and Embryology, 1985. **172**: p. 281-293.
154. Dantzer, V., *Scanning Electron Microscopy of Exposed Surfaces of the Porcine Placenta.* Acta anat., 1984. **118**: p. 96-106.
155. Daniels, R., V. Hall, and A.O. Trounson, *Analysis of Gene Transcription in Bovine Nuclear Transfer Embryos Reconstructed with Granulosa Cell Nuclei.* Biology of Reproduction, 2000. **63**: p. 1034-1040.
156. Niemann, H. and C. Wrenzycki, *Alterations of Expression of Developmentally Important Genes in Preimplantation Bovine Embryos by in vitro Culture Conditions: Implications for Subsequent Development.* Theriogenology, 2000. **53**: p. 21-34.
157. Wells, D.N., B. Oback, and G. Laible, *Cloning livestock: a return to embryonic cells.* Trends Biotechnol, 2003. **21**(10): p. 428-32.
158. Bortvin, A., et al., *Incomplete reactivation of Oct4-related genes in mouse embryos cloned from somatic nuclei.* Development, 2003. **130**(8): p. 1673-80.
159. Johnson, M.H. and B. Maro, eds. *Experimental Approaches to Mammalian Embryonic Development*. Time and Space in the Mouse Early Embryo: A Cell Biological Approach to Cell Diversification. 1986, Cambridge University Press: Cambridge, New York. 35-65.
160. Boerjan, M. and G.t. Kronnie, *The Segregation of Inner and Outer Cells in Porcine Embryos Follows a Different Pattern Compared to the Segregation in Mouse Embryos.* Roux's Archives of Developmental Biology, 1993. **203**: p. 113-116.
161. Piedrahita, J.A., et al., *Differential Gene Expression Between Embryonic Ectoderm and Trophectoderm in the Preimplantation Porcine Embryo [abstract].* Theriogenology, 1994. **41**: p. 274.
162. Gries, L.K., et al., *Uterine secretory alterations coincident with embryonic mortality in the gilt after exogenous estrogen administration.* J Anim Sci, 1989. **67**(1): p. 276-84.
163. Geisert, R.D., et al., *Establishment of pregnancy in the pig: II. Cellular remodeling of the porcine blastocyst during elongation on day 12 of pregnancy.* Biol Reprod, 1982. **27**(4): p. 941-55.
164. Vassilieva, S., Kaomei, G., Pich, U., and Wobus, A.M., *Establishment of SSEA-1- and Oct-4-Expressing Rat Embryonic Stem-like Cell Lines and Effects of Cytokines of the IL-6 Family on Clonal Growth.* Experimental Cell Research, 2000. **258**: p. 361-373.

165. Ginzinger, D.G., *Gene quantification using real-time quantitative PCR: an emerging technology hits the mainstream.* Exp Hematol, 2002. **30**(6): p. 503-12.
166. Livak, K.J. and T.D. Schmittgen, *Analysis of relative gene expression data using real-time quantitative PCR and the 2(-Delta Delta C(T)) Method.* Methods, 2001. **25**(4): p. 402-8.
167. *Relative Quantitation of Gene Expression: ABI PRISM 7700 Sequence Detection System User Bulletin # 2: Rev B*.
168. Barr, A.J., *SAS User's Guide: Statistics*. 1985, Cary, N.C.: Statistical Analysis System Institute Inc.
169. Barr, A.J., et al., *SAS User's Guide*. 1979, Raleigh, NC: SAS Institute. 494.
170. Stewart, C., *Oct-4, Scene 1: The Drama of Mouse Development.* Nature Genetics, 2000. **24**: p. 328-330.
171. De Sousa, P.A., A.J. Watson, and R.M. Schultz, *Transient expression of a translation initiation factor is conservatively associated with embryonic gene activation in murine and bovine embryos.* Biol Reprod, 1998. **59**(4): p. 969-77.
172. Lee, K.F., et al., *A comparative study of gene expression in murine embryos developed in vivo, cultured in vitro, and cocultured with human oviductal cells using messenger ribonucleic acid differential display.* Biol Reprod, 2001. **64**(3): p. 910-7.
173. Bustin, S.A., *Quantification of mRNA using real-time reverse transcription PCR (RT-PCR): trends and problems.* J Mol Endocrinol, 2002. **29**(1): p. 23-39.
174. Bustin, S.A., *Absolute quantification of mRNA using real-time reverse transcription polymerase chain reaction assays.* J Mol Endocrinol, 2000. **25**(2): p. 169-93.
175. Overbergh, L., et al., *Quantification of murine cytokine mRNAs using real time quantitative reverse transcriptase PCR.* Cytokine, 1999. **11**(4): p. 305-12.
176. Giulietti, A., et al., *An overview of real-time quantitative PCR: applications to quantify cytokine gene expression.* Methods, 2001. **25**(4): p. 386-401.
177. Pfaffl, M.W. and M. Hageleit, *Validities of mRNA Quantification Using Recombinant RNA and Recombinant DNA External Calibration Curves in Real-Time RT-PCR.* Biotechnology Letters, 2001. **23**: p. 275-282.
178. Li, W., et al., *Complex DNA Melting Profiles of Small PCR Products Revealed Using SYBR Green I.* Biotechniques, 2003. **35**: p. 702-706.
179. Yeom, Y.I., et al., *Germline regulatory element of Oct-4 specific for the totipotent cycle of embryonal cells.* Development, 1996. **122**(3): p. 881-94.
180. Lan, Z.J., et al., *Expression of the orphan nuclear receptor, germ cell nuclear factor, in mouse gonads and preimplantation embryos.* Biol Reprod, 2003. **68**(1): p. 282-9.
181. Chen, F., et al., *Cloning of a novel orphan receptor (GCNF) expressed during germ cell development.* Mol Endocrinol, 1994. **8**(10): p. 1434-44.
182. Chung, A.C. and A.J. Cooney, *Germ cell nuclear factor.* Int J Biochem Cell Biol, 2001. **33**(12): p. 1141-6.
183. Hummelke, G.C., M.L. Meistrich, and A.J. Cooney, *Mouse protamine genes are candidate targets for the novel orphan nuclear receptor, germ cell nuclear factor.* Mol Reprod Dev, 1998. **50**(4): p. 396-405.

184. Cooney, A.J., et al., *Physiological function of the orphans GCNF and COUP-TF.* Trends Endocrinol Metab, 2001. **12**(6): p. 247-51.
185. Cooney, A.J., et al., *Germ Cell Nuclear Factor: An Orphan Receptor in Search of a Function.* American Zoology, 1999. **39**: p. 796-806.
186. Hummelke, G.C. and A.J. Cooney, *Germ cell nuclear factor is a transcriptional repressor essential for embryonic development.* Front Biosci, 2001. **6**: p. D1186-91.
187. Cooney, A.J., et al., *Germ cell nuclear factor is a response element-specific repressor of transcription.* Biochem Biophys Res Commun, 1998. **245**(1): p. 94-100.
188. Chen, J.D. and R.M. Evans, *A transcriptional co-repressor that interacts with nuclear hormone receptors.* Nature, 1995. **377**(6548): p. 454-7.
189. Yan, Z.H., et al., *Characterization of the response element and DNA binding properties of the nuclear orphan receptor germ cell nuclear factor/retinoid receptor-related testis-associated receptor.* J Biol Chem, 1997. **272**(16): p. 10565-72.
190. Greschik, H., et al., *Characterization of the DNA-binding and dimerization properties of the nuclear orphan receptor germ cell nuclear factor.* Mol Cell Biol, 1999. **19**(1): p. 690-703.
191. Fuhrmann, G., et al., *Mouse germline restriction of Oct4 expression by germ cell nuclear factor.* Dev Cell, 2001. **1**(3): p. 377-87.
192. Lan, Z.J., et al., *The embryonic function of germ cell nuclear factor is dependent on the DNA binding domain.* J Biol Chem, 2002. **277**(52): p. 50660-7.
193. Ying, Y., X. Qi, and G. -Q. Zhao, *Induction of primordial germ cells from murine epiblasts by synergistic action of BMP4 and BMP8B signaling pathways.* PNAS, 2001. **98**(14): p. 7858-7862.
194. Hogan, B.L., *Bone morphogenetic proteins: multifunctional regulators of vertebrate development.* Genes Dev, 1996. **10**(13): p. 1580-94.
195. Zhao, G.Q., et al., *The gene encoding bone morphogenetic protein 8B is required for the initiation and maintenance of spermatogenesis in the mouse.* Genes Dev, 1996. **10**(13): p. 1657-69.
196. Ying, Y. and G.Q. Zhao, *Detection of multiple bone morphogenetic protein messenger ribonucleic acids and their signal transducer, Smad1, during mouse decidualization.* Biol Reprod, 2000. **63**(6): p. 1781-6.
197. Ying, Y. and G.Q. Zhao, *Cooperation of endoderm-derived BMP2 and extraembryonic ectoderm-derived BMP4 in primordial germ cell generation in the mouse.* Dev Biol, 2001. **232**(2): p. 484-92.
198. Ying, Y., et al., *Requirement of Bmp8b for the generation of primordial germ cells in the mouse.* Mol Endocrinol, 2000. **14**(7): p. 1053-63.
199. McLaren, A., *Signaling for germ cells.* Genes Dev, 1999. **13**(4): p. 373-6.
200. Lawson, K.A., et al., *Bmp4 is required for the generation of primordial germ cells in the mouse embryo.* Genes Dev, 1999. **13**(4): p. 424-36.
201. Zhao, G.Q., *Consequences of knocking out BMP signaling in the mouse.* Genesis, 2003. **35**(1): p. 43-56.

202. Dowdy, S.F., *Protein Transduction: Delivery of TAT-Fusion Proteins into Mammalian Cells*. 2000, Howard Hughes Medical Institute: St. Louis, MO. p. Personal Communication.
203. R.K.Scopes and J.A. Smith, *Analysis of Proteins: Supplement 44.* Current Protocols in Molecular Biology, 1998. **10.01-10.020**.
204. Sambrook, J., E.F. Fritsch, and T. Maniatis, *Molecular Cloning: A Laboratory Manual (2nd ed.).* 1989, Plainview, New York: Cold Spring Harbor Laboratory Press.
205. Strachan, T. and A.P. Read, *Human Molecular Genetics 2*. 1999: John Wiley & Sons Inc.
206. Moore, D.D. and D. Dowhan, *Purification and Concentration of DNA from Aqueous Solutions: Supplement 59.* Current Protocols in Molecular Biology, 2002. **2.01-2.-3**.
207. Lorens, J.B., *Rapid and reliable cloning of PCR products.* PCR Methods Appl, 1991. **1**(2): p. 140-1.
208. Heery, D.M., F. Gannon, and R. Powell, *A simple method for subcloning DNA fragments from gel slices.* Trends Genet, 1990. **6**(6): p. 173.
209. Maria, M., U. Mathias, and S. Stahl, *Upstream Strategies to Minimize Proteolytic Degradation upon Recombinant Production in Escherichia coli.* Protein Expression and Purification, 1996. **7**: p. 129-136.
210. Gallagher, S.R., *One-Dimensional SDS Gel Electrophoresis of Proteins: Supplement 47.* Current Protocols in Molecular Biology, 1999. **10.2A1-10.2A.34**.
211. Cleveland, D.W., et al., *Peptide mapping by limited proteolysis in sodium dodecyl sulfate and analysis by gel electrophoresis.* J Biol Chem, 1977. **252**(3): p. 1102-6.
212. Laemmli, U.K., *Cleavage of Structural Proteins during the Assembly of the Head of Bacteriophage T4.* Nature, 1970. **227**: p. 680-685.

VITA

Diana Spencer

Candidate for the Degree of

Doctor of Philosophy

Thesis: *Oct-4* GENE EXPRESSION IN THE PREATTACHMENT POCINE CONCEPTUS AND MURINE EMBRYO WITH REGULATION OF PLURIPOTENCY THROUGH PROTEIN TRANSDUCTION

Major Field: Biomedical Sciences

Biographical:

Personal Data: Born in Wichita Kansas, September 14, 1955, the daughter of Carol E. Blake and Richard E. Blake. Married to Mark F. Spencer on May 28, 1975. Mother of two daughters, Jessica M. Spencer and Julia R. Spencer.

Education: Received a Bachelor of Arts in Biology and Sociology from the University of Houston at Clear Lake City, Texas in 1978; received Master of Science in Math/Science Education from The University of Tulsa in 1994. Completed the requirements for the Doctor of Philosophy degree at Oklahoma State University Center for Health Sciences, Tulsa, Oklahoma in July, 2005.

Experience: Instructor of Physiology and Biology at Tulsa Community College 2004 – present. Instructor of College Preparatory Biology and Anatomy and Physiology Education at Jenks High School, Oklahoma, 1979-2001. Adjunct Instructor of Anatomy and Physiology and Nutrition at Tulsa Community College, 1995-1997. Biology Instructor at Clear Lake High School, Texas, 1978-1979.

Professional Memberships: National Association of Biology Teachers, National Association of Science Teachers

Name: Diana Spencer Date of Degree: July, 2005

Institution: Oklahoma State University Location: Stillwater, Oklahoma

Title of Study: *Oct-4* GENE EXPRESSION IN THE PREATTACHMENT PORCINE CONCEPTUS AND MURINE EMBRYO WITH REGULATION OF PLURIPOTENCY THROUGH PROTEIN TRANSDUCTION

Pages in Study: 150 Candidate for the Degree of Doctor of Philosophy

Major Field: Biomedical Sciences

Scope and Method of Study: To investigate the presence of the Oct-4 transcript in the murine embryo and the preattachment porcine conceptus over time, we quantified the expression of *Oct-4*, a candidate master regulator gene for the maintenance of pluripotent cells. We also examined the cloning and subsequent protein purification of positive and negative regulators of the *Oct-4* gene with the potential for protein transduction therapy. Our first objective was to test the hypothesis that porcine trophoblastic elongation and placental differentiation is associated with the *Oct-4* gene expression. Porcine embryos were collected following days 10 to 17 of development. The quantitative analysis used a Real Time, one-step RT-PCR amplification. Our second objective was to test the hypothesis that individual murine embryos exhibit an up-regulation of Oct-4 in the 4-cell, 8-cell, and blastocyst whole embryos and that the individual pluripotent cells would exhibit an increase in single cell expression. RNA of individual murine embryos was reverse transcribed and Real Time PCR performed. Our final objective was to produce an *Oct-4* gene enhancer TAT fusion protein, an *Oct-4* gene repressor TAT fusion protein and an *Oct-4* TAT fusion protein to be used in subsequent studies. We used site directed PCR mutagenesis to clone the *Bmp8b*, *GCNF* and *Oct-4* genes in prokaryote expression vectors. Through protein expression in *E. coli* and FPLC purification, fusion proteins were verified and tested on living cells.

Findings and Conclusions: Using the comparative C_T method, the porcine Oct-4 expression was greatest on days 10 and 12 of pregnancy and was approximately 2, 8, and 11-fold greater compared to expression on days 13, 15 and 17, respectively. The down regulation of *Oct-4* gene expression between days 12 and 17 is temporally associated with porcine extended trophoblastic elongation and placental differentiation. The murine blastocysts and 8-cell embryos produced 85-fold and 7-fold more Oct-4, respectively, than the four cell embryos. A significant up-regulation of the Oct-4 transcript per totipotent blastocyst cell was demonstrated. The three fusion proteins were produced and verified. The protein transduction initial trials on living cells were unsuccessful in consistently regulating transcription.

ADVISER'S APPROVAL: Lee Rickords, Ph.D.